# Immunotherapy Using a Novel Agonistic Anti-IL-2 Antibody Combined with Epigenetic Modulation Limits Tumor Immune Escape and Controls Tumor Growth

---

**Dissertation**

**zur**

**Erlangung der naturwissenschaftlichen Doktorwürde**

**(Dr. sc. nat.)**

**vorgelegt der**

**Mathematisch-naturwissenschaftlichen Fakultät**

**der**

**Universität Zürich**

**von**

**Natalia Arenas-Ramirez**

**aus**

**Kolumbien**

**Promotionskomitee**

Prof. Dr. Onur Boyman (Leitung)

Prof. Dr. Christian Münz (Vorsitz)

Prof. Dr. François Spertini

**Zürich, 2016**

**Table of contents**

# I. Summary

Interleukin-2 (IL-2) immunotherapy is an attractive approach for the treatment of advanced cancer. However, its short half-life and side effects have compromised its further development into the clinics. Via binding to its IL-2 receptor α (CD25) subunit, IL-2 exerts unwanted effects including stimulation of immunosuppressive regulatory T (Treg) cells and endothelial cell damage. Using a rational based approach, we developed a monoclonal antibody to human IL-2 (hIL-2), termed NARA1, blocking with high affinity the interaction of the cytokine with the CD25 receptor subunit. The structure of the hIL-2/NARA1 complex (IL-2cx) reveals that NARA1 perfectly overlaps with CD25. NARA1 binds to hIL-2 with 10-fold higher affinity compared to CD25 favoring hIL-2 interaction with the dimeric IL-2 receptor. In line with this, IL-2cx immunotherapy leads to potent anti-tumor immunity, by favoring the ratio of tumor-specific and polyclonal cytotoxic $CD8^+$ T cells vs Treg cells, leading to less endothelial cell damage and increasing the half-life of the cytokine. IL-2cx significantly improves survival in transplantable and spontaneous metastatic melanoma models. These data warrant further development of NARA1.

Despite potent and constant stimulation of the immune system upon IL-2cx therapy, cancer cells use several mechanisms to suppress the anti-tumor immune response and to become resistant. The molecular processes of tumor immune escape from immune surveillance remain poorly understood. We were able to show that different tumor immune escape mechanisms are controlled by the histone methyltransferase enhancer of zeste homologue 2 (Ezh2). During IL-2cx immunotherapy, Ezh2 expression increases in melanoma cells, particularly in areas rich in tumor-infiltrating lymphocytes. Ezh2 inhibit the transcription of molecules essential for proper tumor antigen presentation and promote a dedifferentiation program leading to

disease progression and metastasis. Ezh2 blockade reverses these effects in melanoma cells and synergizes with IL-2cx or anti-cytotoxic T-lymphocyte-associated protein 4 (anti-CTLA-4) immunotherapy to control tumor growth. Upon combinatorial treatment interferon-γ-producing $CD8^+$ T cells selectively accumulate in the tumor site and maintain low programmed cell death protein 1 (PD-1) levels, accompanied by programmed death-ligand 1 (PD-L1) downregulation on melanoma cells. On the other hand, immunosuppressive cells such as $FoxP3^+$ $CD4^+$ regulatory T cells and myeloid-derived suppressor cells fail to accumulate intratumorally. These data reveal the importance of Ezh2 playing a key role during tumor immune escape and indicate that combination of EZH2 blockade and immunotherapeutics might be considered for cancer therapy.

# II. Zusammenfassung

Interleukin-2 Immuntherapie ist eine attraktive Strategie zur Behandlung von Krebs in fortgeschrittenen Stadien. Allerdings führt die Bindung von IL-2 an die α-Untereinheit seines Rezeptors (auch CD25 genannt) zu ungewollten Nebenwirkungen, welche einerseits zur Stimulierung von immun-suppressiven regulatorischen T-Zellen (Treg-Zellen) und andererseits zu einer Schädigung des Endotheliums führt. Dank einer rationalen Vorgehensweise konnten wir einen monoklonalen Antikörper namens NARA1 entwickeln, der als hoch-affiner CD25-Imitator wirkt und so die Assoziation von IL-2 mit CD25 verringert. Die Strukturaufklärung dieses neuen hIL-2/NARA1 Komplexes zeigte, dass NARA1 tatsächlich das CD25-Bindungsepitop von IL-2 besetzt, wodurch es zu einer sehr präzisen Überlappung der beiden Epitope kommt. Die Bindung von NARA1 an IL-2 erfolgt mit 10-fach höherer Affinität im Vergleich zu CD25 und führt zu hIL-2/NARA1 Komplexen (IL-2cx), die eine starke Präferenz hinsichtlich der Stimulierung von $CD8^+$ T-Zellen aufweist, während die Stimulierung von Treg-Zellen und die schädliche Wirkung auf das Endothelium reduziert werden. Die Immuntherapie mit hIL-2/NARA1 Komplexen führt zu einer starken Anti-Tumor-Immunantwort durch die Proliferation von Tumor-speziefischen polyklonalen zytotoxischen $CD8^+$ T-Zellen. Diese Therapie führt somit zu einer bedeutenden Verlängerung der Lebenserwartung in Mäusen, in welche entweder Melanomzellen injiziert wurden, oder in anderen Mäusen, welche spontan Melanome entwickeln. Diese Daten dienen als Basis für die Weiterentwicklung von NARA1.

Trotz effizienter und konstanter Stimulierung des Immunsystems mittels IL-2cx entwickeln Tumorzellen verschiedene Mechanismen zur Resistenz gegen das Abtöten durch Immunsystem oder aber Tumorzellen unterdrücken das Immunsystem. Die molekularen

Prozesse, die zur Umgehung der Immunüberwachung des Tumors führen, sind bis jetzt nur unzureichend verstanden. Wir konnten zeigen, dass verschiedene Tumorzell-intrinsische und -extrinsische Mechanismen zur Überwindung einer Immunantwort durch die Histon-Methyltransferase Enhancer of Zeste Homologue 2 (Ezh2) kontrolliert werden. Während der IL-2cx-Immuntherapie steigt die Expression von Ezh2 in Melanomzellen an, insbesondere in Bereichen des Tumors, die intensiv von Lymphozyten infiltriert wurden. Ezh2 fördert ein Dedifferenzierungsprogramm in Tumorzellen, welches an das Fortschreiten der Krankheit erinnert und die Unterdrückung von Schlüsselmolekülen der MHC/Antigen-Präsentation beinhaltet. Die Inaktivierung von Ezh2 macht diese Prozesse rückgängig und führt in Kombination mit IL-2cx- oder anti-CTLA-4-Immuntherapie zu einer erkenntlichen Verlangsamung des Tumorwachstums. Diese Anti-Tumor-Effekte hängen stark von Interferon-γ-produzierenden $CD8^+$ T-Zellen ab, die sich selektiv im Innern des Tumors anreichern. Zudem erhalten diese Zellen ein tiefes PD-1 Niveau aufrecht, während gleichzeitig die Expression von PD-L1 auf Melanomzellen herunter reguliert wird. Im Gegensatz dazu werden immun-suppresive $FoxP3^+$ $CD4^+$ Treg-Zellen und myeloide Suppressorzellen während der Kombinationstherapie bestehend aus Ezh2-Inhibition und IL-2cx-Immuntherapie davon abgehalten in den Tumor einzudringen. Folglich fungiert Ezh2 als molekularer Schalter, der die Überwindung des Immunsystems durch den Tumor kontrolliert. Diese Erkenntnisse implizieren, dass die Blockade von EZH2 zusammen mit Immuntherapien für die Krebstherapie in Betracht gezogen werden könnte.

# III. Introduction

## 1. The immune system

The immune system is a complex network of cells, tissues, lymphoid organs, and messengers, which work together in order to defend our body against pathogens and endogenous malignancies. Epithelial cell barriers form our first line of defense and prevent disease-causing pathogens from invading our body. If pathogens manage to attach to epithelial cells or to cross the epithelial barriers, an immediate defense reaction will take place defined as the innate immune response comprising granulocytes, monocytes, macrophages, innate lymphoid cells, dendritic cells, the complement system, cytokines, chemokines, and acute phase proteins. Because this innate immune reaction has to occur within minutes, it is based on broadly specific pathogen receptors which recognize common structural features present on a variety of pathogens. However, this first line of defense is sometimes insufficient to overcome an infection. Higher organisms have therefore developed an adaptive immune system providing a highly specific defense against invaders, which the innate immune system fails to clear. Adaptive immune responses rely on immune cells featuring antigen receptors and develop within days in response to an infection. These receptor-bearing adaptive immune cells are retained after the pathogens are destroyed and form an immunological memory allowing fast detection and elimination of pathogens by memory lymphocytes upon a second encounter with the same pathogen [1, 2].

### a) The innate immune system

The initial adaptive immune response can take up to 4 to 7 days. Therefore the innate immune response plays an essential role in restraining rapid pathogen growth during this time.

Microorganisms such as bacteria able to cross our epithelial barriers are immediately sensed by phagocytic macrophages present in almost all tissues and able to mount an innate immune response. They express pattern-recognition receptors (PRRs) able to bind to a broad range of bacterial surface constituents triggering phagocytosis [3] and secrete important messenger molecules such as cytokines and chemokines, thus enabling the communication between cells and attracting other immune cells to the site of infections. This is the case for neutrophils and monocytes migrating from the blood stream into infected tissues. Neutrophils are a major type of innate cells observed during an infection, they express in analogy to macrophages, PRRs, and are able to engulf and destroy a variety of microorganisms. The released cytokines and chemokines initiate a state of inflammation in the infected tissue. Inflammation is characterized by an increased permeability of surrounding blood vessels, facilitating immune cell infiltration. In an immature state, dendritic cells (DCs) are also able to engulf pathogens but after maturation they function as specialized antigen presenting cells (APCs). This process will be further described below.

The action of phagocytic cells is aided by the complement system which activates a cascade of proteolytic reactions on the surface of microorganism. The pathogens are thereby coated with fragments of complement components, which can be recognized by phagocytic receptors. At the same time other proteolytic fragments remain soluble and further promote the inflammatory state.

Eosinophils are another cell type of the innate immune system containing cytosolic granules which, upon activation, release molecules such as reactive oxygen species leading to cell death [4]. Basophils and mast cells play an essential role in allergies due to the expression of high affinity receptors for IgE on their surface [5, 6].

Importantly, innate immunity is not only based on phagocytosis of intracellular microorganisms because some pathogens can also exist outside the host cells. Natural killer (NK) cells have the ability to destroy infected and/or malignant cells using two mechanisms: The first relies on binding of their surface Fc receptors to immunoglobulin (Ig) G coated-target cells followed by the release of cytotoxic granules onto the infected cell, a process which is known as antibody-dependent cellular cytotoxicity (ADCC). The second mechanism is based on the discrimination of normal cells from cells that have downregulated for example major histocompatibility complex (MHC) class I molecules as a result of a virus infection [7, 8]. Innate lymphoid cells (ILCs) were recently identified as members of the lymphoid lineage. ILCs do not express surface markers associated with other immune cell lineages and do not respond in an antigen-specific manner. Instead, they play important functions in innate immune responses and in the regulation of homeostasis and inflammation. They are subdivided into three groups according to their cytokine profile: ILC1 (comprising also NK cells), ILC2, and ILC3 releasing type 1, type 2 and T helper (Th) 17 cell-associated cytokines (see below chapter on effector T cells for a more detailed description), respectively [9].

b) The adaptive immune system

The innate immune system is not only involved in the rapid elimination of pathogens but it is also essential for the activation of adaptive immunity in order to develop specific and long-lasting immune responses. In analogy to macrophages and neutrophils, immature DCs can bind to bacterial surface components referred as pathogen-associated molecular patterns (PAMPs) through PRRs and Toll-like receptors (TLRs) triggering their maturation into APCs. Upon activation, DCs enter the lymphatic system and migrate to the nearby draining lymph nodes. After uptake of pathogen-derived antigens at the site of infection, expression levels of

MHC-I, MHC-II and co-stimulatory molecules are up-regulated allowing antigen presentation and priming of antigen-specific T cells through engagement with their respective antigen receptors and co-stimulation (co-stimulatory signals 1 and 2 described below). Additionally, DCs also secrete pro-inflammatory cytokines providing essential signals for the activation of adaptive immune cells, also called lymphocytes. Taken together, DCs are the most important type of APCs bridging innate and adaptive immunity [10].

We can subdivide lymphocytes in two categories, B and T lymphocytes. They both develop from lymphoid progenitor cells in the bone marrow. B cells mature in the bone marrow while T cells migrate to the thymus at an early stage. The specific and diverse production of antigen receptors in both cell types is the result of random recombination of four DNA fragments: variable (V), diversity (D), joining (J) and constant (C) regions by a set of enzymes containing the products of the recombination activating gene 1 (RAG1) and RAG2 [11]. T lymphocytes feature either of two forms of membrane-bound T cell receptors (TCR): TCRα/β or TCRγ/δ chains. The TCR forms a complex with the cluster of differentiation 3 (CD3) protein. The B cell receptor (BCR) is a form of membrane-bound monoclonal immunoglobulin; it binds the antigen and can internalize it playing the role of an APC. Even though gene rearrangement is similar for T and B cell receptors, they bind to antigens in a different manner. The TCR can only bind linear peptides associated with MHC-I or II, which have been previously processed by proteasomes within the APC. By contrast, B cells can bind intact antigens either in their soluble form or presented by APCs. The interplay of innate and adaptive immune cells via different cytokines, co-stimulatory molecules and antigen receptors is illustrated in Figure 1 with the example of some Th cells subsets. A similar cross-talk also exists for cytotoxic T cells and B cells.

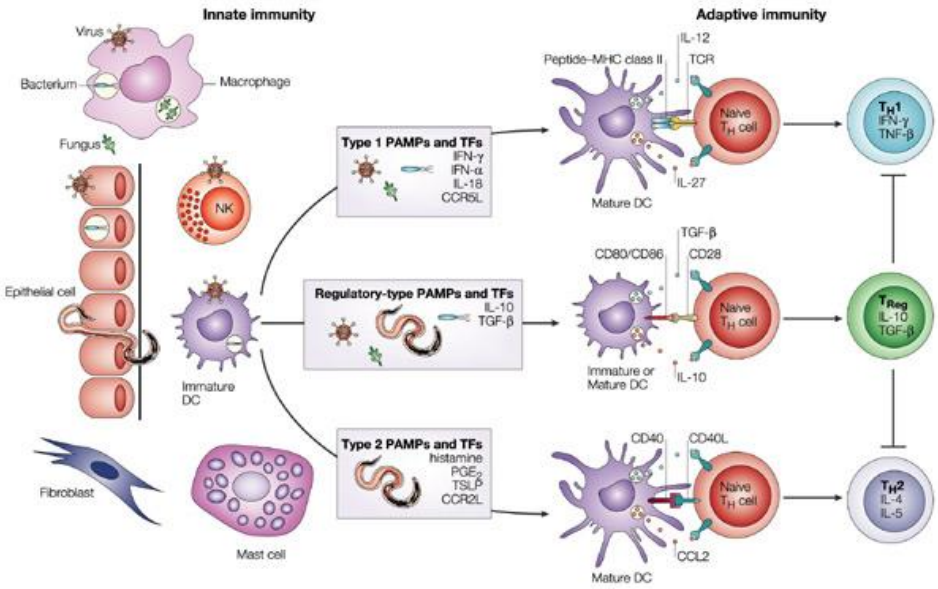


**Figure 1 DCs: Bridging innate and adaptive immunity.** Shown are cells of the innate immune system, including macrophages, mast cells, NK cells and dendritic cells (DC). T helper cells are shown as representatives of adaptive immune cells. Immature DC can be activated by pathogen-associated molecular patterns (PAMPs) or tissues factors (TF) to mature and activate naïve T cells. Adapted from [12].

The random nature of the TCR repertoire requires a tight regulation of the T cell maturation process to remove those cells bearing a TCR specific for an endogenous peptides. This maturation process occurs in several selection steps, termed positive and negative selection, which ensure that TCRs will only recognize a complex formed by a foreign peptide seated within the groove of an MHC molecule [13, 14]. All T cells binding to self-MHC are positively selected in the cortex of the thymus and pass into the cortico-medullary junction where the negative selection of self-reactive T cells occurs. The process of T cell selection generates self-tolerant T cells able to bind foreign antigens presented on self-MHC molecules [15, 16].

Likewise, B lymphocytes will go through the process of central and peripheral tolerance in the bone marrow and in the periphery, which implicates that autoreactive B cells are eliminated via clonal deletion or B cell receptor editing. A new antibody repertoire is generated through somatic hypermutation when a B cell encounters an antigen, and only B cells binding with high affinity survive and become memory B cells [17].

c) Antigen recognition by T cells

The recognition of an antigen by the TCR is different for $CD4^+$ and $CD8^+$ T cells. $CD4^+$ T cells exclusively recognize antigens presented in the context of an MHC-II molecule. This remains important since MHC-II molecules are only expressed by APCs including DCs, B cells and macrophages, able to engulf, digest and present peptides of exogenous pathogens. On the other hand, $CD8^+$ T cells only recognize antigens presented on MHC-I. In this case, the peptide antigens originate from intracellular proteins (such as a tumor antigens) processed via intracellular pathways. The type of MHC molecules presenting the antigen therefore determines different T cell effector functions. Since all nucleated cells express MHC-I on their surface, any cell presenting foreign or mutated peptides can trigger the cytotoxic activity of $CD8^+$ T cells. In contrast, $CD4^+$ T cell activation by APCs leads to cytokine production, subdividing them into specific subtypes depending on the cytokine microenvironment. In order to induce T cell activation, two signals are required: First, engagement of the antigen-MHC complex by the TCR which is associated with CD3 molecules that transmit signal 1 into the cell. The second signal is provided by co-stimulatory molecules such as CD80/CD86 on APC via co-stimulatory receptors like CD28 as shown Figure 2 [18]. In the absence of such co-stimulatory signals or in the presence of co-inhibitory signals, T cells will enter into

anergy or apoptosis. Prominent examples of co-inhibitory receptors are programmed death-1 (PD-1) or cytotoxic T-lymphocyte-associated protein 4 (CTLA-4).

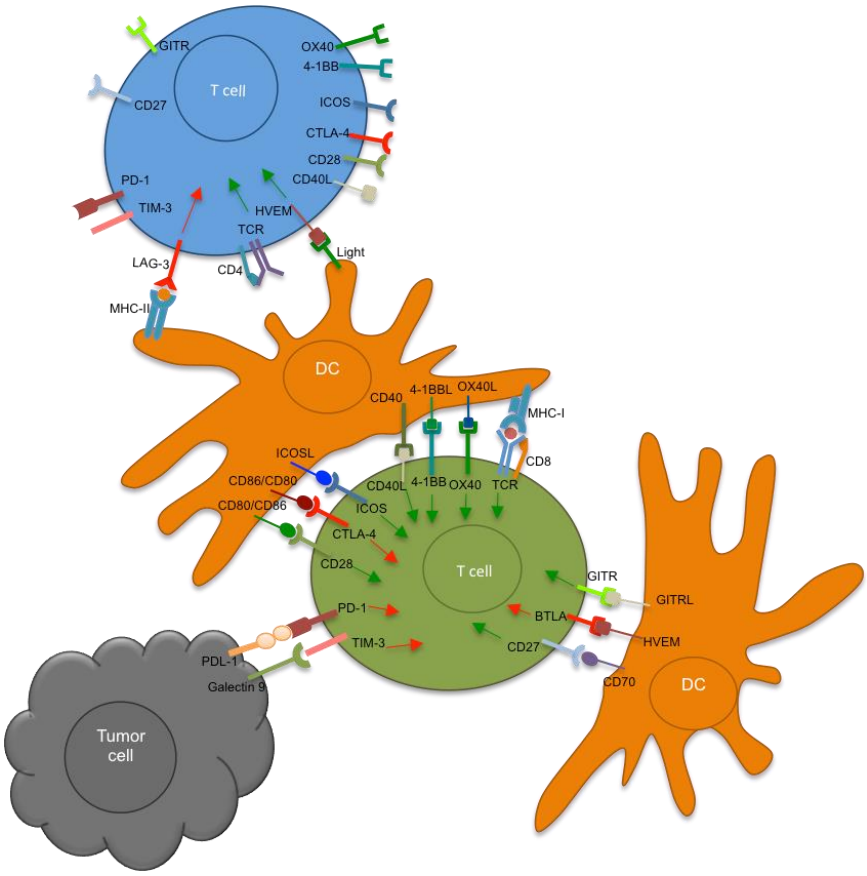


**Figure 2. Co-stimulatory and co-inhibitory receptors on T cells.** Upon interaction of the ligands present on APCs or tumor cells with their corresponding receptors on T cells, either a co-stimulatory (green arrows) or co-inhibitory (red arrows) signal is provided. Adapted from [19].

d) Effector T cells

Two main types of effector T cells have been characterized, including $CD4^+$ T helper (Th) cells and $CD8^+$ cytotoxic T (Tc) cells. As mentioned above, Th cells are subdivided by the pattern of cytokine production driving expression of specific transcription factors. Th 1 lymphocytes are essential in the cellular immune response and in host defense mechanisms to

kill intracellular pathogens. Within the Th 1 cytokines, interleukin 2 (IL-2) plays an essential role in mediating T cell proliferation [20]. Interferon-γ (IFN-γ) is also essential in activating macrophages and stimulates undifferentiated Th 0 cells to become Th 1 cells, while inhibiting Th 2 differentiation. Following this line, activated APCs will produce IL-12, a cytokine promoting the survival and growth of Th 1 lymphocytes. Instead, Th 2 cells mediate the activation and maintenance of the humoral response against extracellular pathogens. Within the Th 2 cytokines, IL-4 is essential in favoring antibody production by the induction of class-switch recombination in B cells and promoting a positive feedback loop to increase Th 2 differentiation. IL-6 mediates B cell maturation into plasma cells and plays a critical role in inflammation and autoimmunity, while IL-5 promotes the generation and proliferation of eosinophils [21]. Other Th immune subsets have been defined as IL-17 expressing T cells (Th 17) promoting neutrophil recruitment and activation. Thus, Th 17 cells are important for the elimination of extracellular bacteria [22]. IL-9 expressing Th 9 cells which play an important role in asthma and IgE class switch recombination have been identified [23, 24]. Follicular helper T cells (T fh) are located in the B cell follicles of secondary lymphoid organs and are involved in B cell antigen presentation and their subsequent maturation in the germinal centers [25]. Forkhead box $P3^+$ (Fox P3) $CD25^+$ $CD4^+$ regulatory T cells (Treg cells) are critical for the maintenance of immune cell homeostasis by producing immunosuppressive ligands and cytokines. As explained before, Tcs are the key effector T cell type for the elimination of infected or abnormal cells. They bind to their specific peptide-MHC complex and kill the target cells by different pathways:

- Perforins released from cytotoxic granules bind to the target cell's membrane and form pores through which pro-apoptotic proteases (granzymes) can enter the target cell.
- Fas ligand (FasL) expressed on the Tc's surface will bind to its receptor Fas expressed on target cells [26].

Both pathways will lead to activation of apoptotic mediators known as caspases [27]. Moreover, Tc produce cytokines such as tumor necrosis factor (TNF), lymphotoxins and IFN-γ. Besides its role in the activation of macrophages [28], IFN-γ is also known for its ability to render adjacent cells resistant to infection and to upregulate the expression of MHC-I molecules and other proteins involved in peptide processing and loading onto MHC-I molecules.

e) <u>B cell development and antibodies</u>

B cell development starts in the bone marrow through the pro-B-cell, pre-B cell and immature B cell stages ($IgM^+$ B cell). Bone marrow stromal cells provide secreted and cell surface factors promoting B cell maturation resulting in antigen-specific cells expressing a functional BCR repertoire, the diversity of which is ensured by the VDJ recombination process as previously described. At this immature stage, self-reactive B cells undergo receptor editing and clonal deletion. Non-self-reactive immature B cells will migrate from the bone marrow to the secondary lymphoid organs (spleen or lymph nodes) where they undergo maturation and become $IgM^{low}$ $IgD^{high}$ B cells. Some cells are driven to become marginal zone B cells, located in the interface between the circulation and lymphoid tissue and able to provide fast responses mainly against blood-borne antigens [29]. B cells can interact with two kinds of antigens: thymus-dependent (TD) and thymus-independent (TI) antigens. In the case of TI

antigens, B cell activation occurs without involvement of Th cells. Co-stimulation is mainly provided by PRR signaling such as TLRs. B cells activated by TI antigens proliferate in the secondary lymphoid organs and differentiate into short-lived plasmablasts providing a fast but weak antibody response. In the case of TD antigens, most of mature B cells will be activated in the B cell follicles (crucial structures for T and B cell interaction) upon antigen binding. B cells will bind and engulf the antigen by BCR-mediated endocytosis, degrade and present to T fh via their MHC-II molecules. T fh are then activated and provide co-stimulatory signals and cytokines essential for B cell activation such as CD40 ligand, IL-21, IL-4 and IL-6 [30]. After activation, some B cells can differentiate into short-lived plasmablasts providing an immediate but weak immune reaction through the secretion of IgM antibodies. Most of the activated B cells will form a germinal center where they will further expand while somatic hypermutation occurs. This step in B cell development is crucial because the introduction of additional mutations within the genes of the antigen-binding domains leads to affinity maturation of the BCR or to apoptosis in the case of disadvantageous mutations. Further selection, isotope class switching and differentiation will take place upon encounter of T fh and follicular dendritic cells resulting in the generation of memory and plasma cell precursors (plasmablasts) [31]. The final stages of differentiation into antibody-secreting plasma cells occur outside of the germinal center. Plasmablasts express high levels of surface Ig which can still switch their antibody isotype. By contrast, fully differentiated plasma cells have very low levels of surface Ig and class-switch recombination is considered complete in these cells. The generated memory B cells and plasma cells can migrate back to the bone marrow where they are responsible for long-term production of antibodies, which are secreted into the bloodstream (Figure 3).

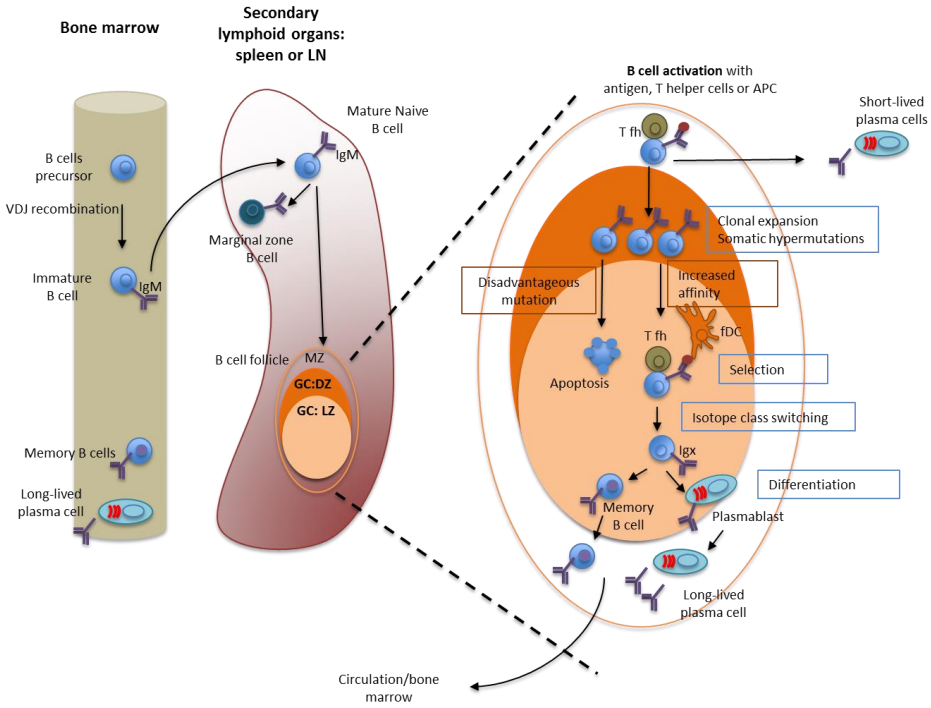


**Figure 3. B cell maturation.** B cells are generated in the bone marrow and migrate to secondary lymphoid organs (spleen or lymph node). Some B cells will become marginal zone B cells but most of them will mature and differentiate in germinal centers (GC) upon antigen encounter. In the dark zone (DZ) of the GC, B cells will expand and BCR diversification takes place through somatic hypermutations. In the light zone (LZ) B cells undergo further selection resulting in isotype class switching and differentiation into memory B cells and plasmablasts. Antibody-producing plasma cells and memory B cells can home back to the bone marrow. T fh: follicular helper T cells; fDC: follicular dendritic cells. Adapted from [29, 31].

The antibodies secreted by plasma cells are Y-shaped proteins, referred to as immunoglobulins (Ig), composed of two heavy and two light chains [32, 33]. Each of these chains has a variable region, containing the antigen binding site, and a constant region (Figure 4). The constant region determines the effector mechanism used to destroy the pathogen. The variability of the amino acid sequences of the variable region is not random but precisely

organized. The greatest variability is located in the areas called hypervariable regions (HV) or complementarity-determining regions (CDRs) within the antigen-binding site.

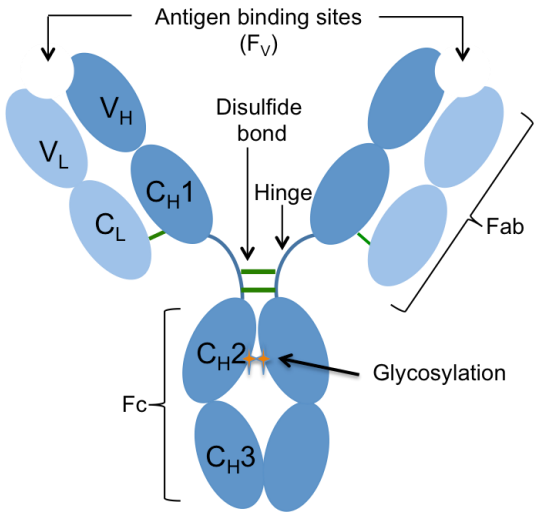


**Figure 4. Structure of an Immunoglobulin (Ig).** An Ig is composed by two identical light (L) and heavy (H) chains; each of them having a constant domain (C) and a variable domain (V). The heavy chain is composed of three constant domains ($C_H1$, $C_H2$ and $C_H3$). Disulfide bonds link the two heavy chains in the hinge region and the light chains to the heavy chain. The antigen-binding part (Fv) of the Ig is formed by pairing VL and VH domains which bring together their CDRs resulting in the antibody's antigen-specificity. The interaction interface with effector molecules (such as C1 complex for the complement system or Fc receptors in immune cells) is located in the Fc part of the Ig. Adapted from [32].

Humans express five different antibody isotypes or classes: IgG, IgM, IgD, IgA and IgE. They differ in their biochemical and serological properties - such as charge, size and solubility - and by their respective tissue distribution and function. Antibodies have the capacity to either neutralize the antigen by binding and inhibiting its function or recruit immune cells such as NK cells, macrophages and neutrophils expressing Fc receptors for IgG (FcγR) that are able to engulf and destroy the bound pathogen or tumor cell through ADCC or phagocytosis. Upon phagocytosis, DCs and other APCs can present the peptide antigens on

MHC-II for the activation of $CD4^+$ T cells. Cross-presentation of peptides derived from lysosomal degradation can also be transferred intracellularly onto MHC-I thereby enabling the priming of cytotoxic $CD8^+$ cells (Figure 5) [34]. This process is important for the detection of tumor antigens and of viruses, which do not infect APCs. IgG-coated antigens can recruit and initiate the complement cascade leading to the destruction of the pathogen, a process known as complement-dependent cytotoxicity (CDC). These antibody-mediated immune reactions are summarized in Figure 5.

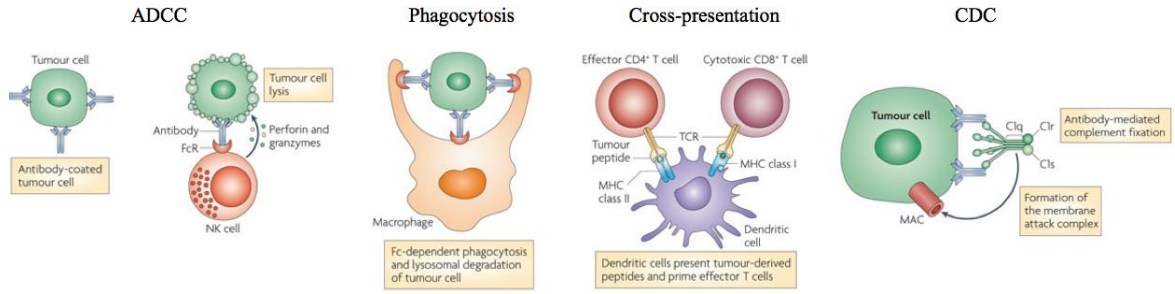


**Figure 5. Antibody-mediated immune reactions.** Antibody-mediated destruction of tumor cells depends on the binding of IgG coated with antigens or malignant cells to FcγR expressed on NK cells, macrophages and neutrophils (ADCC and phagocytosis processes). Lysosomal degradation of cells leads to the release of peptides which can be loaded onto MHC-II and activate $CD4^+$ T cells. DCs can also cross-present peptide antigens on MHC-I molecules and prime $CD8^+$ T cells. IgG-coated tumor cells can recruit C1q (a complement component), initiating the complement cascade and leading to the destruction of the tumor cell by the membrane attack complex (MAC). ADCC: antibody-dependent cell cytotoxicity, CDC: complement-dependent cytotoxicity. Adapted from [33].

f) Antibodies and pharmaceutical applications

In 1975, Köhler and Milstein described the production of immortalized B cells, termed hybridomas, by the fusion of B lymphoblasts with myeloma cells able to consistently produce monoclonal antibodies (mAbs) against defined antigens [35, 36]. Briefly, a host animal (often rodents) is immunized two to three times with the target antigen mixed with an adjuvant in order to properly activate the immune system and generate memory B cells. The antigen is recognized as 'foreign' by the host immune system. During this process B cell activation takes place and differentiation into plasmablasts ensures the production of antigen-specific antibodies. The spleen of the host is then used as the source of B cells and is fused with myeloma cells leading to the formation of hybridomas, which can be selected in a hypoxanthine, aminopterin, thymidine (HAT) media. The initial collection of hybridoma cells is a heterogeneous pool of polyclonal antibodies. A screening and dilution process is therefore needed in order to select for a hybridoma producing the monoclonal antibody of interest. Despite of the elegance of this approach, some limitations regarding immunogenicity have to be overcome for the development of such antibodies as pharmaceutical drugs. Indeed, the administration of a therapeutic antibody produced from rodents leads to the production of anti-drug antibodies in humans [37]. Different strategies were pursued in order to decrease immunogenicity of rodent-derived antibodies. For example, chimeric antibodies combine the variable antigen-binding domains from rodents with a human constant domains [38]. Shortly after, new engineering strategies were developed to further humanize the antibodies by engrafting the CDRs of the parental antibody into the sequence of a fully human antibody [39]. After the introduction of such CDR-grafted, also called humanized mAbs, new technologies have been developed in order to produce fully human mAbs. The generation of

human antibody libraries enabled the in vitro selection of monoclonal antibodies by for example phage or yeast display [40-42]. The repertoire expressed by these phage display libraries exceeding the natural B cell repertoire in terms of diversity and affinity maturation can be achieved *in vitro* by means of random PCR-based mutagenesis. In 1994, genetically engineered mice expressing fully human antibody repertoires were reported [43].

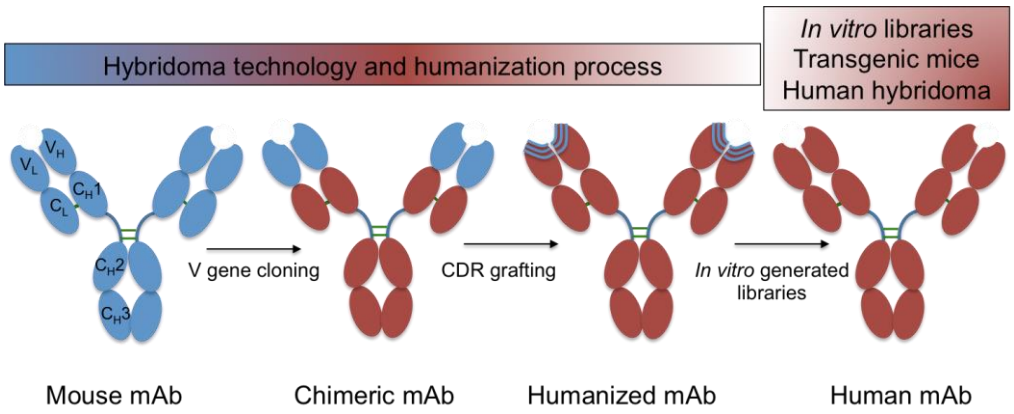


**Figure 6. Engineering of monoclonal antibodies.** The first antibodies were generated using the hybridoma technology obtaining a full mouse monoclonal antibody (mAb; in blue). The cloning of mouse variable genes into human (in red) constant-region results in chimeric antibodies with reduced immunogenicity, which is even lower for CDR-grafted humanized antibodies and virtually inexistent when fully human antibodies are used. Adapted from [32].

The technological advances in antibody generation platforms are reflected by the more than 30 mAbs, which have been approved during the last 30 years to treat various diseases. 'Blockbuster' antibodies such as rituximab, infliximab, trastuzumab and cetuximab directed against CD20, TNF, human epidermal growth factor receptor 2 (HER2) and epidermal growth factor receptor (EGFR), respectively, showed the commercial success of antibodies by generating more than one billion revenue annually. Antibody function and production have been further developed, leading to a second and third generation of molecules such as bispecific antibodies allowing simultaneous binding to two different antigens. Furthermore,

highly potent cytotoxic agents have been conjugated to cancer-directed mAbs resulting in antibody-drug conjugates [44]. Moreover, omitting the Fc part and its effector functions might be an alternative when Fc interactions with immune cells lead to toxic effects (e.g. cytokine release syndrome). Additionally, having a reduced molecular size facilitates the penetration into solid tumors while a shorter half-life may ameliorate systemic target-dependent toxicity. These insights led to the development of different genetically engineered antibody fragments such as single chain variable fragments (scFv), diabodies or minibodies (Figure 7). The advantage of bivalent diabodies and minibodies is that the avidity of a full mAb is conserved while scFv molecules possess only one binding site. Antibody fragments can also be obtained by enzymatic digestion using papain or pepsin of a full IgG, resulting in Fab fragments (heterodimers of VH-CH1 and VL-CL) and their bivalent equivalents $F(ab')_2$ respectively, where the hinge region remains intact to the CH1 domains connected via disulfide bonds (Figure 7).

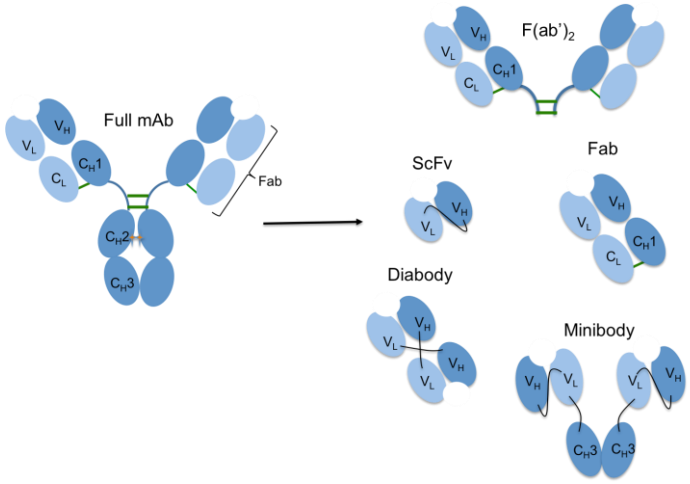


**Figure 7. Antibody-derived fragments.** Using enzymatic digestion or genetic engineering antibody fragments can be generated avoiding their Fc effector functions. These include monovalent and bivalent antibody fragments, whereby bivalent formats predominate in therapeutic applications. Adapted from [45].

2. Interleukin-2

Cytokines are secreted or membrane-bound proteins such as interleukins, interferons, mesenchymal growth factors, chemokines and tumor necrosis factor family members. These particular proteins regulate the growth, differentiation and activation of immune cells by allowing the cells to communicate with each other. Cytokines can have pro-inflammatory (as in the case of IL-1, TNF, and IFN-γ) or anti-inflammatory effects (as for IL-4, IL-13, and IFN-α). Cytokine receptors can be homodimeric, heterodimeric or their ligands can act as trimers assembled then in homotrimeric structures (TNF receptor family). A subunit of the heterodimeric receptors can be shared by different cytokines. This is the case of the common gamma chain ($\gamma_c$) cytokines, comprising IL-2, IL-4, IL-7, IL-9, IL-15 and IL-21. These cytokines bind to receptors comprising the $\gamma_c$ subunit and unique cytokine-specific subunits [46]. Upon binding to their receptors, one or several signal pathways will be activated (Figure 8). Cytokines are essential drivers in the development of a variety of diseases such as rheumatoid arthritis and psoriasis. In the last years many efforts have been pursued to develop antibodies to block pro-inflammatory cytokines or their receptors, such as TNF, IL-6, and IL-17A [47-49]. Moreover, cytokines have also been developed as recombinant proteins in order to use their immune stimulatory activity and treat diseases such as metastatic melanoma, metastatic renal cell carcinoma, chronic granulomatous disease, soft tissue sarcoma, and multiple sclerosis, where cytokines, including IL-2, IFN-γ, TNF-α, and IFN-β, have shown some therapeutic promise [50-53]. The next chapters focus on IL-2, and its relevance for the treatment of advanced cancer.

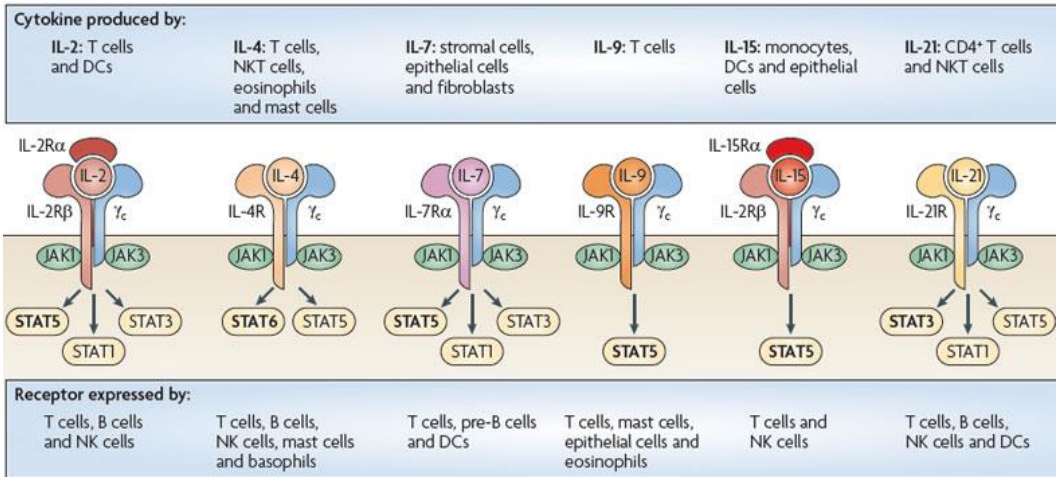


**Figure 8. Common gamma chain cytokines and their receptors.** Shown are receptors for IL-2, IL-4, IL-7, IL-9, IL-15 and IL-21. The common gamma chain subunit will active Janus kinase 3 (JAK3), while the cytokine-specific subunit will activate JAK1. The main signal transducer and activator of transcription (STAT) proteins that are activated by their respective cytokine receptors are shown in bold. Adapted from [46].

a) Biology of IL-2

Parts of this chapter have been adapted from previously published articles [54, 55].

Interleukin-2 (IL-2) is a 15.5-16 kDa four-α-helix bundle cytokine. As a member of the $\gamma_c$ cytokines, it binds to a monomeric (IL-2Rα or CD25), dimeric (IL-2Rβ or CD122 and $\gamma_c$ or CD132) or trimeric receptors (CD25, CD122 and $\gamma_c$), which initiate different downstream signaling cascades [56, 57]. A crystal structure, showing the special organization of IL-2 with its heterotrimeric receptor is shown in Figure 9.

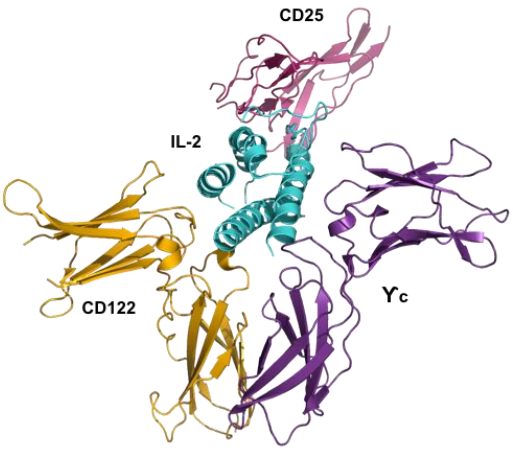


**Figure 9. IL-2/IL-2 receptor complex.** Shown is a ribbon representation of IL-2 (cyan) bound to its receptor subunits CD25 (pink), CD122 (orange) and $\gamma_c$ (purple). Accession code PDB: 2B5I. From [55].

CD25 is not involved in IL-2 signaling but increases the affinity of IL-2 towards CD122 and $\gamma_c$ by about 10 to 100 fold. Signaling is mediated by CD122 and $\gamma_c$. We can therefore discriminate between low-affinity (Kd~$10^{-9}$ M) dimeric and high-affinity (Kd~$10^{-11}$ M) trimeric IL-2 receptors [58]. Dimeric IL-2Rs are found at very high levels on antigen-experienced (memory) $CD8^+$ T cells and NK cells. Intermediate levels of the dimeric receptor can also be found on naïve $CD8^+$ T and memory $CD4^+$ T cells and at lower levels on naive $CD4^+$ T cells [56]. Furthermore, activated B cells express the trimeric IL-2Rs [59]. ILCs and some non-immune cells, such as endothelial cells, have been reported to express low levels of the trimeric IL-2R [60, 61]. Interestingly, DCs have been reported to express CD25 and to use it to present IL-2 *in trans* to T cells expressing dimeric IL-2R [62]. However, the low affinity of CD25 to IL-2 questions the biological relevance of such mechanism. When IL-2 binds to an IL-2R, the cytokine and receptor subunits are internalized. While IL-2, CD122 and $\gamma_c$ are degraded, CD25 can be recycled to the cell surface [57]. Upon binding, a signaling pathway is initiated involving Janus kinase (JAK)-signal transducer and activator of transcription

(STAT), phosphoinositide 3-kinase (PI3K)-AKT and mitogen-activated protein kinase (MAPK) (Figure 10) [55, 56, 63].

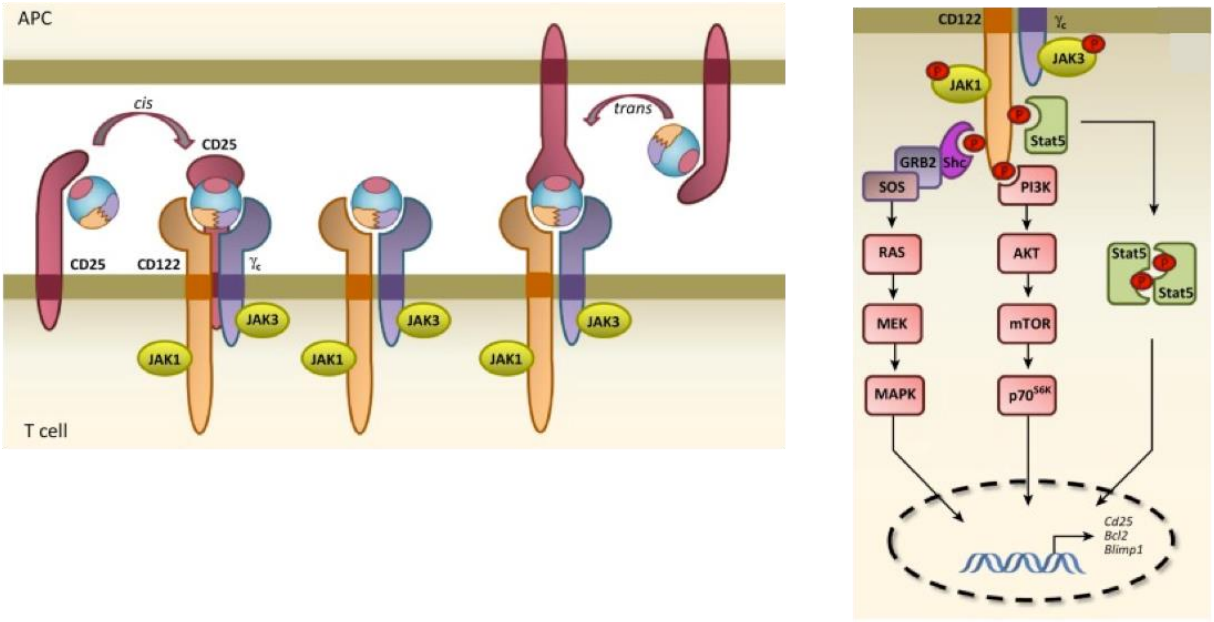


**Figure 10. IL-2 receptor (IL-2R) binding and signaling.** Shown are IL-2 interactions with CD25, CD122 and $\gamma_c$ receptor subunits (left panel). When IL-2 binds to the dimeric IL-2R (right panel) heterodimerization of the cytoplasmic tails initiates the activation and phosphorylation of Janus kinase 1 (JAK1) and JAK3 leading to subsequent recruitment, phosphorylation and activation of the adaptor protein Shc, phosphoinositide 3-kinase and signal transducer and activator of transcription 5 (STAT5) pathways whose products undergo nuclear translocation and bind to genes responsible for cell activation, differentiation and proliferation. Adapted from [55].

IL-2 is continuously produced by resting $CD4^+$ T cells. Upon immune activation, cells such as NK, NKT, DCs and mast cells are also able to produce IL-2 but at levels that are lower compared to the amount produced by activated $CD4^+$ and $CD8^+$ T cells [63]. These activated T cells secrete IL-2 which can lead to autocrine and paracrine signaling events. The production of IL-2 is also regulated by a negative feedback loop depending on the activation levels of STAT-5 and the transcription factor B-lymphocytes-induced maturation protein 1

(Blimp1), leading to the suppression of the *IL-2* gene (Figure 10) [63]. IL-2 production is further regulated at a cellular level involving an equilibrium between IL-2-producing $CD4^+$ T cells and IL-2-consuming regulatory T (Treg) cells. Treg cells are unable to secrete IL-2, while expressing the high-affinity trimeric IL-2R, and they maintain peripheral immune tolerance by dampening effector T cells [64]. IL-2 is crucial for the homeostatic levels of thymus-derived Treg cells [65, 66], while 'induced' Treg cells (peripherally derived) are able to re-differentiate into T h cells and produce IL-2 [67]. Upon IL-2 binding and subsequent signaling on Treg cells, CD25 and FoxP3 are further upregulated promoting the suppressive capacity of Treg cells [56]. The strength and duration of IL-2 signals control $CD4^+$ and $CD8^+$ T cell fates. Upon TCR stimulation, IL-2 production is increased leading to terminal differentiation (followed by CD25 upregulation) of both $CD4^+$ and $CD8^+$ T cell subsets into short-lived effector T cells. Lower IL-2 signals promote $CD4^+$ T cell differentiation into long-lived T fh cells or central memory T cells (Figure 11) [56].

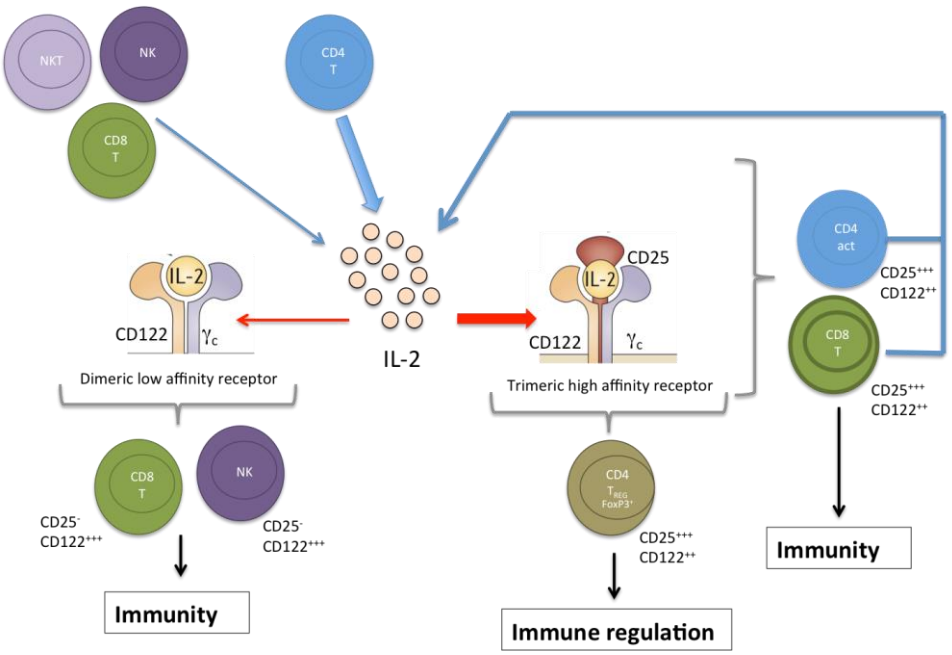


**Figure 11. IL-2 production and regulatory functions.** IL-2 is secreted (as indicated by blue arrows) mainly by $CD4^+$ T cells and to a lower extent by $CD8^+$ T, natural killer (NK), and NKT cells. IL-2 can bind to and be consumed (red arrows) by cells expressing the dimeric low-affinity IL-2 receptor, such as cytotoxic $CD8^+$ T cells and NK cells, or the trimeric high-affinity receptor present at steady-state conditions on $CD4^+$ $Foxp3^+$ regulatory T ($T_{reg}$) cells and, upon antigen-mediated stimulation, on activated $CD4^+$ ($CD4^+_{act}$) and $CD8^+$ ($CD8^+_{act}$) T cells.

b) <u>Clinical relevance and applications of IL-2</u>

As previously described, IL-2 is essential for the homeostasis and suppressive activity of Treg cells and for efficient stimulation of cytotoxic T cells. In order to maintain immune tolerance and immunity, a balance between these subsets has to be in place. The consequences of IL-2 and CD25 deficiencies are well reflected in mice [63] and humans [68, 69] developing autoimmune and/or inflammatory reactions with a higher susceptibility for certain infections. A complete lack of IL-2 or CD25 is rare in humans but partial deficiencies have been linked to several pathologies such as type 1diabetes, multiple sclerosis and rheumatoid arthritis [70,

71]. This resulted in the implementation of clinical trials using low-dose IL-2 in order to promote Treg cell function. Efforts to treat type 1 diabetes [72, 73], autoimmune vasculitis [74] and chronic graft-versus-host-disease [56, 75] led in a subset of patients to clinical improvements [76]. Moreover, the technical difficulties encountered with the isolation, expansion and reinfusion of Treg cells favors IL-2 low-dose administration (500 000-3 000 000 international units (IU) or 15 000-30 000 IU once daily in humans and mice, respectively). On the other hand, administration of IL-2 at higher doses (600 000-720 000 IU/Kg body weight three times daily for up to 14 doses per cycle in humans or 100 000 IU or higher once or twice daily in mice) stimulate cells expressing the dimeric IL-2R such as $CD8^+$ T cells and NK cells once Treg cells have been saturated with IL-2. Such high-dose IL-2 immunotherapy is used for the treatment of certain metastatic cancers [77]. After successful pre-clinical studies in various murine tumor models, high-dose IL-2 has been approved by the Food and Drug Administration (FDA) in humans for the treatment of metastatic renal cell carcinoma in 1992 and metastatic melanoma in 1998. This led to a 15-19% objective clinical response (with 7-9% complete response) in patients [78].

## 3. Cancer immunotherapy

### a) A brief introduction to cancer

Healthy tissues are composed of cells that control the production and release of growth signals in order to maintain a homeostatic level and ensure tissue composition and function. Some cells, by deregulating those homeostatic signals can start a proliferative program resulting in uncontrolled cell growth. The interaction between external carcinogenic agents such as ultraviolet, ionizing radiation, chemical carcinogens (e.g. components of tobacco, aflatoxin), or biological carcinogens (e.g. human papillomavirus) with genetic factors drive

this deregulation, resulting in malignant cell growth, which ultimately can lead to the invasion of surrounding tissues by the cancer and metastasize to distant sites. A lot of efforts went into understanding how cancer cells could proliferate in such manner. In 2000, Hanahan and Weinberg proposed six hallmarks of cancer, including distinctive and complementary capabilities enabling tumor growth and metastatic formation [79]. Cancer cells do not need growth signals in order to proliferate and they become insensitive to extrinsic and/or intrinsic processes preventing their own division. Their survival is also linked to their capacity to evade programmed cell death, their limitless replicative potential and their sustained angiogenesis (blood vessels formation), allowing them to spread and invade surrounding tissues. The complexity and diversity of solid tumors and haematologic malignancies has led to an extended set of ten cancer hallmarks in 2010 by the same authors (Figure 12) [80]. A better understanding of the biology of tumor development has led to the generation of therapeutics targeting pathways of almost all hallmarks of cancer.

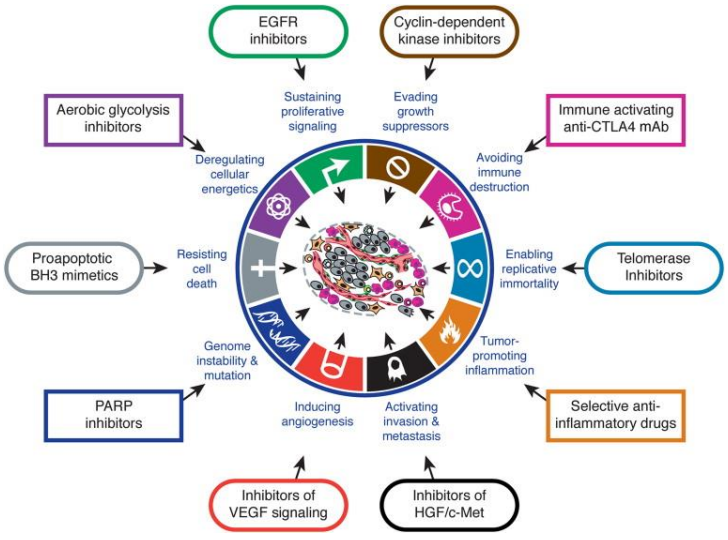


**Figure 12. The updated hallmarks of cancer and corresponding therapeutic approaches.** From [80].

b) Anti-cancer immunity

The term ‘cancer immunotherapy’ appeared for the first time in 1891, when William Coley began to study intratumoral injections of live inactivated *Streptococcus pyogenes* and *Serratia marcescens, later called Coley’s toxins,* and observed complete tumor remission of sarcomas in patients [81]. Assuming that the immune system is able to cause inflammation and destroy pathogens as previously described, the theory of William Coley could be explained by the activation of the immune system through the stimulation of antibacterial phagocytes that could also attack tumor cells. Although a certain efficacy was observed, results were difficult to reproduce and the risk associated with the administration of infectious agents led oncologists to rely on surgery and effective methods such as radiation therapy and chemotherapy. In the early 1900s, Paul Ehrlich suggested that immune cells may hold cancerogenic cells in check but it took over 50 years until the first demonstration of the existence of tumor antigens [82], which can be recognized by immune cells. In the past two decades, extensive efforts were taken to understand how cancer evades the immune system and how this process can be prevented or reversed. This led to studies postulating the cancer immunosurveillance hypothesis where adaptive immunity is thought to prevent cancer progression in healthy hosts. Follow-up studies by Stutman and colleagues did not support this theory, leading to a controversy about the term cancer immunity. The development of immunodeficient mouse models on defined genetic backgrounds gave the basis to further investigate the role of the immune system in cancer development. Mice lacking responsiveness to IFN-γ or components of adaptive immunity developed faster tumors showing the relevance of immune-mediated tumor control [83]. Since then a large number of research studies contributed to the understanding of the steps needed to get an effective anti-

tumor immune response, including the stimulation of innate immune recognition promoting antigen-presentation therefore leading to the generation of protective T cell responses which have the capacity to overcome immunosuppression at the tumor site. DCs have to take up and cross-present antigens derived from tumors. DCs receiving sufficient co-stimulation are then able to migrate to lymph nodes to properly mount an immune response. In a last step, primed Tc and/or NK cells need to migrate to the tumor site where they exert their cytotoxic function and thereby eliminate tumor cells (Figure 13).

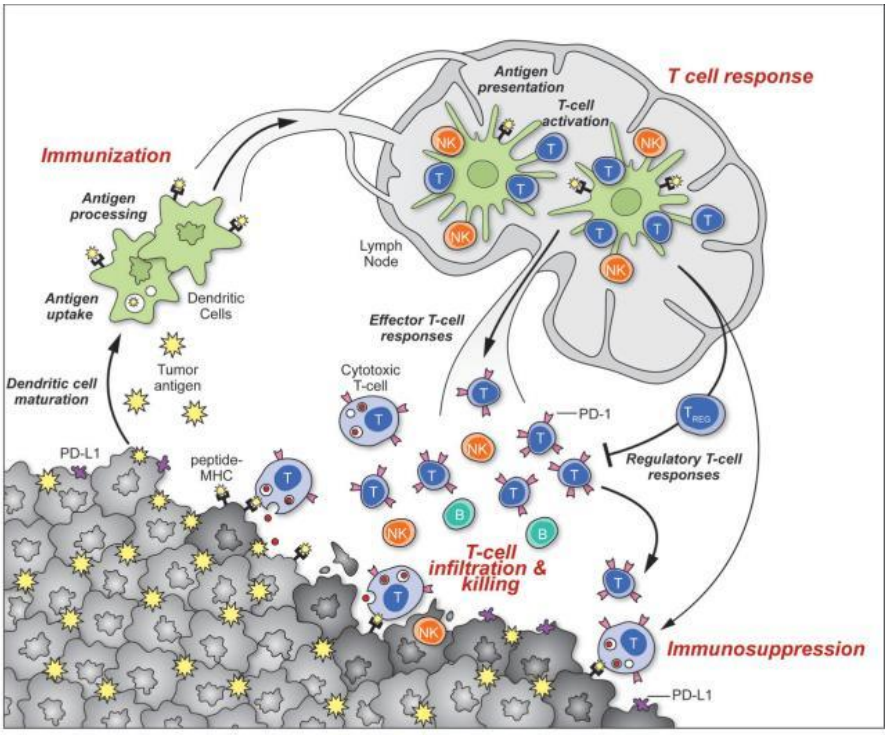


**Figure 13. The generation and regulation of anti-tumor immune responses.** Adapted from [84].

c) Cancer vaccines

In the late 1980s, the capacity to obtain cytotoxic T lymphocytes from patients with melanoma unable to act against normal cells but against cells expressing mutated proteins

allowed the identification of different tumor antigens [85]. Those antigens can be different for a given type of cancer and may result from mutations which occurred during the transformation of normal cells into malignant cells. Other tumor antigens can be products of genes preferentially expressed by cancer cells such as cancer-testis antigens [86-89], differentiation antigens against which peripheral or thymic tolerance has not been completely established, or antigens associated with the tissue where the cancer originates from such as melanocyte-specific antigens [90-92]. Based on these findings therapeutic vaccination strategies were developed, relying on the systemic administration of tumor antigens. However, these therapeutic approaches showed only limited efficacy in the clinics [93]. A possible explanation may be that DC maturation relies on optimal activation through endogenous signals (such as necrotic tumor cells releasing factors), co-stimulatory molecules (such as CD40L) or cytokines. These signals, like TLR ligands or agonistic antibodies activating receptors such as CD40, are also called adjuvants when administered to a patient or animal [94].

When a cancer is of viral origin, such as cervical cancer mainly caused by infection with the human papillomavirus (HPV), a prophylactic vaccine can be used to prevent the formation of HPV-induced malignant cells. The development of therapeutic vaccines has been tested and improved in the last years. The idea behind this approach is the administration of peptides known to be recognized as ‘foreign’ and supposedly expressed by tumor cells, in combination with adjuvants in order to activate DCs that will engulf and present the peptide on MHC-I molecules to then activate Tc cells. One example was the use of peptides derived from the HPV-16 E6 and E7 oncoproteins administered in incomplete Freund’s adjuvant to women with vulvar intraepithelial neoplasia. Tumor regressions in 15 of 19 women were correlating

with the generation $CD8^+$ and $CD4^+$ T cells secreting large amounts of IFN-γ and being specific for the HPV oncoproteins [95]. The property of virus to elucidate strong immune responses is currently exploited in order to develop vaccines where tumor antigens will be encoded by viral vectors [96]. Moreover, a particular interest in developing DC-based vaccines has emerged. The specialized APCs are isolated from cancer patients, *ex vivo* stimulated with peptides and re-infused back to patients [97]. In order to break self-tolerance, the immunogenicity of peptides has to be above a certain threshold as shown by the p53 vaccine leading to only weak T cell response [98]. This is why full length proteins are being investigated as targets for cancer vaccinations [99]. Cancer vaccines represent a powerful tool for tumor immunotherapy but a lot of limitations need to be overcome such as optimal tumor target and adjuvant in order to induce strong anti-tumor T cell responses with the capacity to overcome tumor-induced immune suppression.

d) Adoptive cell therapy

The adoptive transfer of autologous, *in vitro* expanded tumor-infiltrating lymphocytes (TILs), termed adoptive cell therapy (ACT), has shown durable clinical responses in 50% of patients with melanoma [100]. The efforts in T cell engineering opened further perspectives in ACT. One example was the development of chimeric antigen receptor (CAR) T cell therapy, which relies on genetically modified T cells expressing an antigen-binding domain (e.g. a scFv) on their surface which mimics a tumor antigen-specific TCR [101].

e) Antibody therapy of cancer

The use of mAbs for cancer therapy has been successfully developed in the last several years [33]. They can target tumor antigens and kill tumor cells either by induction of apoptosis

[102], the delivery of cytotoxic agents (antibody drug conjugates) or immune-mediated cell killing mechanisms such as ADCC or CDC (see also Figure 5) [103].

As previously discussed, the specificity of T cells for tumor cells is mediated by the interaction of their TCR with an MHC molecule displaying the processed tumor antigen on the cell surface. However, T cell activation also relies on the engagement of co-regulatory receptors expressed on the surface of T cells binding to cognate ligands displayed on APCs or tumor cells. The discovery and study of these co-stimulatory or co-inhibitory receptors provided a number of potential targets for the development of agonist antibodies directed against 4-1BB, OX40, CD27 and CD28. Notably, agonist mAbs directed to CD28 resulted in unexpectedly life-threatening conditions of patients in early clinical trials resulting from rapid release of cytokines by activated T cells [104]. These events have shown the power of our immune system and the necessity to tightly control it. Other approaches, which were far more clinically successful due to better therapeutic windows and side-effect profiles, are targeting immunosuppressive co-inhibitory molecules [105] with antagonist antibodies directed against LAG-3, CTLA-4 [106] and PD-1 [107, 108] (Figure 14).

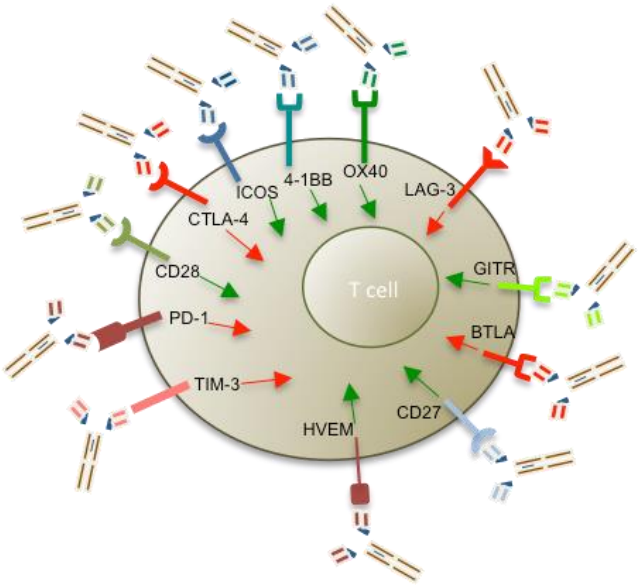


**Figure 14. Activating and inhibitory receptors on T cells.** T cell receptors transmit stimulatory or inhibitory signals upon binding to their ligands, which can be expressed by APCs or tumor cells. Such molecules represent targets for antibody-mediated cancer immunotherapy. Adapted from [84].

The potential of blocking CTLA-4 was first demonstrated in 1996 and provided the basis for the development of two fully human mAbs: ipilimumab and tremelimumab. Clinical trials in patients were successful leading to an increased survival in patients with metastatic melanoma. Side effects related to tissue-specific inflammatory responses were observed in patients, but could be controlled without affecting the efficacy of the therapy [106]. The success of these inhibitory TCR blockers, commonly referred to as immunological check point inhibitors, led to the development of fully human mAbs blocking PD-1. These mAbs, namely nivolumab and pembrolizumab, showed promising responses in patients with melanoma, renal cell carcinoma, non-small-cell lung cancer, and colorectal cancer [107]. It will be important to follow-up the treated patients in order to know whether the responses will be durable and which side effects will come along with the therapy. A summary of antibody therapeutics approved for use in oncology is provided in

| Antibody | Engineering | Isotype | Target | FDA approved indication year |
|---|---|---|---|---|
| Bevacizumab (Avastin®) | Humanized | IgG1 | VEGF-A | Colorectal/lung cancer 2004 |
| Cetuximab (Erbitux®) | Chimeric Murine/Human | IgG1 | EGF receptor (EGFR) | Colorectal cancer 2004 |
| Panitumumab (Vectibix®) | Human | IgG2 | EGFR | Colorectal cancer 2006 |
| Ipilimumab (Yervoy®) | Human | IgG1 | CTLA-4 | Metastatic melanoma 2011 |
| Pembrolizumab (Keytruda®) | Humanized | IgG4 | PD-1 | Metastatic melanoma 2014 |
| Nivolumab (Opdivo®) | Human | IgG4 | PD-1 | Metastatic melanoma 2014 |

Table 2.

| Antibody | Engineering | Isotype | Target | FDA approved indication year |
|---|---|---|---|---|
| Rituximab (Rituxan®) | Chimeric Murine/Human | IgG1 | CD20 | Lymphoma 1997 |
| Trastuzumab (Herceptin®) | Humanized | IgG1 | HER2 | Breast cancer 1998 |
| Alemtuzumab (Campath®) | Humanized | IgG1 | CD52 | Chronic lymphocytic leukemia 2001 |
| Ofatumumab (Arzerra®) | Human | IgG1 | CD20 | Lymphoma 2009 |
| Pertuzumab (Perjeta®) | Humanized | IgG1 | HER2 | Breast cancer 2012 |
| Obinutuzumab (Gazyva®) | Humanized-glycoengineered | IgG1 | HER2 | Breast cancer 2013 |

**Table 1a. Unconjugated monoclonal antibodies approved for the treatment of cancer targeting cancer cells.** Adapted from [33, 109, 110].

| Antibody | Engineering | Isotype | Target | FDA approved indication |
|---|---|---|---|---|

| | | | | year |
|---|---|---|---|---|
| Bevacizumab (Avastin®) | Humanized | IgG1 | VEGF-A | Colorectal/lung cancer 2004 |
| Cetuximab (Erbitux®) | Chimeric Murine/Human | IgG1 | EGF receptor (EGFR) | Colorectal cancer 2004 |
| Panitumumab (Vectibix®) | Human | IgG2 | EGFR | Colorectal cancer 2006 |
| Ipilimumab (Yervoy®) | Human | IgG1 | CTLA-4 | Metastatic melanoma 2011 |
| Pembrolizumab (Keytruda®) | Humanized | IgG4 | PD-1 | Metastatic melanoma 2014 |
| Nivolumab (Opdivo®) | Human | IgG4 | PD-1 | Metastatic melanoma 2014 |

**Table 2b. Unconjugated monoclonal antibodies approved for the treatment of cancer having a different mode of action.** Adapted from [33, 109, 110].

Moreover, the efforts in antibody engineering led to new therapeutic applications. Notably, bispecific molecules targeting tumor antigen and the TCR-associated CD3 have the ability to bring tumor cell and the Tc in close proximity, which enables efficient Tc-mediated tumor cell killing [111]. Other approaches to overcome tumor-induced immunosuppression include targeting immunosuppressive cells such as Treg or myeloid-derived suppressor cells, found at higher counts in the tumor site [112]. These cells release immunosuppressive cytokines such as IL-10, TGF-β, arginase 1 and 2, and nitric oxide synthase 2 (NOS2), which block Tc proliferation and induce apoptosis of these cells.

There are different tumor escape mechanisms to antibody treatment including the heterogeneous level of tumor antigen expression and the biophysical properties of antibodies (such as size and half-life) influencing their ability to access the intratumoral microenvironment. Immune escape mechanism such as ineffective FcγR binding and immune suppression can lead to poor clinical responses [113]. Moreover, the ability of antibodies to

generate T cell responses towards tumor antigens depends on various factors, such as antigen cross-presentation by DCs and immune escape mechanism mediated by Treg cells and myeloid derived suppressor cells (MDSCs) [114].

f) Immunotherapy using cytokines

Various cytokines are produced in the tumor microenvironment and play an essential role during cancer progression or control. The role of some of these molecular messengers in tumor formation and development has been elucidated using immunodeficient mice. For example, IFN-γ inhibits chemical carcinogenesis and lymphoma development [115, 116], granulocyte-macrophage-colony stimulating-factor (GM-CSF) inhibits lymphomas and carcinomas in combination with IFN-γ [117]. By contrast, other pro-inflammatory cytokines such IL-1 can promote tumor invasion and angiogenesis [118]. The study of the cytokine microenvironment has led to their therapeutic use for cancer treatment. Systemic IL-12 has shown strong anti-tumor effect in mice, but clinical trials have been stopped due to toxicity [119]. Recombinant IFN-α has been shown to potentiate the anti-tumor response in various cancers [120] and GM-CSF has proven some benefit in melanoma and prostate cancer [121, 122]. As previously mentioned, IL-2 has been used for treatment of metastatic melanoma and metastatic renal cell carcinoma. Its therapeutic application plays a pivotal role for the treatment of patients with metastatic melanoma resistant to cytotoxic chemotherapy [123]. However, also this treatment is limited by the IL-2-related side effects and the short half-life of the cytokine itself, as IL-2 is rapidly cleared via the kidneys (3 to 5 minutes in mice and 7 to 10 minutes in humans) [124, 125]. The side effects have been linked to an indirect NK cell-mediated mechanism involving the release of vasoactive mediators, such as TNF-α, as well as to CD25-dependent endothelial cell damage induced by the binding of IL-2 to the endothelial

surface receptors leading to the vascular leak syndrome (VLS) [56, 60]. One line of research aims to improve the clinical application of IL-2 by e.g. incorporating IL-2 in fusion proteins aiming to target the cytokine to the tumor site [126-128]. The drawback of such applications is the simultaneous expansion of Treg cells, which could suppress the effect of the activated Tcs [129, 130]. Of note, IL-15-based immunotherapy is also under investigation. It differs from IL-2 in terms of receptor binding; IL-15 has a high affinity for its IL-15 receptor α subunit and causes therefore lower CD25-mediated cytotoxicity. This has led to the development of molecules where IL-15 has been fused to its soluble receptor IL-15Rα showing better tumor control in mouse models [131, 132].

g) Improved IL-2 immunotherapy using IL-2cx

IL-2 can bind and stimulate $CD8^+$ T cells and NK cells expressing the dimeric IL-2R ($CD122^{high}$ cells) but also Treg cells expressing the trimeric IL-2R. Using specific anti-IL-2 mAbs, which bind IL-2 and form so-called IL-2/mAb complexes (IL-2cx), IL-2 can be preferentially directed to $CD122^{high}$ or $CD25^{high}$ cells. This selectivity has been previously demonstrated in animals receiving IL-2cx or IL-2 alone [60, 133, 134]. Five to seven daily injections of mouse IL-2 (mIL-2) complexed with an anti-mIL-2 (mAb clone S4B6 or S4B6 like antibodies) led to the expansion of $CD122^{high}$ cells by 20-40 fold versus a 2 to 5 fold expansion of Treg cells. In line with this finding, lower mIL-2 doses (15 000 IU when complexed with mAb) are needed compared to mIL-2 alone (200’000 IU) in order to get preferential stimulation, leading to significantly reduce IL-2-related side effects correlating with less binding to $CD25^+$ endothelial cells [60, 133]. The therapeutic outcome of IL-2/S4B6 complexes are in line with the recent structural data showing that S4B6 associates and inhibits the CD25 binding epitope of mIL-2 [55, 135]. On the other hand, when mIL-2 is complexed

with a specific mAb such as clone JES6-1A12, three to seven daily injections increases Treg cell numbers by 7 to 15 fold compared to mIL-2 alone (Figure 15) [133, 134, 136]. When IL-2 is complexed to a mAb the half-life of IL-2 is increased by 10 to 20 fold [133, 137]. The increased half-life is mediated by neonatal Fc receptors but, interestingly, FcγR do not seem to play an important role on the observed *in vivo* effects of IL-2-cx [133, 137]. Until to date, mIL-2/S4B6 complexes have been tested in various tumor and acute and chronic infection models showing their pre-clinical efficacy [60, 138, 139].

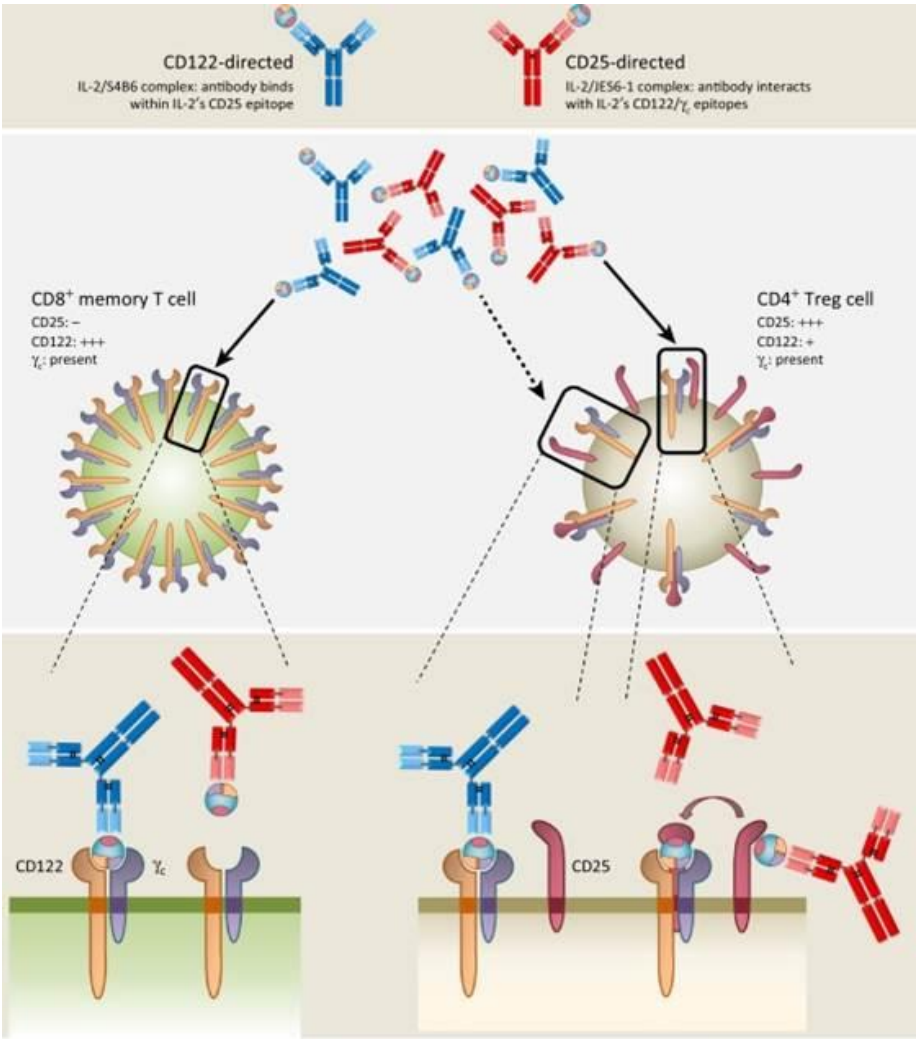


**Figure 15. T cell subtype-specific receptor interactions of IL-2cx.** IL-2/S4B6 complexes (blue) preferentially stimulate CD122$^{high}$ cells including memory CD8$^{+}$ T cells (green) and

NK cells (not shown). On the other hand, IL-2/JES6-1 complexes (red) only stimulate $CD25^{high}$ cells such as Treg cells (brown). From [55].

h) IL-2 muteins

Another approach to increase IL-2 efficacy and/or reduce its associated side effect is the generation of IL-2 mutants, or so-called IL-2 muteins. The first mutational studies were done in order to decrease IL-2's affinity for CD122. The idea behind goal was to limit NK cell activation and release of TNF-α, which were thought to be the central players of vasodilation and therefore VLS at that time. However, the developed N88R (BAY50-4798) and the D20T mutants of IL-2 (Selectikine) did not show lower toxicity levels in clinical applications [54, 140, 141]. The decreased side effects observed with IL-2/S4B6 complexes disfavoring the stimulation of $CD25^{+}$ cells (including endothelial cells) and preferentially expanding $CD122^{high}$ cells led to the development of the next generation of IL-2 muteins. These IL-2 mutants (H9 or D10) being modified on amino acids 80 to 92, showed that the substitutions L80F, L85V and I86V were essential in order to get 200 fold higher affinity for CD122, better tumor control and less side effects compared to IL-2 alone [142]. An alternative approach was to generate an IL-2 mutein with lower affinity for CD25. The resulting IL-2 mutant, the so-called 'no-α-muteins', displayed superior tumor control and reduced side effects when compared to IL-2 alone. Another mutant termed F42A, also having a decreased affinity for CD25 performed similarly *in vivo* [54, 142, 143].

i) Combination therapy

The success of cancer immunotherapy depends on a coordinated recruitment of innate and adaptive immunity, including soluble and cellular factors. In such a case, the tumor cells can be destroyed before becoming invasive. However, some tumor cells can survive and enter an

equilibrium phase, as postulated in 2011 by Schreiber and colleagues and termed 'The cancer immunoediting concept' [83]. At this stage, an adaptive immune response is needed in order to prevent uncontrolled tumor growth and metastasis. Unfortunately, as a consequence of immune selection pressure some tumor cells may not be any more recognized as foreign by loss of antigenicity and/or develop resistance to cellular cytotoxicity [144, 145]. Simultaneously, tumor cells may induce and maintain an immunosuppressive environment allowing them to escape and grow in an uncontrolled manner. In order to prevent such immune evasion, a strategy targeting different effector arms of the immune system using combinatorial approaches is of great clinical interest [146]. Various pre-clinical models have shown the benefit of therapy combinations like the administration of anti-CTLA-4 or anti-PD-1 in combination with vaccines leading to better tumor control [147, 148]. Moreover, the synergy observed with combinatorial CTLA-4 and PD-1 blockade in animals prompted the clinical testing of this combination [149]. However, such combinations need to be properly tested in order to limit additive immune-mediated toxicities [150].

4. Epigenetic modulation of tumor control

Conrad Waddington introduced the term epigenetics in the early 1940 [151]. It refers to the molecular pathways modulating the expression of genes that are not due to any alteration in the DNA sequence. The mechanisms involved in epigenetic gene regulation include methylation of cytosines in DNA and enzymatic modification state of histones. Several enzymes are known to be involved in mediating post-translational histone modifications such as methylation or deacetylation. Acetylation of histone (H) lysines (K) is generally associated with transcriptional activation while the consequence of histones methylation depends on the residue and the site of methylation [152]. For example, methylation of H3 at K4 is linked to

transcriptional activation [153] but methylation of H3 at K9 or K27 leads to transcriptional repression. Low levels of DNA methylation have been found in human cancer tissues [154]. Moreover, hypermethlyation of DNA regions containing many adjacent cytosine and guanine nucleotides (referred as 'CpG islands') in the promoter regions of tumor suppressors regions, have been found in many types of cancers [155-157]. The hypermethylation state of genes closely depends on histone modifications. The enhancer of zeste homologue 2 (EZH2) makes part of the multiprotein polycomb repressive complex 2 (PRC2, Figure 16). EZH2 is a highly conserved histone methyltransferase found to be overexpressed in many cancers such as melanoma and breast cancer [158-160]. It mediates the tri-methylation of lysine 27 on histone 3 (H3K27me3), thus inducing chromatin compaction and leading to transcriptional repression of target genes (Figure 16) [160-162]. EZH2 is essential in early development but it is downregulated in normal adult tissues [163]. High EZH2 levels have been linked to a stem cell-like state in cancer by repressing genes involved in differentiation while allowing expression of genes involved in cell division [164].

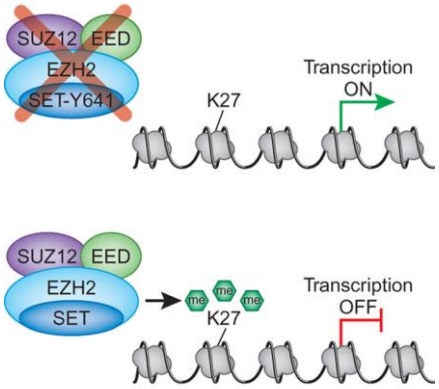


**Figure 16. Multiprotein polycomb repressive complex 2 (PRC2).** Polycomb repressive complexes (PRCs) are essential mediators of transcriptional repression. In PRC2 the co-factors SUZ12 and EED interact with nucleosomes and induce EZH2 catalytic activity

responsible for trimethylation of lysine 27 on histone H3, thus leading to transcriptional repression. Adapted from [161].

Mutations within the catalytic site of EZH2 lead to a permanent tri-methylation state and have been identified in 22% of lymphomas [165-167]. Furthermore, high levels of EZH2 have been associated with more aggressive forms of melanoma and increased proliferation and invasion of cancer cells [168]. Likewise, it has been shown that EZH2 mediates the repression of different tumor suppressors and differentiation genes [169]. The key role played by EZH2 in malignant melanoma progression was shown in a genetic mouse model of cutaneous melanoma [170]. Interestingly, EZH2 overexpression has been linked to inefficient T cells immune response in uveal melanoma [171]. Because of its role in cancer, EZH2 has been validated as a promising target for the development of small molecule inhibitors. Several inhibitors are currently being tested in preclinical and clinical studies. The first drug described was the molecule DZNep. It acts through the inhibition of the S-adenosyl homocysteine hydrolase causing the degradation of proteins members of the PRC2 complex and leading to H3K27 demethylation [172]. Even though the drug has shown some success, its lack of specificity led to the development of more selective inhibitors such as GSK126 [166], GSK343, and GSK503. *In vivo* studies of such inhibitors demonstrated the correlation between tumor control and decreased levels of H3K27me3 [173]. Within the present thesis, we have evaluated the inhibitor GSK503 in combination with human IL-2cx in various melanoma models.

# IV. Aims

As previously described, IL-2 immunotherapy can be enhanced by delivering IL-2 as IL-2cx, which preferentially stimulate $CD122^{high}$ cells. Currently, no monoclonal antibody (mAb) to human (h) IL-2 suitable for clinical development in cancer immunotherapy is available. The first aim of my thesis was to develop a rational approach to generate an anti-hIL-2 antibody acting as CD25 mimic (which we have termed NARA1). The generation is followed by *in vitro* characterization of the antibody allowing us to precisely define the binding epitope on hIL-2. Then the *in vivo* properties of the hIL-2/NARA1 complex (IL-2cx) need to be tested in order to check for its specificity (stimulation of $CD122^{high}$ cells) and anti-tumor effects. Despite potent and constant stimulation of the immune system using IL-2cx in aggressive melanoma models, tumors use several mechanisms (through genetic and/or epigenetic alterations) to become resistant to apoptosis or to counterattack the immune system. The second aim of my thesis was to the check if IL-2cx immunotherapy would promote epigenetic modifications leading to tumor cell dedifferentiation, loss of immunogenicity and immune escape. Once we observed a clear correlation between up-regulation of the histone methyltransferase enhancer of zeste homologue 2 (Ezh2) and IL-2cx immunotherapy, we aim to test and elucidate the mechanisms of the combination therapy consisting of Ezh2 blockade and IL-2cx in order to better control tumor growth *in vivo*.

# V. Results

1. Rational generation of CD25-mimobody specific for human IL-2

Adapted from a manuscript submitted to Science Translational Medicine.

**'Improved cancer immunotherapy by rational generation of CD25-mimobody conferring selectivity to human interleukin-2'**

Natalia Arenas-Ramirez[1], Chao Zou[2], Simone Popp[2], Catherine Regnier[2], Barbara Brannetti[2], Emmanuelle Wirth[2], Thomas Calzascia[2], Jiri Kovarik[2], Daniel Zingg[3], Lukas Sommer[3], Gerhard Zenke[2], Andreas Katopodis[2], and Onur Boyman[1]*

[1] Department of Immunology, University Hospital Zurich, University of Zurich, CH-8091 Zurich, Switzerland

[2] Novartis Institutes for Biomedical Research, Novartis Pharma AG, CH-4002 Basel, Switzerland

[3] Cell and Developmental Biology, Institute of Anatomy, University of Zurich, CH-8057 Zurich, Switzerland

* Corresponding author: onur.boyman@uzh.ch

a) Rational based screening for generation of selective anti-human IL-2 antibodies

We have previously hypothesized that CD122-directed IL-2/antibody complexes are made of anti-IL-2 mAbs that occupy IL-2's CD25-binding site [55, 133, 134]. Hence, we established a screening approach for such mAbs (fig. S1A). As the affinity of recombinant hCD25 to hIL-2 is low ($K_d$ ~$10^{-8}$ M) and thus unsuitable for use in a sandwich enzyme-linked immunosorbent assay (ELISA), we tested various available anti-hIL-2 mAbs, when complexed to hIL-2, for their ability to expand either $CD25^{high}$ cells (termed $mAb_{cap}$) or $CD122^{high}$ cells (termed $mAb_{det}$) *in vivo*. We verified that binding of $mAb_{det}$ to hIL-2 prevented the binding of hCD25 to the same hIL-2 molecule. We then used $mAb_{cap}$ and $mAb_{det}$ as capture and detection antibodies, respectively, in a competitive sandwich ELISA to screen newly-generated anti-hIL-2 mAbs for their ability to prevent $mAb_{det}$ binding to hIL-2 and to preferentially expand $CD122^{high}$ $CD8^+$ T cells and $NK1.1^+$ DX5 $(CD49b)^+$ NK cells *in vivo* (fig. S1B). About 0.2% of all anti-hIL-2 mAbs were efficiently displacing $mAb_{det}$, even at low concentrations, and showed selective and potent expansion of $CD122^{high}$ lymphocytes *in vivo*, of which clone NARA1 was most promising.

b) Structure of hIL-2/NARA1 complex shown analogy of NARA1 to CD25

We used surface plasmon resonance (SPR), to assess whether binding of hIL-2 to NARA1 prevented further binding to hCD25. To this end, hIL-2 was loaded on immobilized NARA1 prior to injection of recombinant hCD25 or hCD122. In this setting, hCD25 was unable to bind, even at high concentrations, while hCD122 readily associated with NARA1-bound hIL-2 (Fig. 1A, and fig. S2A). Conversely, hIL-2 loaded on immobilized $mAb_{cap}$ allowed efficient association with hCD25, but not with hCD122 (fig. S2, B and C). The affinity of NARA1 to hIL-2 was ~$10^{-9}$ M, as determined by SPR fitting curves, showing a lower off-rate (fig. S3).

Unlike $mAb_{det}$, NARA1 showed no cross-reactivity with mouse IL-2 (mIL-2; fig. S4, A and B). To gain further insight into the structural and mechanistic properties of NARA1, we determined the crystal structure of the hIL-2/NARA1 (Fab) complex to a resolution of 1.95 Å. The association of hIL-2 and NARA1 relied mainly on electrostatic interactions (Fig. 1B). In comparison to the structure of the quaternary complex of hIL-2 with its trimeric hIL-2R [174, 175] NARA1 bound hIL-2 'on top', that is dorso-laterally, and at an angle similar to hCD25 (Fig. 1, C and D). Overlaying the structures of the hIL-2/NARA1 and hIL-2/hIL-2R complexes showed that position and angle of NARA1, particularly the $V_H$ domain of NARA1, closely overlapped with hCD25 (Fig. 1E).

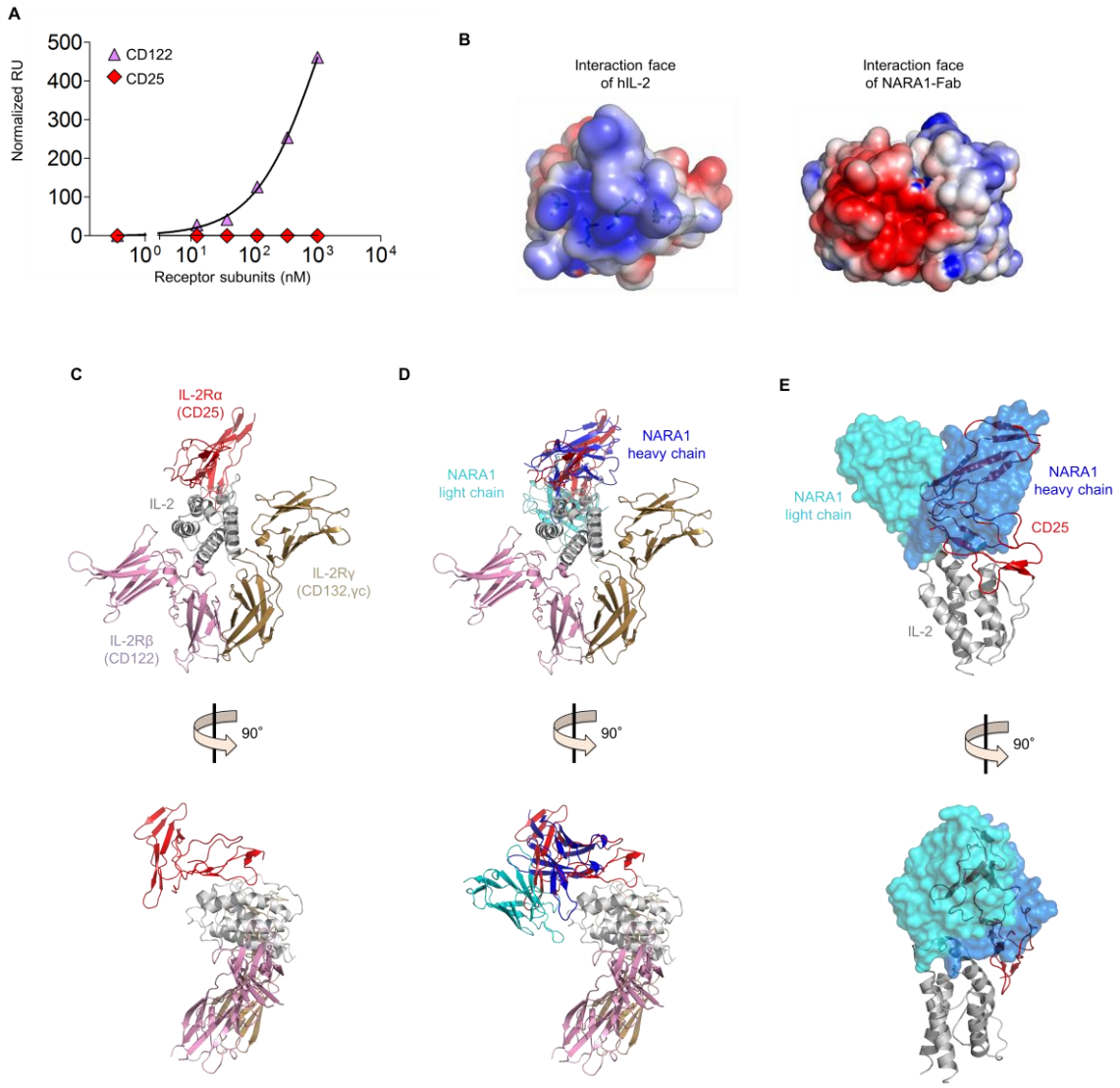


**Figure 1. Three-dimensional structure of NARA1/IL-2 complex shows strong analogy of NARA1 to CD25.** (**A**) Equilibrium surface plasmon resonance titration of human (h) CD122 and hCD25 interacting with immobilized NARA1 bound to hIL-2 at saturating concentration. Data are representative of three independent experiments. (**B**) View of electrostatic interaction interfaces between hIL-2 and NARA1. (**C**) Ribbon representation of hIL-2/hIL-2R quaternary complex (IL-2, grey; CD25, red; CD122, purple; $\gamma_c$, gold; PDB accession code: 2B5I;[174]). (**D**) Overlay of NARA1 on hIL-2/hIL-2R quaternary complex with NARA1 heavy and light chains in blue and cyan, respectively. (**E**) Overlay of NARA1 (surface representation), hIL-2, and hCD25.

c) IL-2 residues contacting CD25 are involved in binding to NARA1

Analysis of the interface between hIL-2 and NARA1 revealed that hIL-2 residues P34, K35, R38, T41, Q74, and K76 were most prominent in forming the epitope, with R38 being the most crucial (Fig. 2, A and B). These residues had the possibility of forming 10 and more direct intermolecular contacts with NARA1, as measured by the number of NARA1 atoms within 4 Å of hIL-2, and showed reduced solvent-accessible ('buried') surface of 50 $Å^2$ and more after binding to NARA1 (Fig. 2A). Significantly, R38 and its neighboring residues formed a hot spot comprising a loop and a short α-helix connecting helices A and B of hIL-2, which contained the most important hIL-2 residues contacting hCD25 (Fig. 2, A and B) [176]. Moreover, the residues Q74 and K76 participated in a smaller secondary interaction spot in a loop connecting helices B and C, of which L72 has been involved in hCD25 interaction [175, 176]

d) NARA1 binding sites differ from S4B6 and $mAb_{det}$ epitopes on IL-2

We next compared the hIL-2/NARA1 complex with a recently published structure of a CD122-directed mIL-2/anti-mIL-2 (clone S4B6) antibody complex [135]. In the reported structure of mIL-2/S4B6 complex, S4B6 occupied part of IL-2's CD25 epitope, leaving R38 and some other CD25-interacting IL-2 residues unbound [55, 135]. Moreover, unexpectedly, S4B6 affected IL-2 binding to CD122 by exerting two seemingly antagonistic effects consisting of a slight steric clash between S4B6 and CD122 versus an affinity-enhancing structural change of IL-2's CD122-binding loop [55, 135]. The latter is reminiscent of a hIL-2 mutein (termed 'IL-2 superkine') with increased CD122 binding [142]. In comparison to NARA1 associating with hIL-2 mainly via a short α-helix stretch connecting helices A and B (Fig. 2C), S4B6 bound mIL-2 residues that were located in helices B and C (Fig. 2D, and

[135]), consistent with earlier data from S4B6 epitope mapping studies [177]. Consequently, NARA1 and S4B6 interacted with mostly unrelated IL-2 epitopes (fig. S5), resulting in binding to IL-2 at different angles (Fig. 2E). Moreover, hCD25 fitted nicely into the density graph of NARA1, while overlap of S4B6 with hCD25 was notably different, with significant parts of CD25 still exposed (Fig. 2E). Interestingly, NARA1-bound hIL-2 adopted the allosteric changes in helix C (fig. S6) observed with binding of hIL-2 to hCD25 or described for the IL-2 superkines [142, 174], although these changes in hIL-2/NARA1 complex did not lead to increased signaling or proliferation of responder cells *in vitro* (see below).

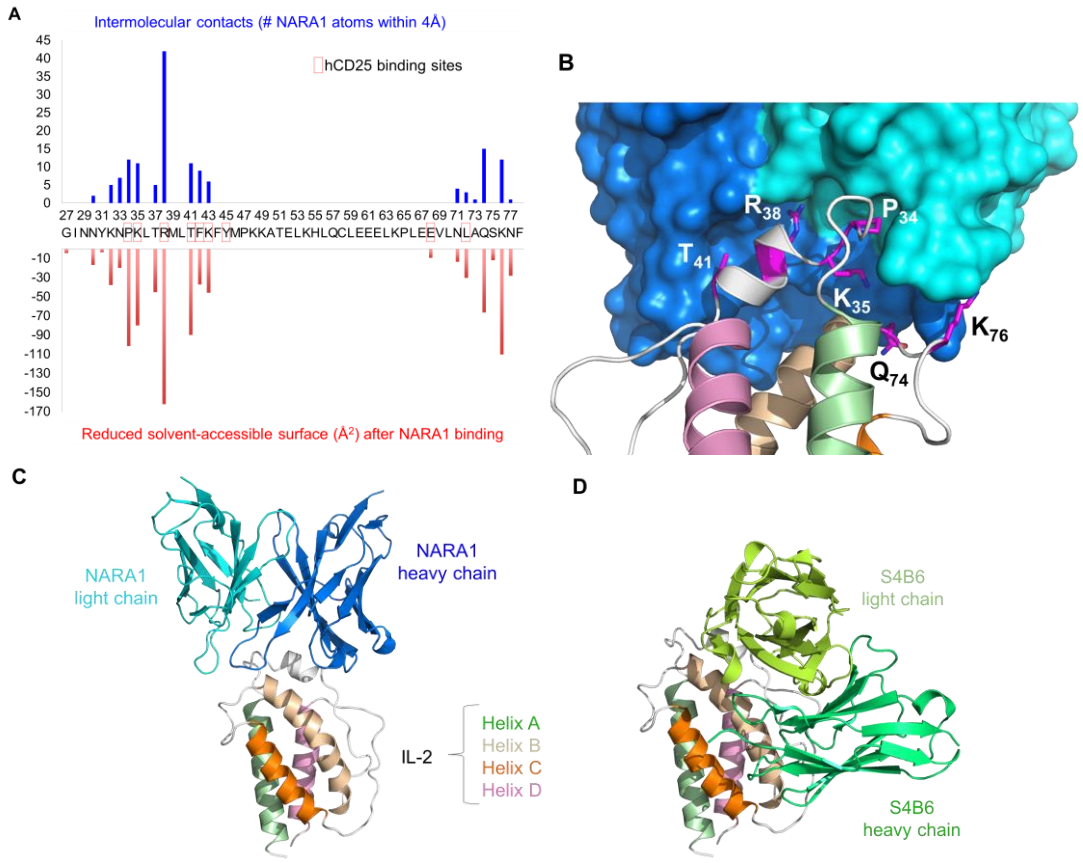

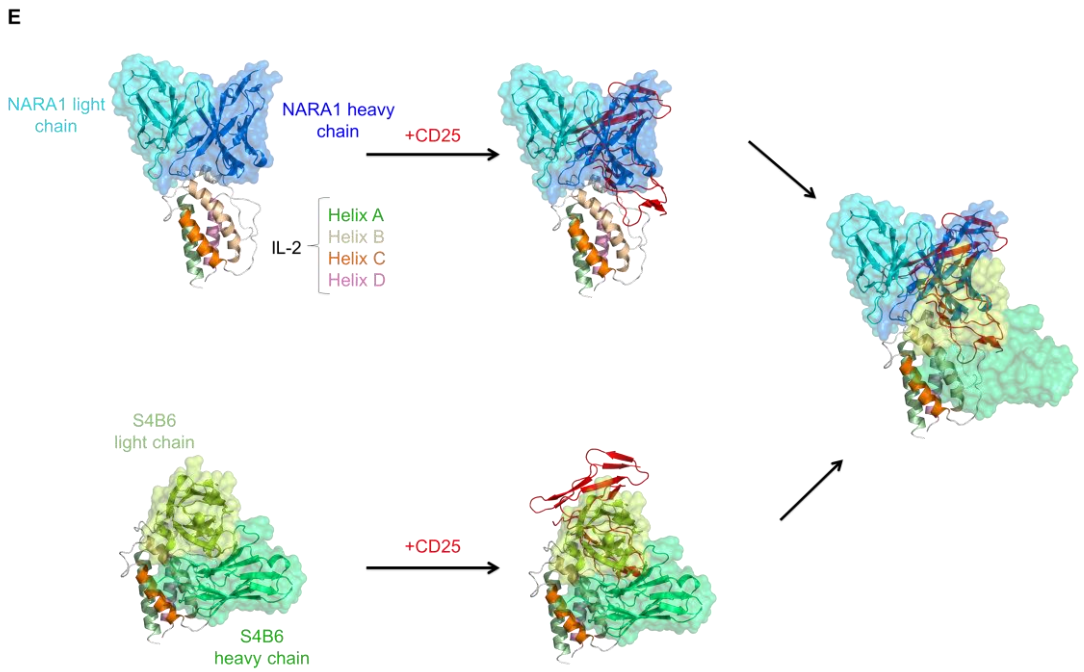


**Figure 2. Key IL-2 residues mediating contact with CD25 are also involved in binding to NARA1 antibody.** (**A**) Number of NARA1 (Fab) atoms within 4 Å of hIL-2 indicating direct intermolecular contacts (blue bars) and reduced solvent-accessible surface ($Å^2$) of hIL-2 after binding to NARA1 (red bars). Numbers in the middle of the graph represent hIL-2 residues, with red boxes indicating residues involved in hCD25 binding [55]. (**B**) Close view of NARA1 binding site to hIL-2 with key residues indicated. NARA1 heavy and light chains are shown in blue and cyan, respectively. (**C–E**) Ribbon and surface representation of hIL-2 (helix A, green; helix B, gold; helix C, dark orange; helix D, pink) with NARA1 (**C**) or mIL-2 with S4B6 (**D**; light chain, lime; heavy chain, light green), and overlay of these complexes with hCD25 (red) (**E**).

Generation of hIL-2 muteins containing a single amino acid mutation at R38 or F42 revealed that R38, but not F42, was essential for binding to NARA1. Conversely, linear peptide mapping to identify linear hIL-2 sequences binding to the anti-hIL-2 mAbs did not show any significant interaction with NARA1, whereas $mAb_{det}$ readily bound to hIL-2 linear peptides containing amino acids 37 to 42 (Fig. 3A). Accordingly, introduction of an F42A mutation abrogated binding to $mAb_{det}$, but not to NARA1 (Fig. 3B). These results indicate that NARA1

binds to a three-dimensional epitope of hIL-2 that is different from $mAb_{det}$ and S4B6 and contains the most prominent hCD25-interacting residues.

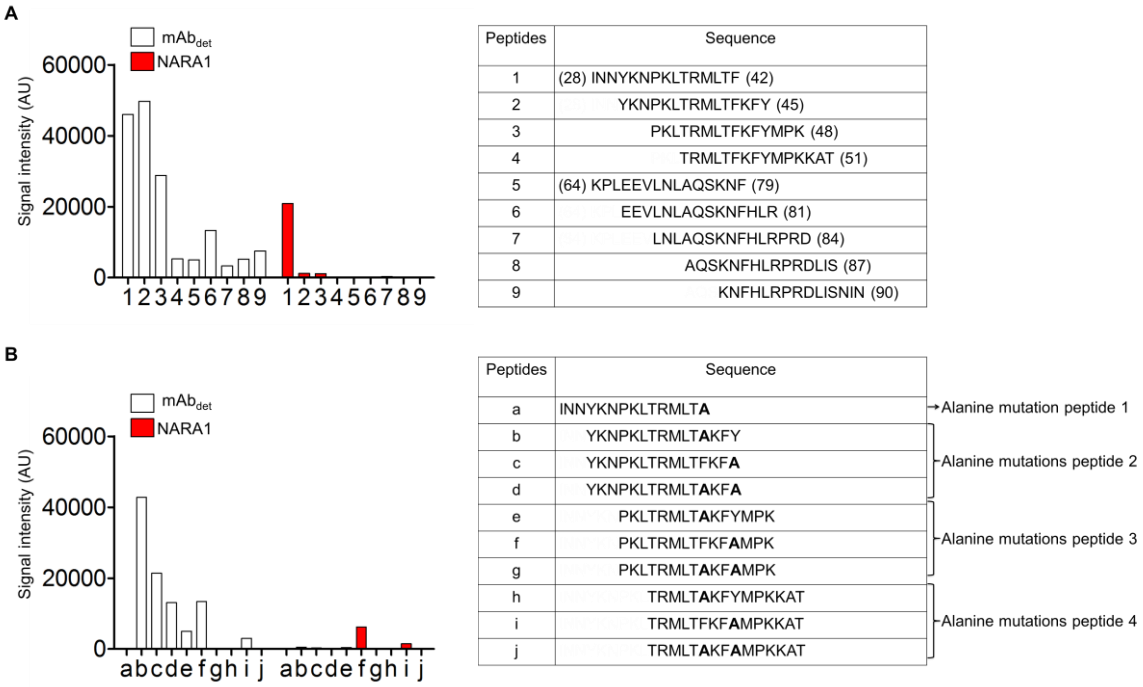


**Figure 3. NARA1 binding sites differ from $mAb_{det}$ epitopes on IL-2.** (**A** and **B**) Linear peptide mapping of NARA1 and $mAb_{det}$ binding sites to unmodified hIL-2 (**A**) or after mutation of F42, Y65 and L92 to an alanine residue (**B**). Shown is the signal intensity for both antibodies after subtraction of control signal (AU). Sequences of peptides and residue numbers in brackets are provided. Data are representative of two independent experiments.

e) hIL-2/NARA1 complex stimulates T cells independently of IL-2R crosslinking

To assess the functional properties of NARA1, we compared hIL-2 to hIL-2 complexed to NARA1 at a 2:1 ratio (hIL-2/NARA1 complex) *in vitro*. Binding of IL-2 to its receptor leads to phosphorylated STAT5 (pSTAT5) [55, 64]. Compared to hIL-2, hIL-2/NARA1 complex led, at all concentrations assessed, to very similar pSTAT5 levels in IL-2-responsive CTLL-2 cells (Fig. 4A) expressing trimeric IL-2Rs. In contrast, mIL-2 complexed to S4B6 at a 2:1 ratio (mIL-2/S4B6 complex) was about 10-fold less potent than mIL-2 (Fig. 4C, and [135]), consistent with our previous finding that mIL-2/S4B6 complex was discretely less active than mIL-2 in mediating proliferation of $CD122^{high}$ $CD8^{+}$ cells *in vitro* [134]. These effects might result from aforementioned steric clash between S4B6 and CD122 [135]. Conversely, hIL-2/NARA1 and mIL-2/S4B6 complexes were equipotent to hIL-2 and mIL-2 in driving proliferation of CTLL-2 cells (Fig. 4, B and D). Moreover, pSTAT5 induction and proliferation of purified human $CD8^{+}$ T cells (Fig. 4, E and F) was comparable for hIL-2 and hIL-2/NARA1 complex. The stimulatory activity of hIL-2/NARA1 complex did not depend on cross-linking of two IL-2Rs by the bivalent mAb, as demonstrated by similar pSTAT5 and proliferation kinetics of complexes made with either whole mAb versus Fab or $F(ab')_2$ fragments of NARA1 (Fig. 4, G and H), the latter of which retained efficient hIL-2 binding (fig. S7).

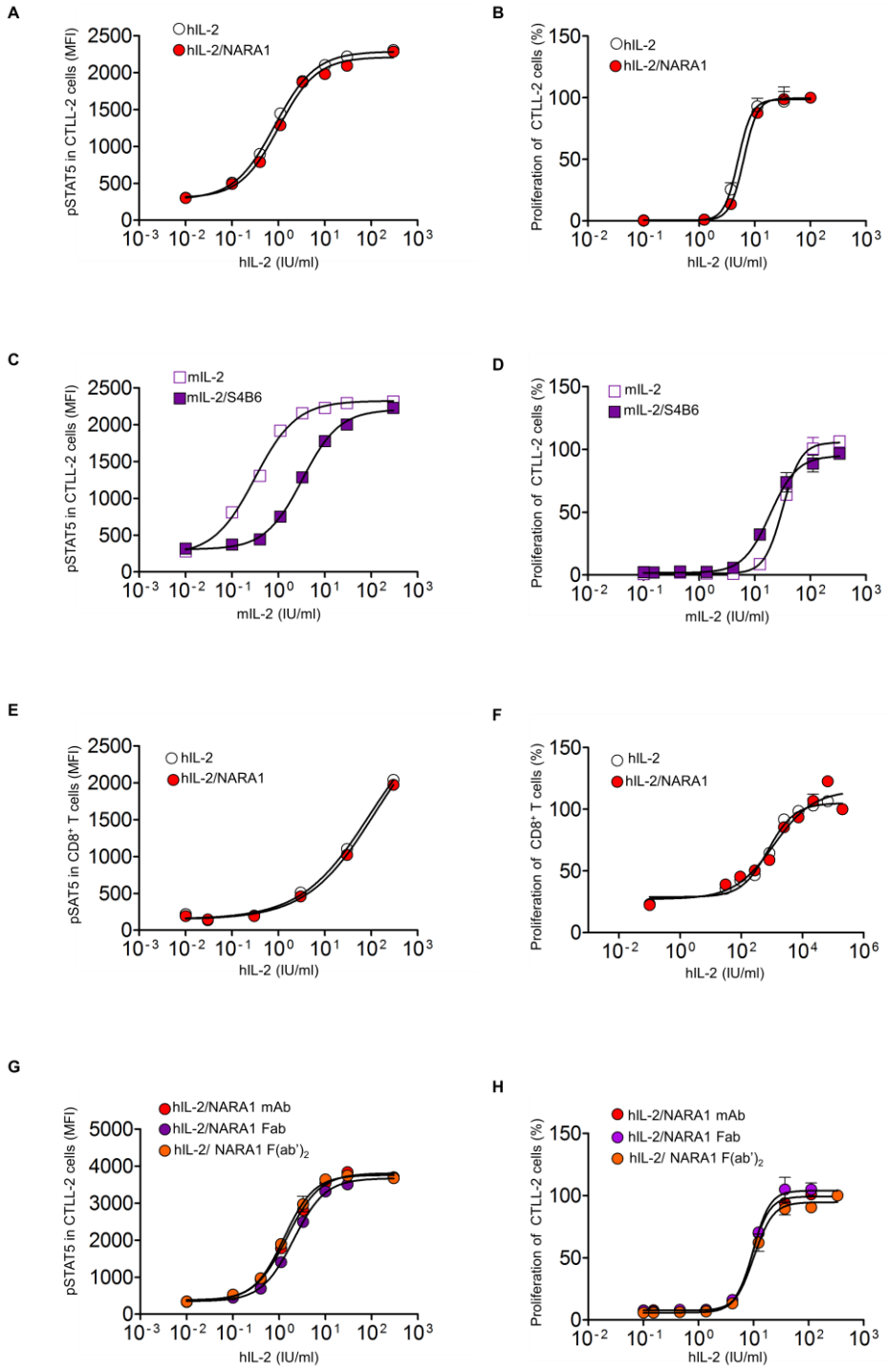


**Figure 4. Efficient binding and stimulation of T cells by IL-2/NARA1 complex is independent of IL-2R crosslinking.** (**A** to **D**) Phosphorylated STAT5 (pSTAT5) levels (**A** and **C**) and proliferation (**B** and **D**) of CTLL-2 cells in response to titrated hIL-2 versus hIL-

2/NARA1 complex (**A** and **B**) or mIL-2 versus mIL-2/S4B6 complex (**C** and **D**). (**E** and **F**) pSTAT5 levels (**E**) and proliferation (**F**) of purified human $CD8^+$ T cells to titrated hIL-2 versus hIL-2/NARA1 complex. (**G** and **H**) pSTAT5 (**G**) and proliferation (**H**) of CTLL-2 cells to hIL-2/NARA1 complex using NARA1 as full antibody, $F(ab')_2$ fragment, or Fab fragment. Shown are mean fluorescence intensity (MFI) of intracellular pSTAT5 levels (**A**, **C**, **E**, and **G**) and proliferation using WST-1 reagent (**B**, **D**, **F**, and **H**) of two to three independent experiments.

f) <u>hIL-2/NARA1 complex selectively expands anti-tumor effector lymphocytes</u>

Injection of mice with hIL-2/NARA1 complex for 4 days led to vigorous proliferation and expansion of $CD122^{high}$ $CD8^+$ T cells (Fig. 5A) and $NK1.1^+$ $DX5^+$ NK cells in lymph nodes and spleen (Fig. 5B-D). Although $CD25^{high}$ $CD4^+$ Treg cells were also stimulated by this treatment, expansion of $CD8^+$ T cells was much more prominent (Fig. 5B-D).

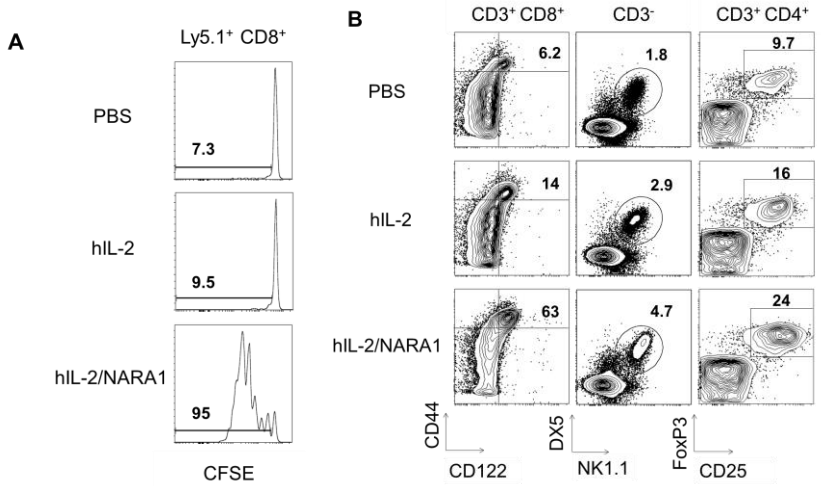

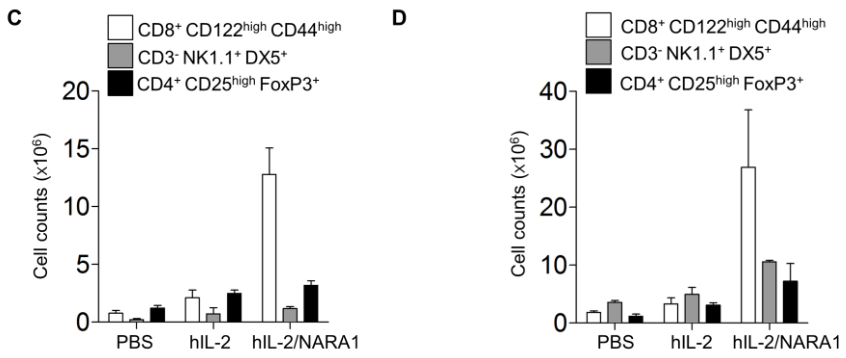


**Figure 5. Use of IL-2/NARA1 complex mediates efficient expansion of CD122$^{high}$ cells.** (**A** to **D**) Carboxyfluorescein succinimidyl ester (CFSE)-labeled CD8$^+$ T cells from Ly5.1 (CD45.1)-congenic animals were adoptively transferred to recipient mice, which subsequently received 4 daily intraperitoneal injections of PBS, hIL-2, or hIL-2/NARA1 complex. On day 5, lymph nodes (LNs) were collected and analyzed by flow cytometry for CFSE dilution (indicating cell proliferation) in Ly5.1$^+$ CD8$^+$ T cells (**A**) and for levels of the indicated immune subsets (**B**). Total counts of indicated cell subsets in LNs (**C**) and spleen (**D**) of mice treated as in A. Data are representative of three independent experiments.

Treatment of mice harboring a syngeneic intradermal B16-F10 melanoma nodule revealed that 1 course of 4 injections of hIL-2/NARA1 complex was sufficient to suppress tumor growth by 80%, whereas hIL-2 alone decreased tumor growth only minimally (Fig. 6A). The improved anti-tumor response correlated with an increase in CD8$^+$ T cells in tumor-draining lymph nodes (TDLNs; Fig. 6B) and tumor-infiltrating lymphocytes (TILs; Fig. 6C). In contrast to CD8$^+$ T cells, intratumoral CD25$^{high}$ forkhead box p3 (Foxp3)$^+$ CD4$^+$ Treg cells were disfavored by hIL-2/NARA1 complex treatment compared to hIL-2 (Fig. 6C), which altogether led to a 5 fold higher ratio of CD8$^+$ to Treg cells (Fig. 6D). A similar paucity was observed for CD11b$^+$ Gr-1$^+$ myeloid-derived suppressor cells (Fig. 6C) [112]. Compared to their counterparts isolated from mice treated with hIL-2, CD8$^+$ TILs from animals receiving hIL-2/NARA1 complex expressed significantly lower programmed death-1 levels (Fig. 6C) [146], suggesting the cells were less exhausted. In line with this finding, CD90.1$^+$ gp100-

specific and CD90.1$^{-}$ polyclonal CD8$^{+}$ T cells from TDLNs and TILs produced significant amounts of interferon-γ, a crucial cytokine involved in anti-tumor immunity [83], upon *ex vivo* stimulation with gp100 or a polyclonal trigger, respectively (Fig. 6, E and F). Also pulmonary nodules of B16-F10 melanoma were reduced by over 77% following 4 injections of hIL-2/NARA1 complex, while high-dose hIL-2 treatment achieved only 48% reduction (Fig. 6G). However, as expected [60], high-dose hIL-2 treatment caused significant pulmonary edema, whereas hIL-2/NARA1 complex was much better tolerated (Fig. 6H).

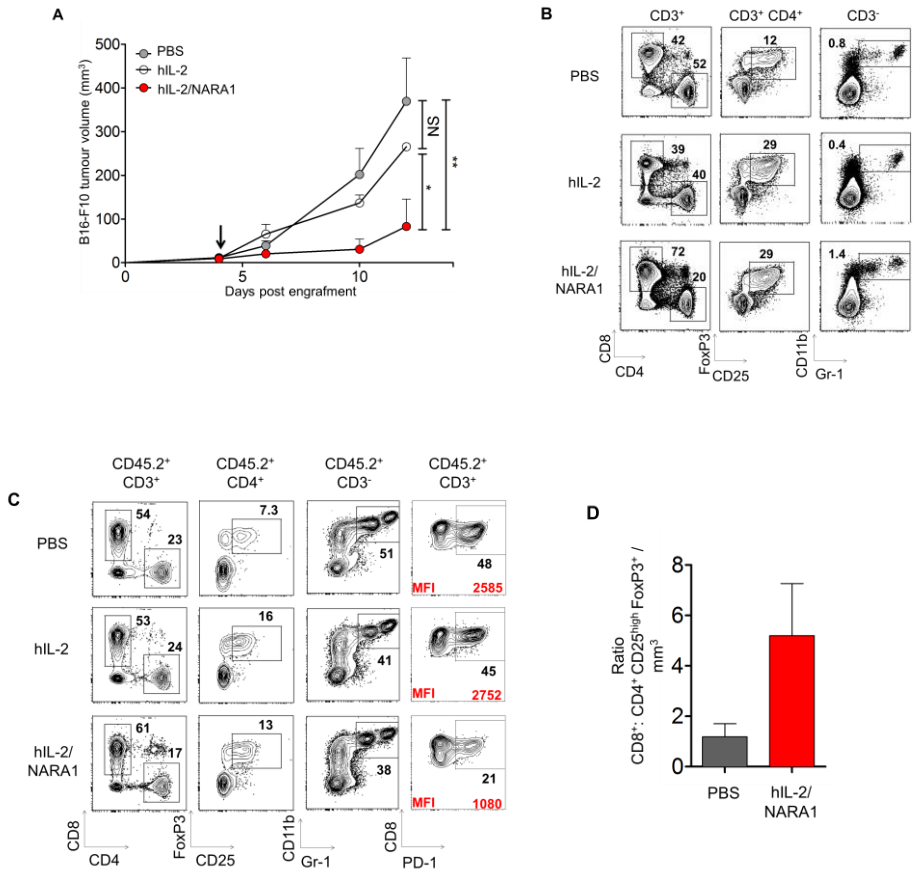

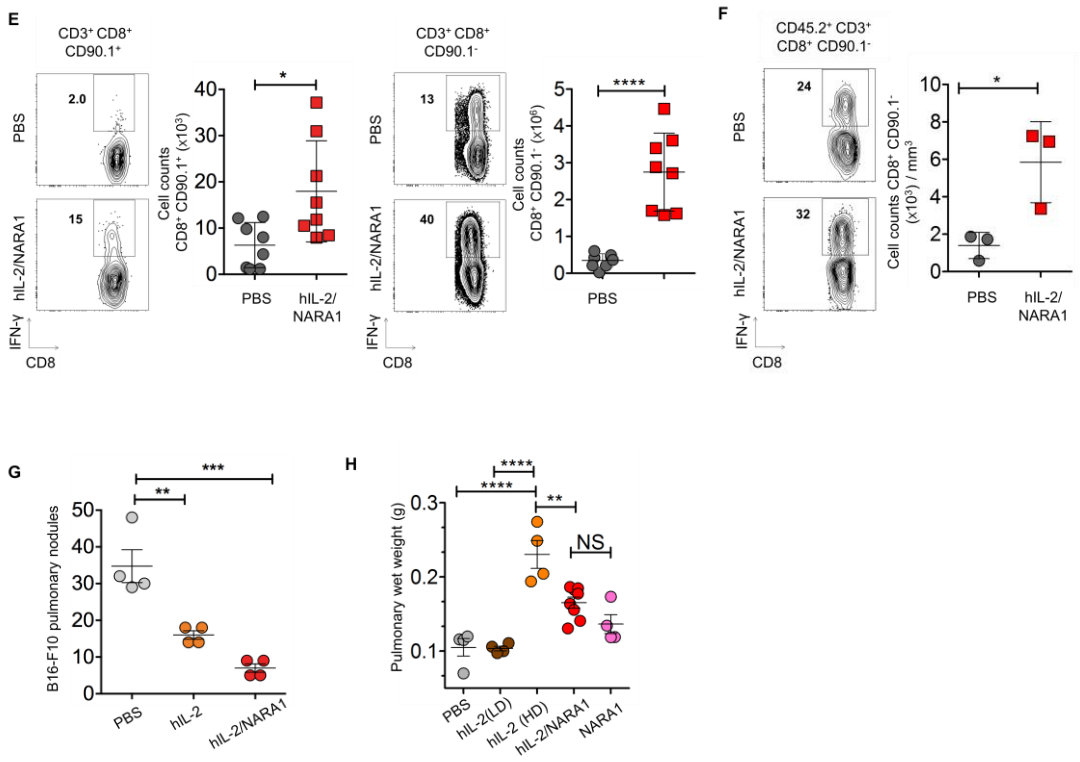


**Figure 6. Use of IL-2/NARA1 complex mediates efficient CD8$^+$ T cell proliferation and anti-tumor immune response in the B16-F10 melanoma model.** (**A** to **D**) Animals were injected intradermally with B16-F10 melanoma cells, followed by 4 injections of PBS, hIL-2, or hIL-2/NARA1 complex. Shown is tumor volume, with arrow indicating start of treatment (**A**), and indicated immune cell subsets within tumor-draining lymph nodes (TDLNs, **B**) and tumor-infiltrating lymphocytes (TILs, **C**). Red numbers refer to MFI of programmed death-1 expression in CD8$^+$ T cells (**C**). (**D**) Ratio of CD8$^+$ T cells to CD4$^+$ CD25$^{high}$ FoxP3$^+$ T cells in TILs from mice treated as in A. (**E** and **F**) Mice were adoptively transferred with CD90.1$^+$ gp100-specific T cell receptor-transgenic CD8$^+$ T cells, followed by treatment as in A. Shown is IFN-γ production in CD90.1$^+$ gp100-specific and CD90.1$^-$ polyclonal CD8$^+$ T cells and their quantification from tumor-draining lymph nodes (TDLNs, **E**) and TILs (**F**). (**G**) Animals were injected intravenously with B16-F10 melanoma cells, followed by treatment as in A. On day 16, lungs were removed and quantification of melanoma nodules was performed, as previously described [60]. (**H**) Mice received PBS, hIL-2 at 1.5 µg (low dose, LD) or 20 µg (high dose, HD), NARA1 (15 µg), or hIL-2/NARA1 complex (1.5 µg/15 µg) for 4 days. On day 5, lungs were removed in order to determine pulmonary wet weight, as previously described [60]. Data are represented as mean ± s.e.m. of three independent experiments, *n* = 3

to 4 (**A** to **D**), *n* = 8 (**E**), *n* = 3 (**F**), *n* = 4 (**G**), *n* = 4 (**H,** PBS, hIL-2 [LD], hIL-2 [HD], NARA1), and *n* = 7 (**H,** hIL-2/NARA1). For TILs, samples of mice receiving the same treatment were pooled prior to analysis. Differences between groups were analyzed using one-way ANOVA with Bonferroni's post-test correction. **P*<0.05, ***P*<0.01, ****P*<0.001, *****P*<0.0001.

g) <u>hIL-2/NARA1 complex immunotherapy is efficacious in a spontaneous melanoma model</u>

Finally, we assessed hIL-2/NARA1 complex treatment in transgenic *Tyr::N-Ras*$^{Q61K}$ *Ink4a*$^{-/-}$ mice, which spontaneously develop metastatic melanoma within 6 months of age [170, 178, 179]. Using 10 weekly courses of hIL-2/NARA1 complex we were able to prolong tumor-free survival in these mice by 2.3–2.7 times (Fig. 7A). Likewise, at time-point of sacrifice, hIL-2/NARA1 complex-treated mice showed a significant reduction in skin melanoma counts (Fig. 7B) and lung metastases (Fig. 7C).These effects correlated with an increase in CD8$^{+}$ T cells, particularly CD44$^{high}$ cells, in lymph nodes and spleen (Fig. 7D). Notably, such prolonged treatment did not lead to any overt signs of toxicity or autoimmunity.

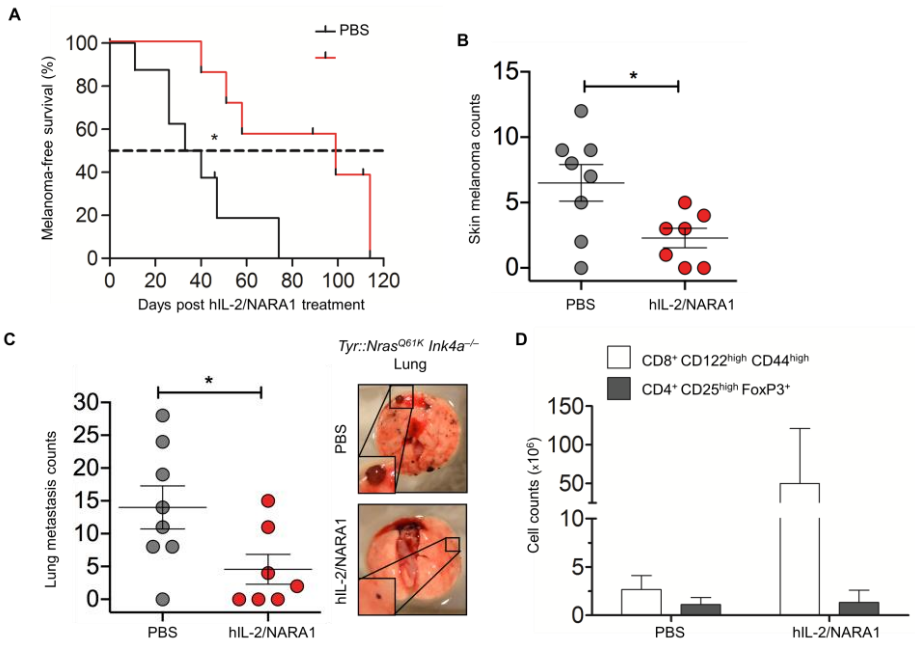

**Figure 7. Use of IL-2/NARA1 complex mediates efficient tumor and metastasis development immune control in a spontaneous melanoma model.** (**A** to **D**) Skin melanoma-free survival (**A**), skin melanoma counts (**B**) and lung metastasis counts (**C**) of *Tyr::N-Ras*$^{Q61K}$ *Ink4a*$^{-/-}$ mice, developing spontaneous melanoma, treated with 10 weekly courses of 4 injections of PBS or hIL-2/NARA1 complex. Shown are representative pictures of lung metastases. LNs and spleen were collected at the end of the experiment. Shown are total counts of indicated cell subsets in LNs (**D**). Data are represented as mean ± s.e.m. of one experiment with $n$ = 7-8. Differences between groups were analyzed using log-rank Mantel-Cox test (**A**) and unpaired Student's $t$-test (**B** to **C**).*$P$<0.05, **$P$<0.01, ***$P$<0.001, ****$P$<0.0001.

h) Conclusion

Using a rational screening approach we have identified a very rare anti-hIL-2 antibody, which based on structural, biophysical and functional data behaves as a high-affinity hCD25-mimetic. Application of hIL-2/NARA1 complex in established preclinical models of metastatic melanoma preferentially stimulates CD8$^+$ T and NK cells and favorably changes the intratumoral balance of effector to suppressor-type immune cells. Thus, hIL-2/NARA1 complex immunotherapy is particularly suitable for achieving strong anti-tumor immune responses. Moreover, the properties of hIL-2/NARA1 complex give insight into IL-2 biology and IL-2-based selective immunotherapy [55, 56].

In conclusion, use of hIL-2/NARA1 complex potentiates IL-2's *in vivo* bioactivity, while reducing its CD25-mediated adverse effects, thus warranting further development of this biologic for clinical cancer immunotherapy.

i) Supplementary information

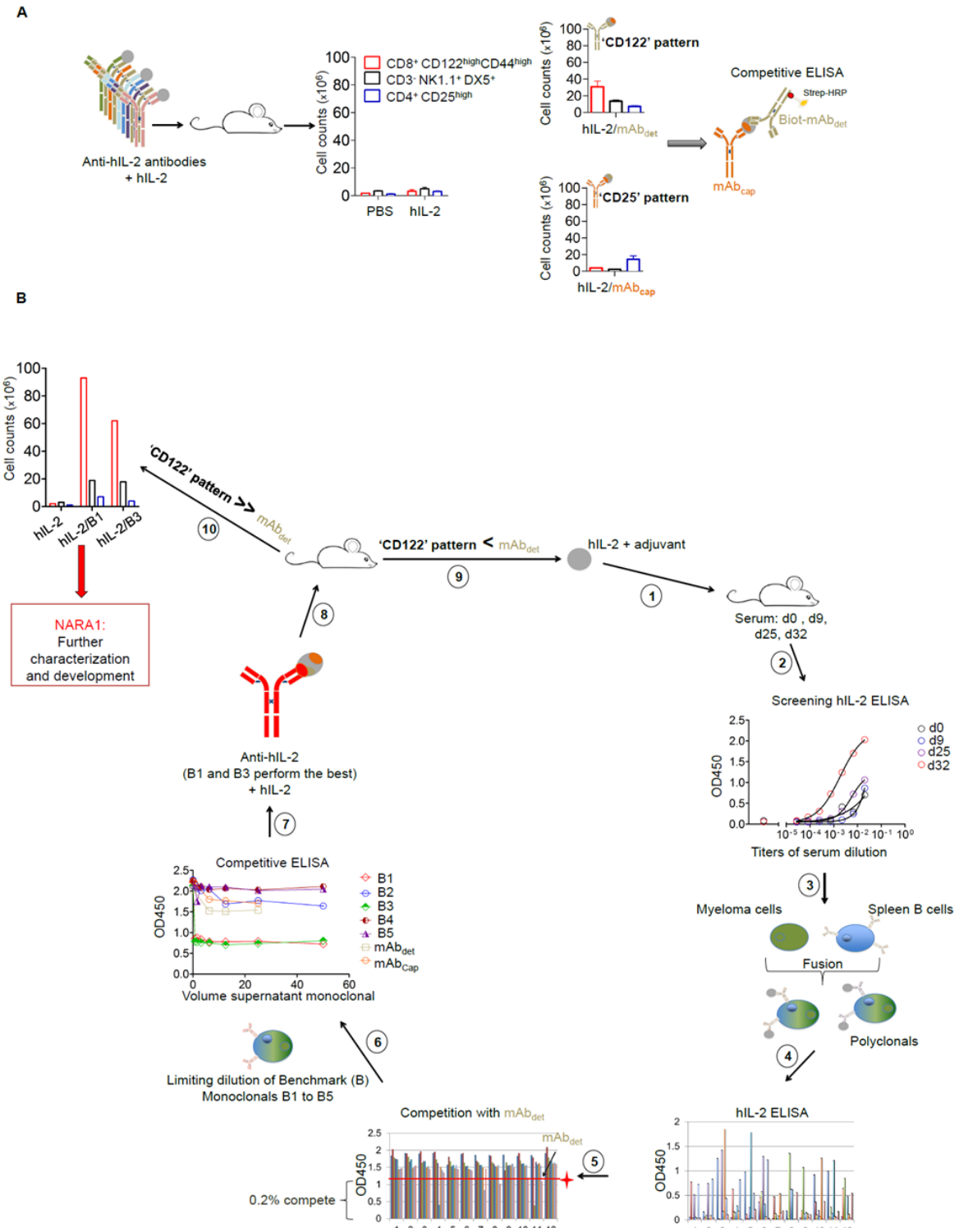

**Fig. S1. Rational biased screening method for generation of selective anti-human IL-2 antibodies.** (**A** and **B**) Complexes of human (h) IL-2 (1.5 µg) and various anti-hIL-2 monoclonal antibodies (mAbs; 15µg) were injected daily for 4 consecutive days. On day 5, lymph nodes (LNs) and spleen were analyzed for $CD122^{high}$ cells [60, 134], that is $CD44^{high}$ $CD8^{+}$ T cells and $CD3^{-}$ $NK1.1^{+}$ $DX5^{+}$ NK cells, versus $CD25^{high}$ $CD4^{+}$ T cells. The antibodies $mAb_{cap}$ and $mAb_{det}$ were chosen to establish a screening and competition ELISA (**A**, see Methods). Following immunization of mice with hIL-2, serum antibodies and polyclonals obtained from hybridomas were screened for hIL-2 binding and for their specificity in the competition ELISA. Candidates were diluted in order to obtain monoclonals which were further tested for competition and for *in vivo* expansion of the above-mentioned immune cell subsets. This process was repeated until appropriate anti-hIL-2 mAbs were identified (**B**).

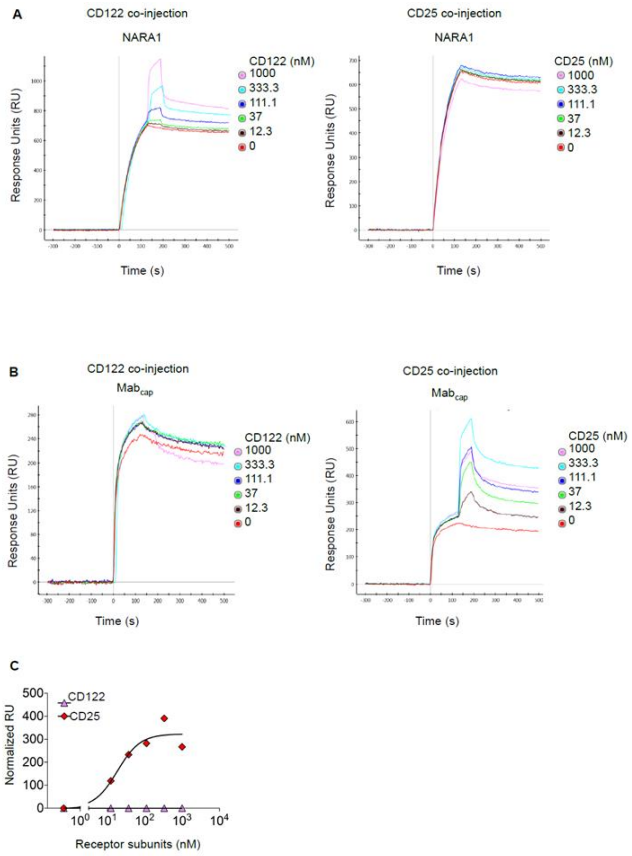


**Fig. S2. IL-2 interaction with CD122 and CD25 is different when bound to NARA1 or $mAb_{cap}$.** (**A** and **B**) Surface plasmon resonance (SPR) kinetic profiles of hCD122 and hCD25 interacting with immobilized NARA1 (**A**) or $mAb_{cap}$ (**B**) bound to hIL-2 at saturating concentration. (**C**) Equilibrium SPR titration of hCD122 and hCD25 interacting with

immobilized $mAb_{cap}$ bound to hIL-2 at saturating concentration. Data are representative of three independent experiments.

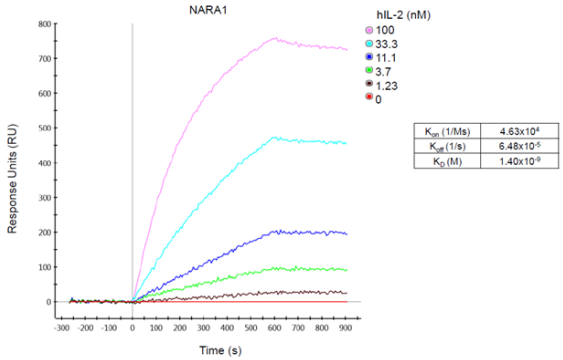


**Fig. S3. NARA1 binds to IL-2 with high affinity.** SPR kinetic profile of hIL-2 in 3-fold dilutions starting at 100 nM interacting with immobilized NARA1. Data are representative of three independent experiments.

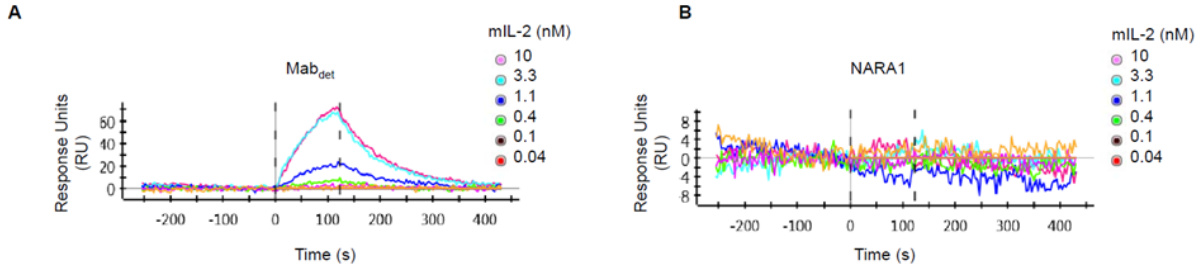


**Fig. S4. NARA1 does not crossreact with mouse IL-2.** (**A** and **B**) SPR kinetic profiles of mouse IL-2 (3-fold dilutions starting at 10 nM) with immobilized $mAb_{det}$ (**A**) or NARA1 (**B**). Data are representative of two independent experiments.

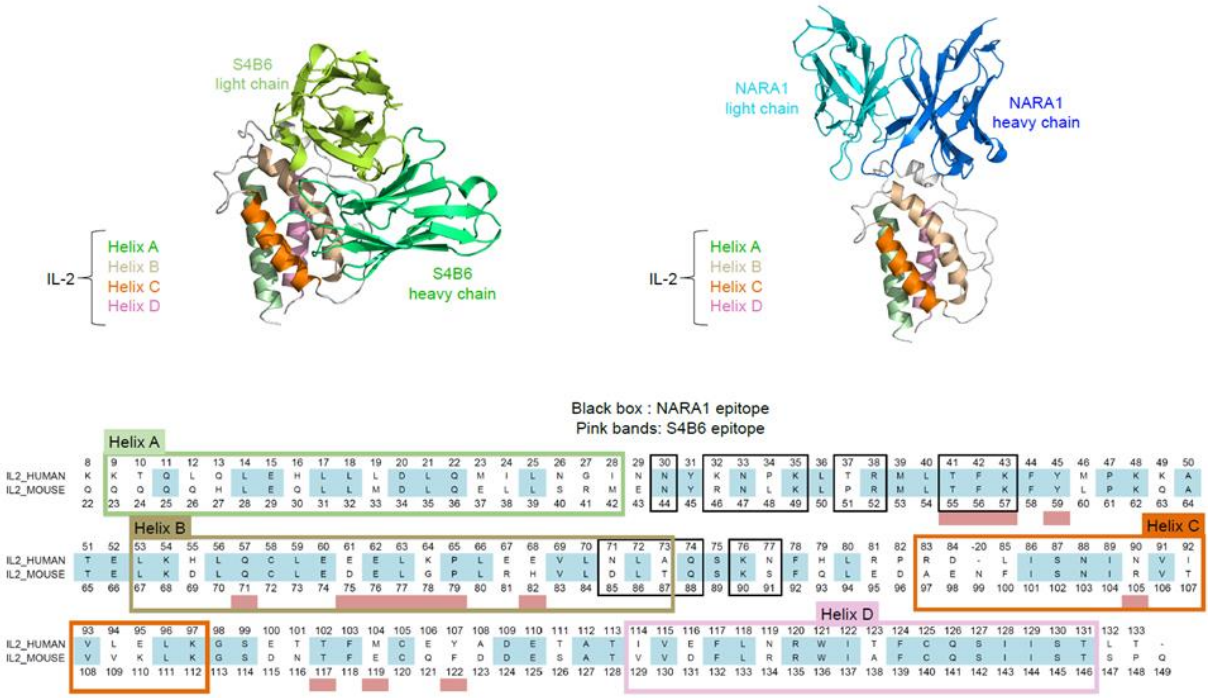


**Fig. S5. NARA1 binding sites differ from S4B6 epitopes on IL-2.** Alignment of human and mouse IL-2 sequences with indication of α-helices A, B, C, and D, and showing NARA1 (black boxes) and S4B6 epitopes (pink bands).

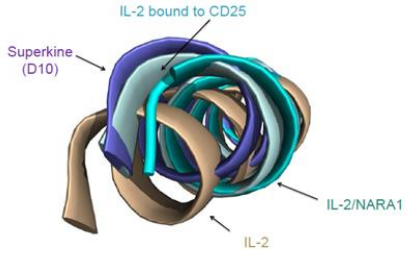


**Fig. S6. Binding to NARA1 induces a slight conformational change in hIL-2's helix C.** Shown are ribbon representations of helix C in unbound hIL-2 (gold; [174]), hIL-2 associated with hCD25 (cyan; ref. [174]), D10 hIL-2 mutein ('IL-2 superkine'; purple; [142]), and hIL-2 bound to NARA1 (turquoise).

.

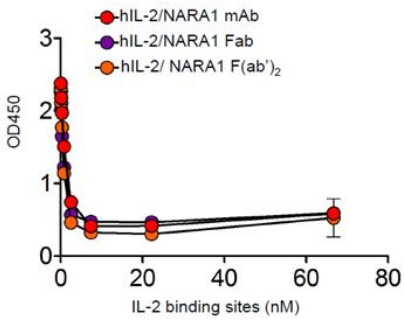


**Fig. S7. NARA1 Fab and F(ab')$_2$ fragments retain hIL-2 binding.** Equimolar amounts of hIL-2 binding sites of NARA1 full mAb, Fab or (Fab')$_2$ fragments were added to hIL-2 bound to mAb$_{cap}$. Biotinylated mAb$_{det}$ was added to check for competition of NARA1 antibody and fragments. Data are representative of two independent experiments.

| Antigen | Fluorophore | Company | Serial number |
|---|---|---|---|
| CD11b | BV650 | BD Biosciences | 563402 |
| CD122 | PE | eBioscience | 12-1221 |
| CD25 | APC | BD Biosciences | 557192 |
| CD3 | BV510 | BD Biosciences | 563024 |
| CD3 | FITC | eBioscience | 11-0031 |
| CD4 | BV605 | BioLegend | 100451 |
| CD44 | APC | eBioscience | 17-0441 |
| CD45.2 | Alexa-700 | BioLegend | 109822 |
| CD45.2 | BUV395 | BD Biosciences | 564616 |
| CD8a | Alexa 488 /efluor 450 | eBioscience | 53-0081/48-0081 |
| CD8b | APC-efluor 780 | eBioscience | 47-0083 |
| CD90.1 | eFluor 450 | eBioscience | 48-0900 |
| FoxP3 | PE | eBioscience | 12-5773 |
| Gr-1 | Alexa 488 | eBioscience | 53-5931 |
| IFN-γ | PE | eBioscience | 12-7311 |
| NK1.1 | FITC | eBioscience | 11-5941 |
| PD-1 | BV605 | BioLegend | 135219 |
| STAT5(pY694) | Alexa Fluor647 | BD Biosciences | 562076 |

**Table S1. Antibodies used for flow cytometry.**

2. Epigenetic modulation limits tumor escape during IL-2cx complex immunotherapy

Adapted from a manuscript submitted to Nature Medicine (Letter format)

**'The epigenetic repressor Ezh2 controls tumor escape mechanisms during immunotherapy'**

Natalia Arenas-Ramirez[1]*, Daniel Zingg[2]*, Rodney A. Rosalia[1], Ana T. Antunes[2], Jessica Haeusel[2], Lukas Sommer[2]† & Onur Boyman[1]†

[1] Department of Immunology, University Hospital Zurich, University of Zurich, CH-8091 Zurich, Switzerland

[2] Cell and Developmental Biology, Institute of Anatomy, University of Zurich, Winterthurerstrasse 190, CH-8057 Zurich, Switzerland

* These authors contributed equally to this work.

† These authors jointly supervised this work.

Correspondence: O.B. (onur.boyman@uzh.ch), L.S. (lukas.sommer@anatom.uzh.ch)

Keywords: cancer immunoediting, cancer immunosurveillance, immunotherapy, epigenetics, Ezh2, melanoma, CTLA-4, IL-2, PD-1, PD-L1

a) hIL-2/NARA1 antibody complexes (IL-2cx) immunotherapy is followed by selective suppression of EZh2 target genes

Engraftment of murine melanoma cells either of B16-F10 origin or isolated from tumors spontaneously developing in *Tyr::N-Ras*$^{Q61K}$ *Ink4a*$^{-/-}$ mice (termed RIM-3) [170] onto syngeneic *C57Bl/6* wild-type (*Wt*) mice (Extended Data Fig. 1) resulted in rapidly-growing melanoma nodules. Remarkably, in both B16-F10 and RIM-3 melanomas, interleukin-2 (IL-2)/NARA1 antibody complex (IL-2cx) [60, 134] immunotherapy caused an increase in Ezh2 expression (Extended Data Fig. 2). Interestingly, Ezh2$^{high}$ cells were found in tumor areas rich in CD45$^{+}$ leukocytes, whereas tumor sites with little immune cell infiltrates showed lower Ezh2 levels (Fig. 1a, b), suggesting that immune cells created a microenvironment promoting Ezh2 upregulation. Moreover, gain in Ezh2 was accompanied by a global increase in H3K27me3, indicating enhanced Ezh2 activity (Fig. 1c and Extended Data Fig. 2). Indeed, IL-2cx treatment of B16-F10-harbouring animals led to an enrichment of Ezh2 and H3K27me3 in promoter regions of major histocompatibility complex class I (MHC-I) molecules *H2-D1* and *H2-K1*, transporter associated with antigen *Tap1* and *Tap2*, proteasome subunits β8 and β9 (*Psmb8* and *Psmb9*), and a set of melanocyte lineage genes, including *Sox10*, *Mitf*, *Dct*, *Tyr*, *Tyrp1*, *Pmel*, *Mlana* and *Oca2* (Fig. 1d and Extended Data Fig. 3) [179, 180]. The products of these targets are involved in antigen processing and presentation and constitute known melanoma antigens, such as Trp2 and Pmel (also known as gp100) [181, 182]. As a result, these Ezh2 target genes (ETGs) became transcriptionally silenced in B16-F10 and RIM-3 melanomas from IL-2cx-treated mice. In contrast, expression of several genes previously connected to melanoma dedifferentiation and metastatic progression, including *Sox9*, *Snai1*, *Zeb1* and *CD271*, substantially increased (Fig. 1e and Extended Data Fig. 4)

[144, 183-185]. Notably, these changes were again most apparent in tumor areas with high immune cell infiltration (Fig. 1f, g). To demonstrate that IL-2cx-induced changes in gene expression were dependent on Ezh2, we blocked Ezh2 function using either a short hairpin RNA against *Ezh2* transcript (shEzh2) or GSK503, an EZH2-specific chemical inhibitor [173]. RNA interference (RNAi) effectively reduced Ezh2 levels *in vitro* and *in vivo*, while both approaches led to a considerable loss of H3K27me3 in melanoma samples, even in animals receiving IL-2cx (Fig. 1c and Extended Data Fig. 2). Importantly, upon *Ezh2* silencing, loss of Ezh2 and H3K27me3 was observed specifically in promoter regions of the aforementioned ETGs shown to be downregulated upon IL-2cx immunotherapy (Fig. 1d and Extended Data Fig. 3). Accordingly, Ezh2 inactivation resulted in upregulation of these ETGs and reduced expression of dedifferentiation genes, despite concomitant IL-2cx immunotherapy (Fig. 1e and Extended Data Figs. 4 and 5). This was most conspicuous for areas rich in $CD45^+$ immune cell infiltrates (Fig. 1f, g).

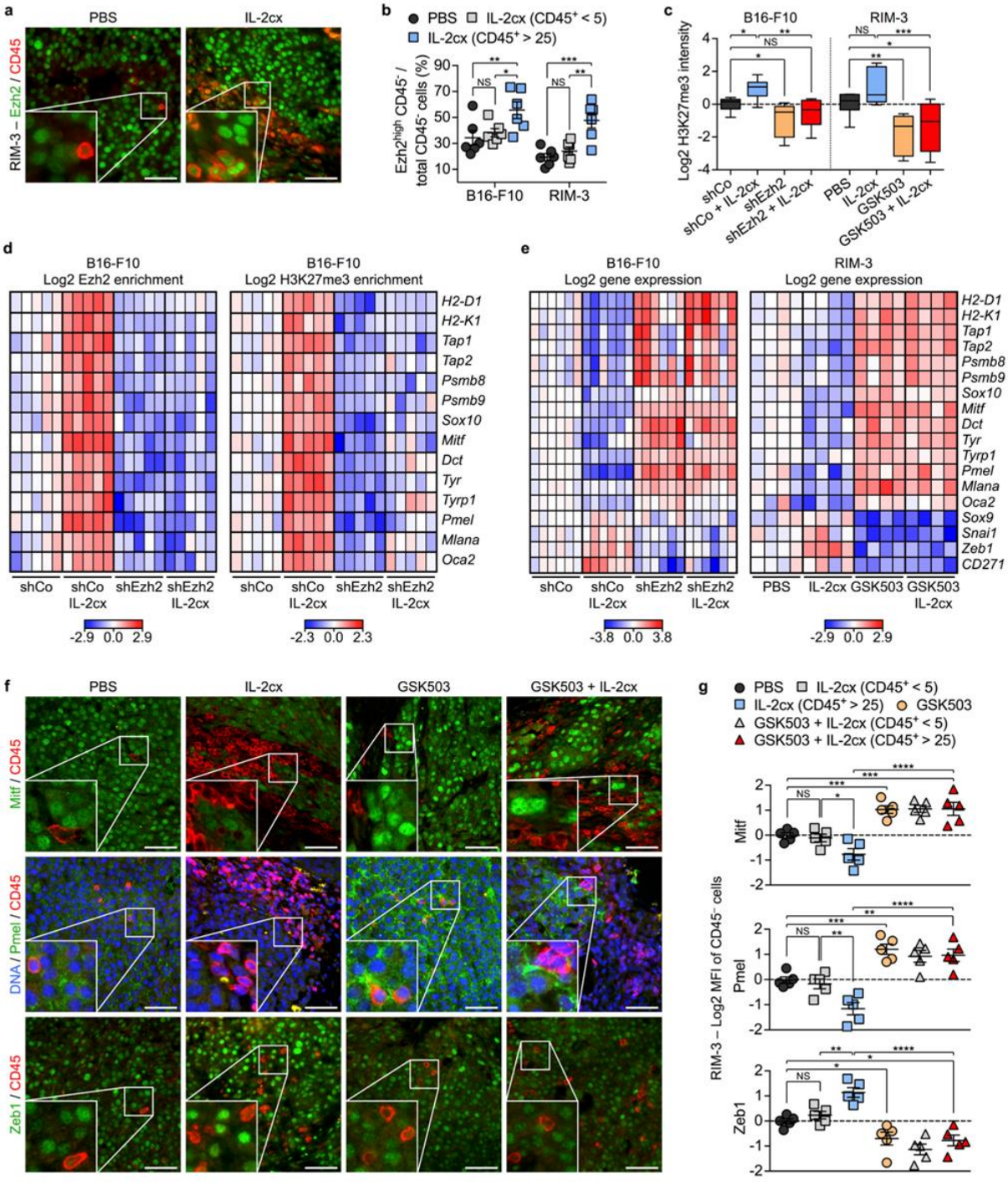


**Figure 1. Immunotherapy-induced Ezh2 promotes melanoma dedifferentiation and loss of immunogenicity. a**, **b**, Immunofluorescence staining for Ezh2 and CD45 and quantification of Ezh2$^{high}$ CD45$^{-}$ cells in areas poor or rich in CD45$^{+}$ cells (CD45$^{+}$ $n < 5$ versus $n > 25$ / field) in B16-F10 and RIM-3 from PBS or IL-2cx-treated mice. Scale bars, 50

μm. **c**, Quantification of Western blots for H3K27me3 (Extended Data Fig. 2c, d) on B16-F10 and RIM-3 following IL-2cx and/or Ezh2 inactivation with shEzh2 or GSK503. **d**, ChIP for Ezh2 and H3K27me3 and subsequent qPCR in promoter regions of selected loci on B16-F10 after IL-2cx and/or *Ezh2* silencing with shEzh2. Heat maps show values relative to intergenic region 1 (*Interg1*) and control (shCo) and summarise data from Extended Data Fig. 3. **e**, RT-qPCR for selected genes on B16-F10 and RIM-3 after IL-2cx and/or Ezh2 inactivation with shEzh2 or GSK503. Heat maps show values relative to control (shCo or PBS) and summarise data from Extended Data Fig. 4. **f**, **g**, Immunofluorescence stainings for Mitf, Pmel, Zeb1 and CD45 on RIM-3 following PBS, IL-2cx, GSK503, or GSK503 + IL-2cx to quantify mean fluorescence intensities (MFI) of Mitf, Pmel and Zeb1 in areas poor or rich in $CD45^+$ cells ($CD45^+$ $n < 5$ versus $n > 25$ / field). Scale bars, 50 μm. Data are represented as mean ± standard error of the mean (s.e.m.) of $n = 6$ (**b**), $n = 5$ (**g**), median ± 100% range of $n = 7$ (**c**) of two independent experiments. *P*-values calculated with analysis of variance (ANOVA) and Fisher's least significant difference (LSD) test. NS, not significant, $*P < 0.05$, $**P < 0.01$, $***P < 0.001$, $****P < 0.0001$.

b) <u>Ezh2 blockade synergizes with IL-2cx immunotherapy favoring the intratumoral accumulation of cytotoxic T cells</u>

Our data suggested that Ezh2 inactivation was sufficient to reverse immunotherapy-induced immune escape in melanoma cells. Indeed, *Ezh2* RNAi or IL-2cx as individual approaches were able to slow down B16-F10 growth *in vivo*, although tumors ultimately progressed. Significantly, a combination of both IL-2cx and *Ezh2* RNAi was most potent, reducing tumor volume by more than 80% (Fig. 2a and Extended Data Fig. 1). Similar effects were observed in mice harboring B16-F10 following injection of GSK503 + IL-2cx or GSK503 plus a blocking monoclonal antibody (mAb) against CTLA-4 (Fig. 2b, c and Extended Data Fig. 1). To uncover the mechanism of these anti-tumor effects, we dissected the cellular immune composition within tumors, analysing tumor-infiltrating lymphocytes (TILs), in comparison to tumor-draining lymph nodes (TDLNs) and spleen. Compared to control, IL-2cx

immunotherapy led to increased $CD8^+$ T cell counts in TILs, TDLNs and spleen, unlike GSK503, which affected neither proliferation nor expansion of these cells (Fig. 2d, e and Extended Data Fig. 6). Strikingly, accumulation of $CD8^+$ T cells was more prominent upon GSK503 + IL-2cx than in IL-2cx monotherapy, while $CD8^+$ T cell levels were comparable for both treatments in TDLNs and spleen (Fig. 2d, e and Extended Data Fig. 7). Contrarily, percentages and counts of other T cell subsets, including total $CD4^+$ T cells, $CD4^+$ $CD25^+$ $FoxP3^+$ Treg cells, natural killer (NK) cells, MHC-$II^+$ B and antigen-presenting cells, and $CD11b^+$ Gr-$1^+$ MDSCs were not significantly changed in TILs upon treatment, although some differences were noted in TDLNs and spleen (Fig. 2d, e and Extended Data Fig. 8). These effects resulted, upon GSK503 + IL-2cx combination therapy, in favorable ratios of $CD8^+$ T cells over Treg cells (15:1) and over MDSCs (45:1), respectively (Fig. 2f, g). These ratios were lower upon IL-2cx monotherapy and barely changed during GSK503 treatment in comparison to control animals. Thus, the anti-tumor effects of IL-2cx combined with Ezh2 blockade correlated with accumulation of effector $CD8^+$ T cells selectively within the tumor in disfavor of suppressor-type immune cells.

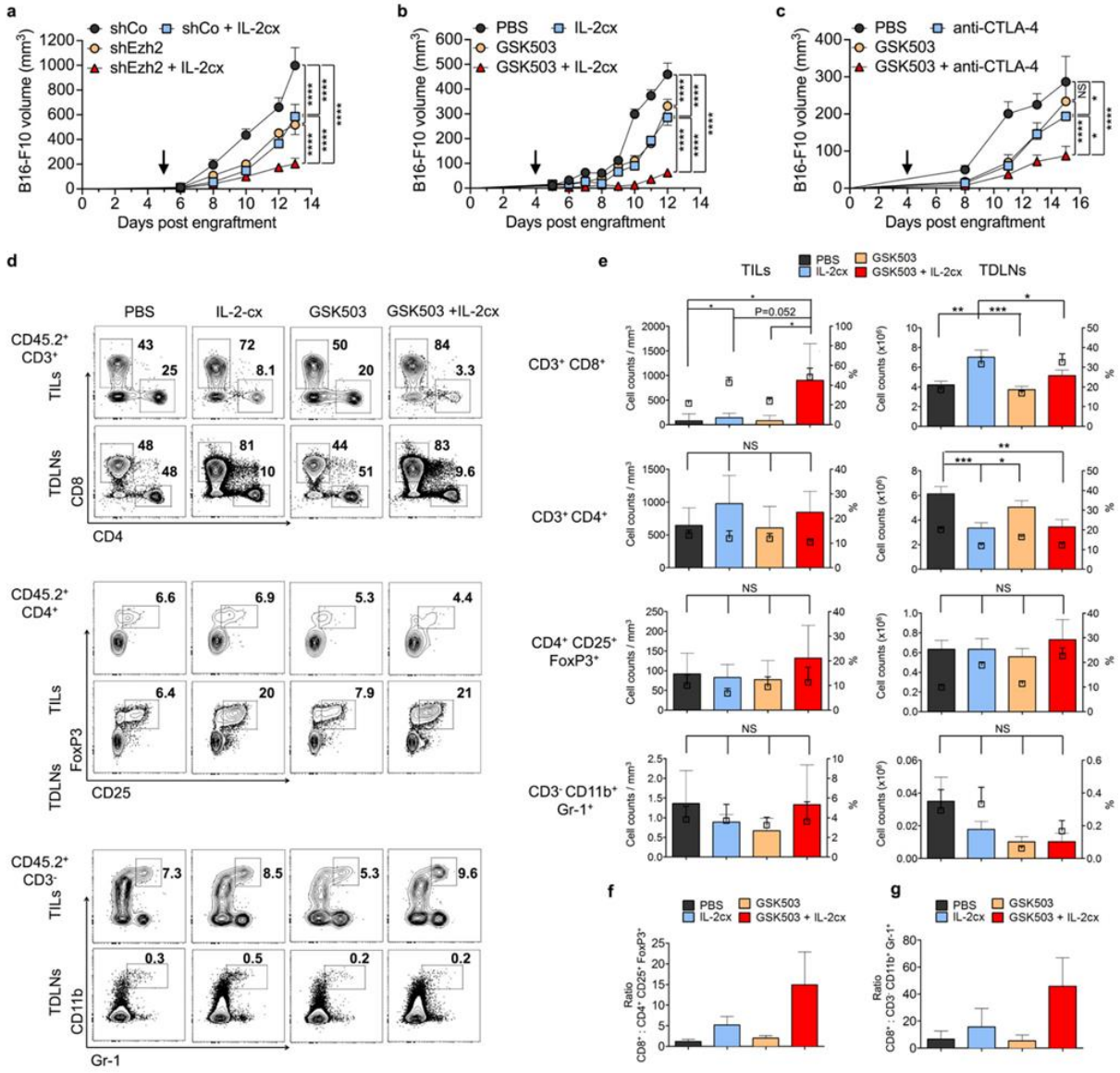


**Figure 2. Ezh2 inactivation enhances anti-melanoma immunotherapy by facilitating intratumoral CD8$^+$ T cell accumulation. a–c**, Tumor growth kinetics in mice engrafted with shCo or shEzh2-transfected B16-F10 melanoma cells and receiving PBS or IL-2cx (**a**), engrafted with B16-F10 cells and receiving PBS, IL-2cx, GSK503, or GSK503 + IL-2cx (**b**), or PBS, anti-CTLA-4 mAb, GSK503, or GSK503 + anti-CTLA-4 mAb (**c**). Black arrows indicate time-point of treatment start. **d**, **e**, Flow cytometry analyses of tumor-infiltrating lymphocytes (TILs) and tumor-draining lymph nodes (TDLNs) from mice harbouring B16-F10 and treated as in (**b**), with quantifications of total cell counts (**e**, left axes, coloured bars) and percentages (**e**, right axes, square points) of indicated immune cell subsets. **f**, **g**, Ratios of CD8$^+$ T cells versus CD4$^+$ CD25$^+$ FoxP3$^+$ regulatory T cells (**f**)

and $CD3^-$ $CD11b^+$ $Gr\text{-}1^+$ myeloid-derived suppressor cells (**g**). Data are represented as mean ± s.e.m. of $n = 15$ (**a**), $n = 25$ (**b**), $n = 4$ (**c,** PBS), $n = 6$ (**c,** GSK503), $n = 5$ (**c,** anti-CTLA-4 +/- GSK503), $n = 6$ (**e**, $CD8^+$ and $CD4^+$ TILs), $n = 4$ (**e**, $CD4^+$ $CD25^+$ $FoxP3^+$ and $CD3^-$ $CD11b^+$ $Gr\text{-}1^+$ TILs), $n = 17$ (**e**, $CD8^+$, $CD4^+$ and $CD4^+$ $CD25^+$ $FoxP3^+$ TDLNs), $n = 9$ (**e**, $CD3^-$ $CD11b^+$ $Gr\text{-}1^+$ TDLNs), $n = 4$ (**f**) and $n = 3$ (**g**) of three (**a**), six (**b**, **d**–**g**), and two independent experiments (**c**). For TILs, samples of mice receiving the same treatment were pooled prior to analysis. *P*-values calculated with ANOVA and Fisher's LSD test (**a**–**c**), unpaired Student's *t*-test (**e,** total cell counts). $*P < 0.05$, $**P < 0.01$, $***P < 0.001$, $****P < 0.0001$.

c) Ezh2 blockade and IL-2cx immunotherapy combination suppress the PD-1/PDL-1 pathway in the tumor site

Negative costimulatory molecules, including PD-1 and its ligand PD-L1, contribute to an immunosuppressive tumor microenvironment [83, 105, 108]. High PD-1 expression marks effector T cells that become exhausted when faced with antigen persistance and progressively lose effector functions, including IFN-γ production [145]. In contrast to TDLNs where PD-1 levels on $CD8^+$ T cells were low in all groups, $CD8^+$ T cells from TILs of control mice expressed very high levels of PD-1, both in percentages and mean fluorescence intensity (MFI) (Fig. 3a). Conversely, percentages of $PD\text{-}1^+$ $CD8^+$ T cells were roughly halved in TILs of animals receiving either IL-2cx or GSK503, and even further decreased with combination therapy (Fig. 3a, b), indicating that GSK503 + IL-2cx prevented tumor-infiltrating $CD8^+$ T cells from rapid exhaustion.PD-L1 is frequently elevated on tumor cells [105, 108]. Interestingly, IL-2cx immunotherapy promoted PD-L1 upregulation in $Pax3^+$ melanoma cells, particularly in areas rich in $CD3^+$ TILs (Fig. 3c, d). This was in line with the observed increase of Zeb1 upon IL-2cx (Fig. 1 and Extended Data Fig. 4), which has been shown to transcriptionally enhance PD-L1 expression [186]. However, Ezh2 inactivation led to reduced

PD-L1 mRNA levels and a decrease in PD-L1$^{+}$ Pax3$^{+}$ melanoma cells, which was maintained during concomitant IL-2cx treatment (Fig. 3c, d and Extended Data Fig. 9). The downregulation of the immunosuppressive PD-1–PD-L1 axis by Ezh2 blockade plus IL-2cx combination therapy was remarkably efficient, even when treatment was initiated only after the formation of visible tumor nodules. Consequently, addition of a blocking anti-PD-1 mAb did not further improve the anti-tumor effects of GSK503 or IL-2cx (Fig. 3e).

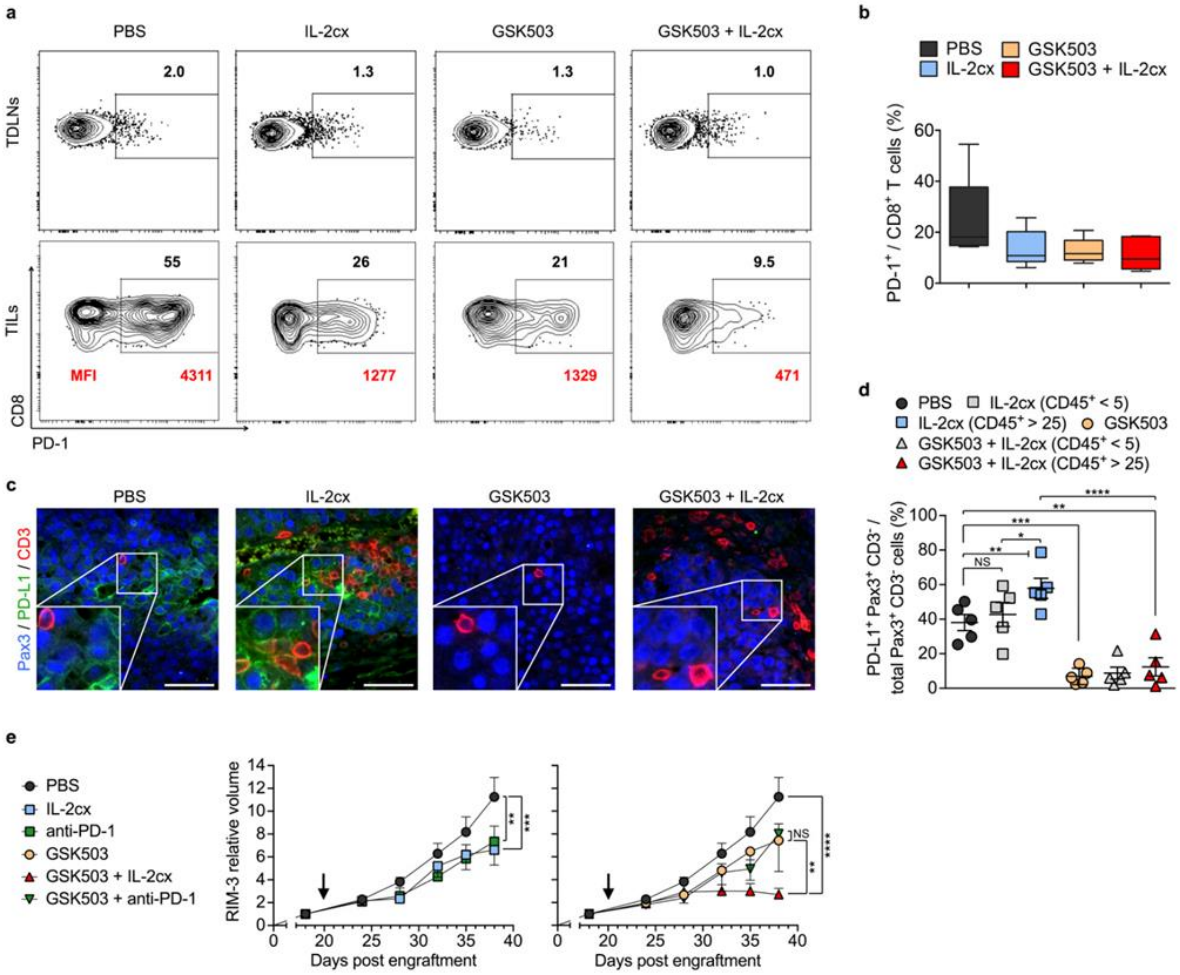


**Figure 3. Immunotherapy and Ezh2 blockade synergistically suppress PD-1–PD-L1 axis. a**, **b**, PD-1 expression on CD8$^{+}$ T cells by percentages (**a**, **b**) and MFI (**a**) in TDLNs (**a**, upper panels) and TILs (**a**, lower panels, and **b**). **c**, **d**, Immunofluorescence staining for Pax3, PD-L1 and CD3 on RIM-3 following PBS, IL-2cx, GSK503, or GSK503 + IL-2cx, and

quantification of $Pax3^+$ $PD\text{-}L1^+$ cells in areas poor or rich in $CD3^+$ cells ($CD3^+$ $n < 5$ versus $n > 25$ / field). Scale bars, 50 μm. **e**, Growth of RIM-3 tumors during IL-2cx, anti-PD-1 mAb, GSK503, or indicated combinations thereof. Black arrows indicate time-point of treatment start. Data are represented as mean ± s.e.m. of $n = 5$ (**b, d**, **e**) of six (**b**) and two independent experiments (**e**). For TILs, samples of mice receiving the same treatment were pooled prior to analysis. *P*-values calculated using ANOVA and Fisher's LSD test. $*P < 0.05$, $**P < 0.01$, $***P < 0.001$, $****P < 0.0001$.

d) IFN-γ producing CD8+ T cells mediate the anti-tumor effects observed upon IL-2cx immunotherapy and Ezh2 blocked

The demonstration in animals receiving Ezh2 inhibitor plus IL-2cx that $CD8^+$ T cells predominated TILs and expressed very low PD-1 levels suggested that tumor control depended on these effector cells. We thus compared combination therapy using GSK503 + IL-2cx in *Wt* mice versus animals lacking both T cell receptor (TCR)$\alpha\beta^+$ and TCR$\gamma\delta^+$ T cells (*Tcrbd*$^{-/-}$ mice). Moreover, we used mice deficient in the recombinase-activating gene 1 (*Rag1*$^{-/-}$), as they lack T and B cells, but harbor functional NK cells. The anti-melanoma effect of combination therapy was lost in both *Tcrbd*$^{-/-}$ and *Rag1*$^{-/-}$ mice (Fig. 4a), thus demonstrating that T cells, but neither B nor NK cells, exerted the tumoricidal effects. Further experiments using specific depleting mAbs showed that $CD8^+$, but not $CD4^+$ T cells, played a crucial role in the anti-tumor response. Thus, during GSK503 + IL-2cx treatment, tumor control was lost in animals injected with anti-CD8 depleting mAb, while mice receiving anti-CD4 depleting mAb were able to fully suppress tumor growth (Fig. 4b). Previously, $CD8^+$ T cell anti-tumor function has been linked to IFN-γ and TNF-α production [83, 115, 144]. Notably, the anti-tumor effect of IL-2cx plus Ezh2 blockade depended on IFN-γ production, whereas TNF-α was dispensable or even pro-tumorigenic, as demonstrated using *Ifng*$^{-/-}$ and *Tnfa*$^{-/-}$ mice (Fig. 4c). In line with these data, TNF-α production by $CD4^+$ and $CD8^+$ T cells

was not significantly altered in GSK503 + IL-2cx-treated animals (Extended Data Fig. 10). However, both CD90.1$^{-}$ polyclonal CD8$^{+}$ and, upon adoptive transfer, also CD90.1$^{+}$ Pmel-specific TCR-transgenic CD8$^{+}$ T cells produced high IFN-γ levels when isolated from mice receiving GSK503 + IL-2cx combination therapy, whereas IFN-γ production was lower in cells originating from the other groups as well as in CD4$^{+}$ T cells (Fig. 4d and Extended Data Fig. 10). This correlated with the strong intratumoral Pmel upregulation upon Ezh2 inactivation (Fig. 1d-g and Extended Data Figs. 3 and 4) and suggested that intratumoral IFN-γ production facilitated killing of tumor cells. Accordingly, *ex vivo* cytotoxic activity of CD8$^{+}$ T cells, as assessed using the degranulation marker CD107a, was highest following combination immunotherapy, as shown by higher numbers of CD107a$^{+}$ CD8$^{+}$ T cells within TILs from animals treated with IL-2cx plus Ezh2 blockade (Fig. 4e).

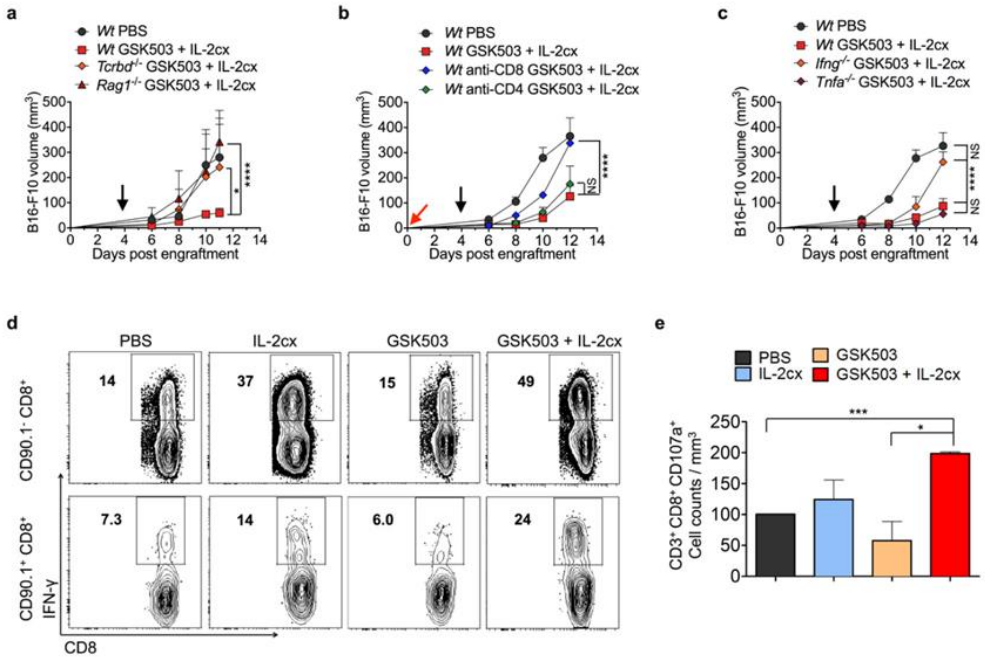


**Figure 4. Ezh2 inhibition plus IL-2 immunotherapy depends on IFN-γ-producing cytotoxic CD8$^{+}$ T cells. a**–**c**, Growth of B16-F10 tumors during PBS versus GSK503 + IL-2cx combination therapy in *Wt*, *Tcrbd*$^{-/-}$, and *Rag1*$^{-/-}$ (**a**), *Wt* depleted of CD4$^{+}$ or CD8$^{+}$ T cells using mAbs (**b**), or *Ifng*$^{-/-}$ and *Tnfa*$^{-/-}$ mice (**c**). Black arrows indicate time-point of

treatment start, red arrow start of mAb injection. **d**, IFN-γ production by CD90.1$^{-}$ endogenous (upper) and CD90.1$^{+}$ Pmel-specific CD8$^{+}$ T cells (lower panels) from TDLNs of B16-F10-grafted mice receiving PBS, IL-2cx, GSK503, or GSK503 + IL-2cx. **e**, Degranulating CD107a$^{+}$ CD8$^{+}$ T cells per mm$^{3}$ tumor from mice treated as in (**d**). Data are represented as mean ± s.e.m. of $n = 8$ (**a**), $n = 6$ (**b**), $n = 9$ (**c**), $n = 2$ (**e**) of two (**a**–**c**, **e**) and three independent experiments (**d**). For TILs, samples of mice receiving the same treatment were pooled prior to analysis. *P*-values calculated with ANOVA and Bonferroni correction (**a**–**c**), unpaired Student's *t*-test (**e**). *$P < 0.05$, **$P < 0.01$, ***$P < 0.001$, ****$P < 0.0001$.

e) Conclusion

Collectively, we show that, during immunotherapy, increased Ezh2 activity reshapes the epigenomic landscape resulting in melanoma dedifferentiation, loss of immunogenicity and upregulation of the PD-1–PD-L1 axis. These mechanisms favour tumor cell-intrinsic and extrinsic immune escape through exhaustion of IFN-γ-producing cytotoxic CD8$^{+}$ T cells and likely complement the recently demonstrated epigenetic repression of CD8$^{+}$ T cell-trafficking to the tumor site [187]. Therefore, Ezh2 inactivation locks melanoma in an immunogenic state and facilitates efficient CD8$^{+}$ T cell-mediated anti-tumor responses during immunotherapy. Thus, targeting of EZH2 is an attractive strategy to combine with cancer immunotherapy.

f) Supplementary information

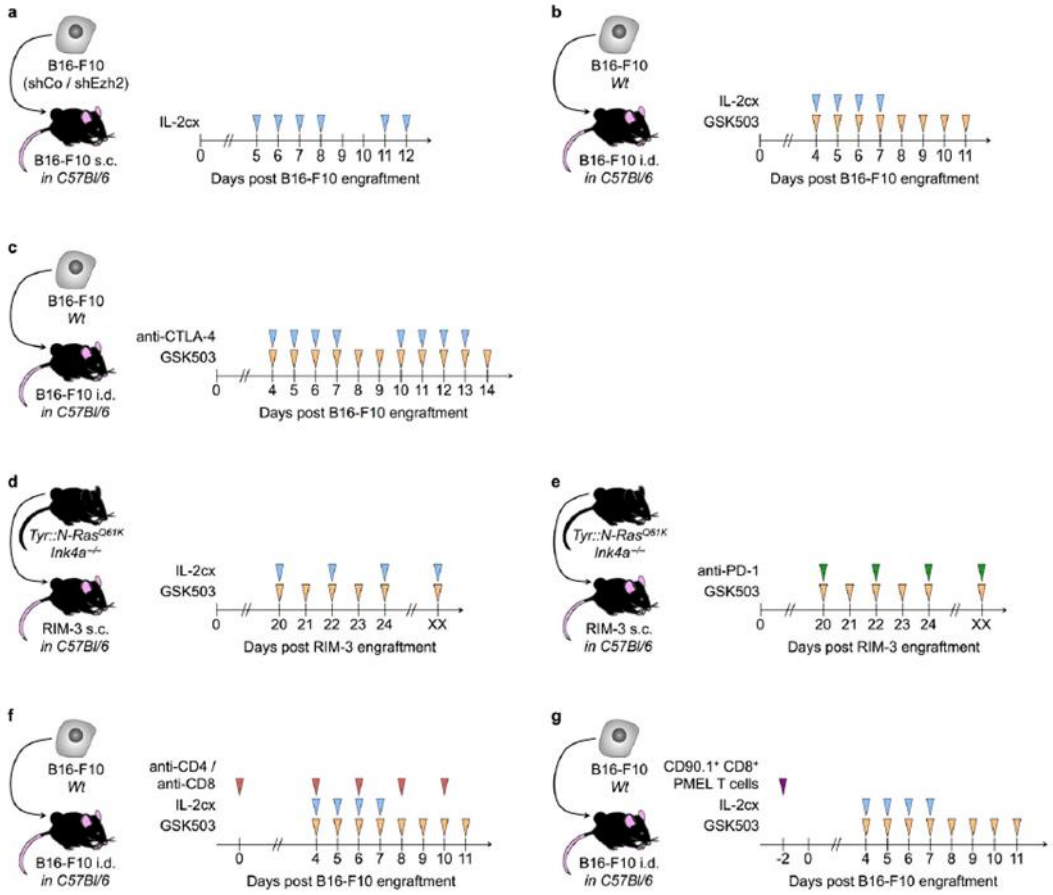


**Extended Data Figure 1. Experimental setups used. a**, Strategy used to administer IL-2/anti-IL-2 antibody complexes (IL-2cx) to mice harbouring shCo or shEzh2-transfected B16-F10 melanoma. **b**–**e**, Strategies used to administer IL-2cx, anti-CTLA-4 monoclonal antibody (mAb), anti-PD-1 mAb immunotherapy and GSK503 Ezh2 inhibitor to mice harbouring B16-F10 or RIM-3 (*Tyr::N-Ras*$^{Q61K}$ *Ink4a*$^{-/-}$ melanoma 3). **f**, **g**, Strategies used to deplete CD4$^{+}$ and CD8$^{+}$ cells (**f**) or to adoptively transfer CD90.1$^{+}$ CD8$^{+}$ Pmel T cells (**g**) in mice harbouring B16-F10 and treated as in **c**.

i.d., intradermal; s.c., subcutaneous.

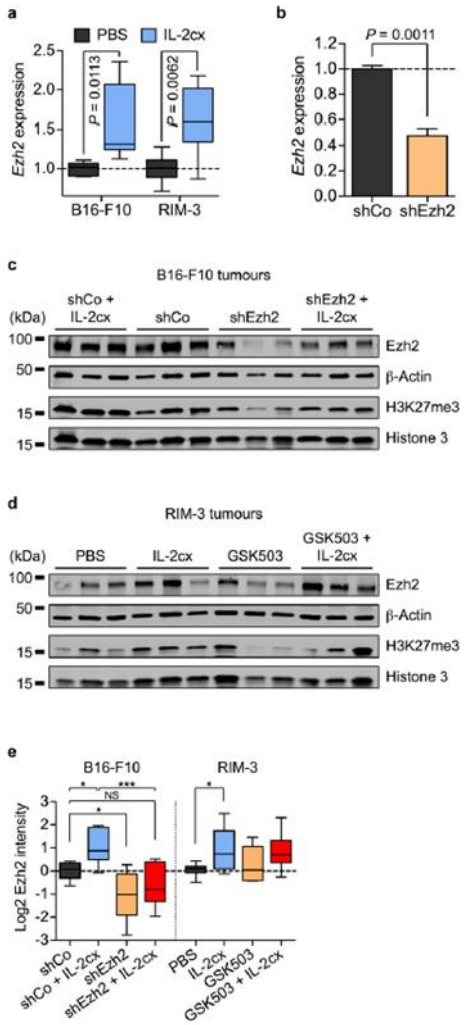


**Extended Data Figure 2. Ezh2 inactivation reverses IL-2cx-promoted Ezh2 activity.a**, RT-qPCR for *Ezh2* on B16-F10 and RIM-3 melanoma biopsies after IL-2cx application as in Extended Data Fig. 1.**b**, RT-qPCR for *Ezh2* on *in vitro*-cultured B16-F10 cells after transfection with a scrambled shRNA (shCo)-expressing or a shEzh2-expressing plasmid. **c**–**e**, Western blots for Ezh2 and H3K27me3 on B16-F10 (**c**) and RIM-3 (**d**) after IL-2cx application and/or Ezh2 inactivation using shEzh2 or GSK503 and quantifications of Ezh2 protein levels (**e**). H3K27me3 level quantifications are shown in Fig. 1c. Data are represented as median ± 100% range of $n = 6$ (**a**), mean ± s.e.m. of $n = 3$ (**b**) of two independent (**a**, **e**) and one experiment (**b**). *P* values calculated with Student's *t*-test. NS, not significant, $*P < 0.05$, $**P < 0.01$, $***P < 0.001$, $****P < 0.0001$.

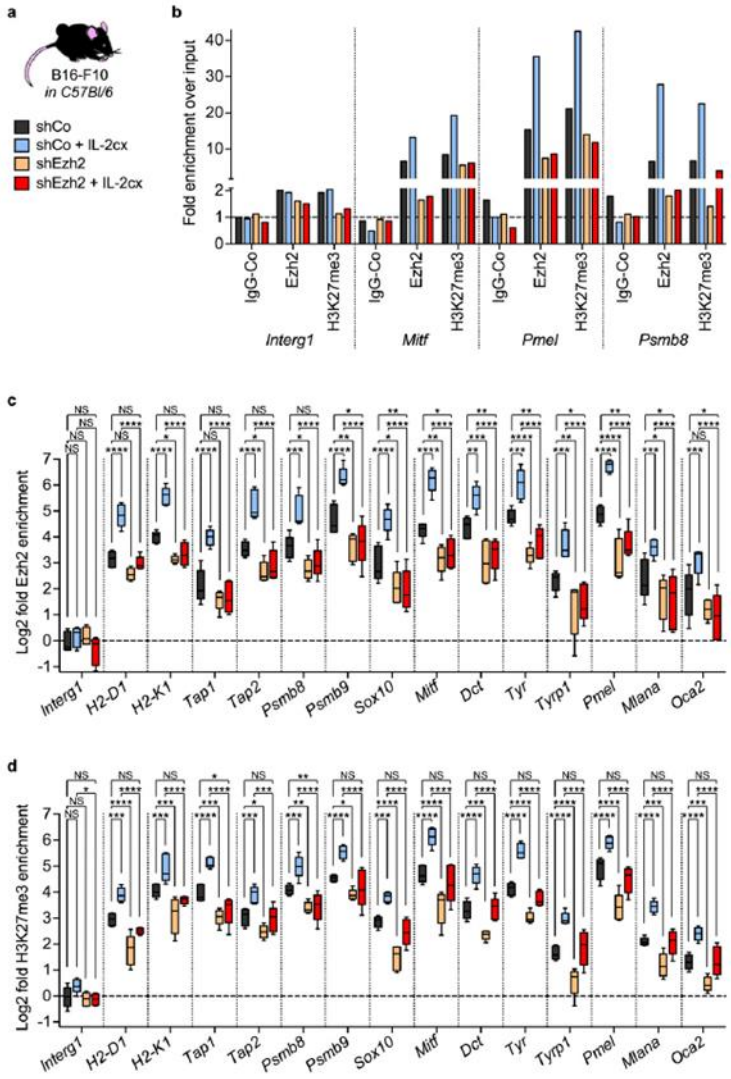


**Extended Data Figure 3. Ezh2 silencing reverses IL-2cx-promoted Ezh2 and H3K27me3 enrichment at promoters of selected loci. a**, Graphical representation of model system and colour coding for experimental groups. **b**, ChIP using IgG control antibody (IgG-Co) and antibodies against Ezh2 and H3K27me3 and subsequent qPCR for promoters of selected loci and intergenic region 1 (*Interg1*) on B16-F10 melanomas after IL-2cx administration and/or Ezh2 depletion using shEzh2. **c**, **d**, Ezh2 and H3K27me3 specific ChIP and subsequent qPCR for promoters of selected loci and *Interg1* on B16-F10 melanomas after IL-2cx administration and/or Ezh2 depletion using shEzh2. Data summarized in heat maps of Fig. 1d. Data are represented as mean of $n = 2$ (**b**), median ± 100% range of $n = 5$ (**c**, **d**) of one experiment (**a**)

and two independent experiments (**c**, **d**). *P*-values calculated using ANOVA and Fisher's LSD test. **P* < 0.05, ***P* < 0.01, ****P* < 0.001, *****P* < 0.0001.

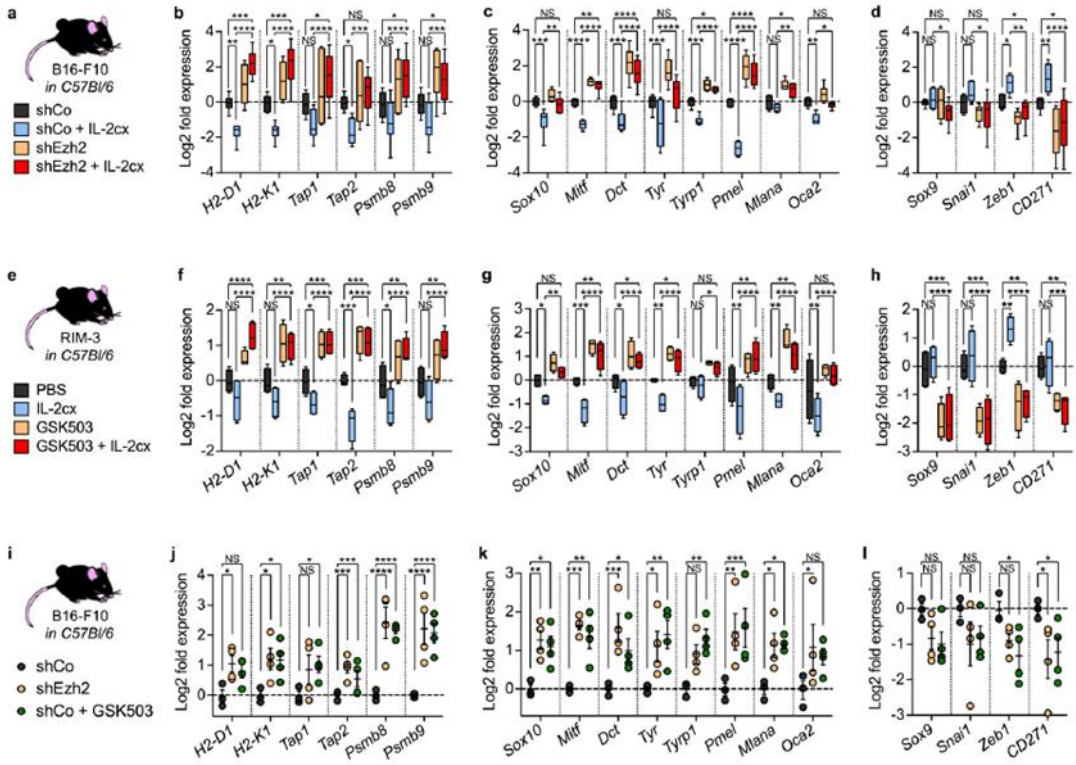


**Extended Data Figure 4. Ezh2 silencing reverses IL-2cx-promoted changes in gene expression. a**, **e**, **i**, Graphical representations of model systems and colour coding for experimental groups. **b**–**d**, **f**–**h**, RT-qPCR for selected genes on B16-F10 or RIM-3 melanomas after IL-2cx administration and/or Ezh2 inactivation using shEzh2 or GSK503. Data summarized in heat maps of Fig. 1e. **j**–**l**, RT-qPCR for selected genes on B16-F10 melanomas after Ezh2 inactivation using either shEzh2 or GSK503. Data are represented as median ± 100% range of *n* = 6 (**b**–**d**), *n* = 4 (**f**–**h**), mean ± s.e.m. of *n* = 3 (**j**–**l**, shCo), *n* = 4 (**j**–**l**, shEzh2, shCo + GSK503) of two independent experiments (**a**–**h**) and one experiment (**i**–**l**). *P* values calculated with ANOVA and Fisher's LSD test. **P* < 0.05, ***P* < 0.01, ****P* < 0.001, *****P* < 0.0001.

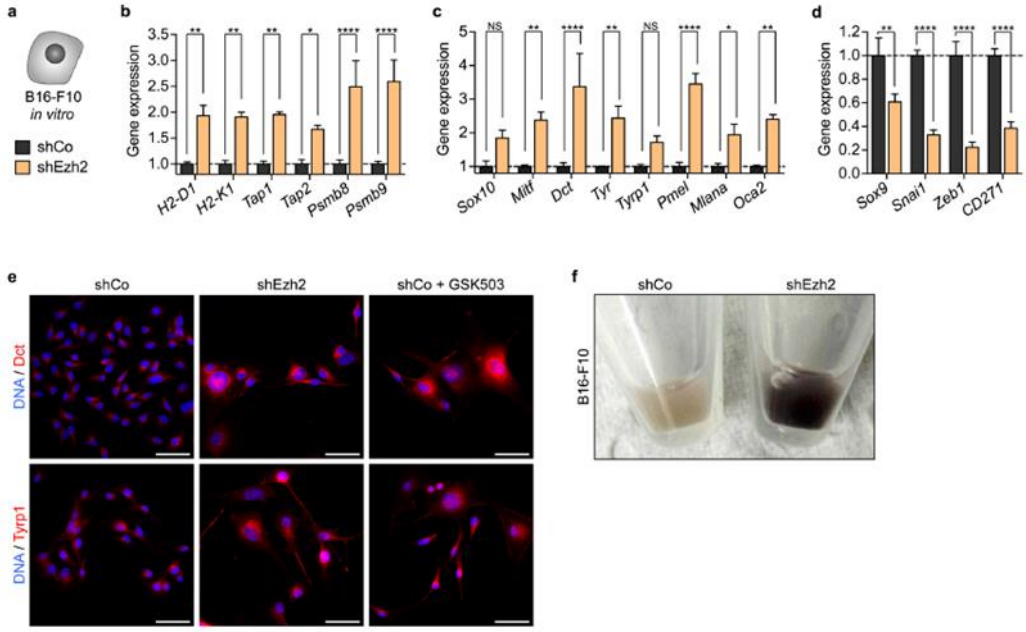


**Extended Data Figure 5. Ezh2 silencing induces *in vitro* B16-F10 differentiation. a**, Graphical representations of model system and colour coding for experimental groups. **b**–**d**, RT-qPCR for selected genes on B16-F10 cultures after *Ezh2* silencing using shEzh2. **e**, Immunofluorescent staining for Dct and Tyrp1 on B16-F10 cells after Ezh2 inactivation using either shEzh2 or GSK503. Scale bars, 50 μm. **f**, Macroscopic picture of B16-F10 cell pellets after *Ezh2* silencing using shEzh2. Data are represented as mean ± s.e.m. of $n = 3$ of two independent experiments. *P*-values calculated with ANOVA and Fisher's LSD test. *$P < 0.05$, **$P < 0.01$, ***$P < 0.001$, ****$P < 0.0001$.

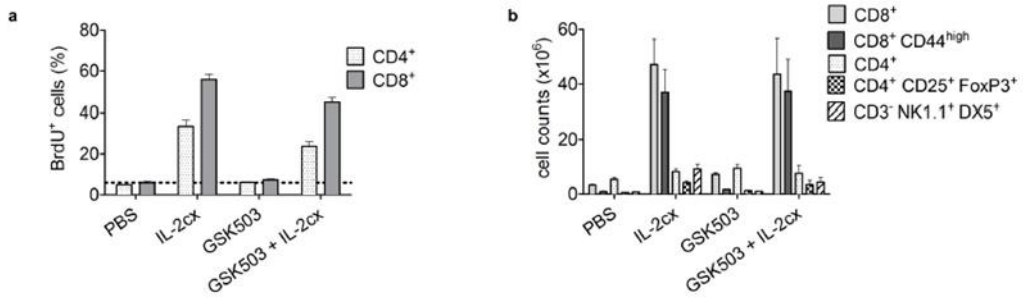


**Extended Data Figure 6. Ezh2 inhibition does not affect cell proliferation or expansion of T cells and NK cells. a**, **b**, Mice received PBS, IL-2cx, GSK503, or GSK503 + IL-2cx for four days. On the last 3 days animals also received bromodeoxyuridine (BrdU; 0.8 mg/ml) in

their drinking water. On day 5, mice were euthanized and analysed for proliferating $BrdU^+$ $CD4^+$ and $CD8^+$ T cells (**a**) and total cell counts of $CD8^+$ T cells, memory-phenotype $CD44^{high}$ $CD8^+$ T cells, $CD4^+$ T cells, $CD4^+$ $CD25^+$ forkhead box P3 $(FoxP3)^+$ regulatory T cells, and $CD3^-$ $NK1.1^+$ $DX5^+$ natural killer (NK) cells in spleen (**b**). Data are represented as mean ± s.e.m. of $n = 2$ (PBS), $n = 3$ (GSK503 and IL-2cx), $n = 4$ (GSK503 + IL-2cx) of two independent experiments.

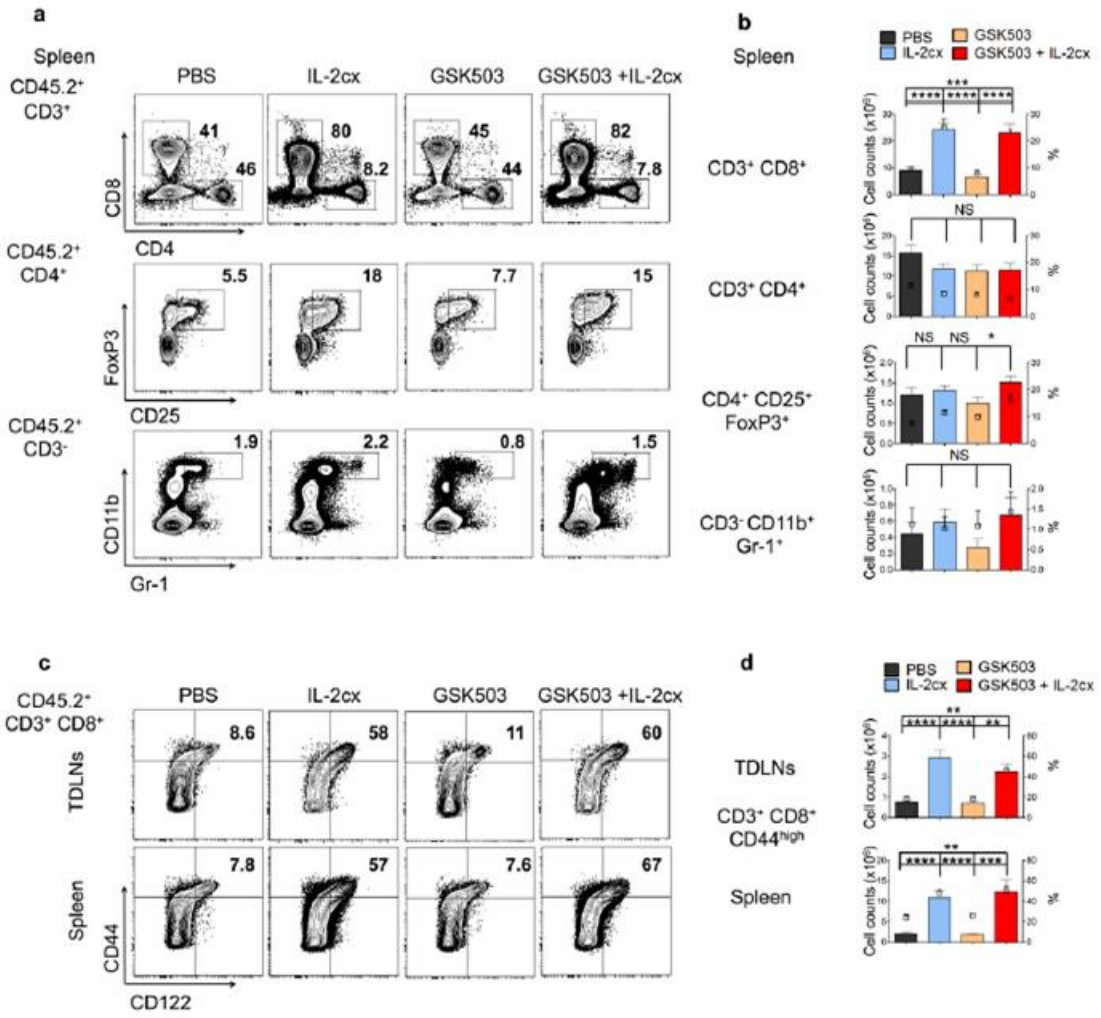


**Extended Data Figure 7. Effects on T cell subsets and suppressor-type immune cells upon combination of Ezh2 inhibition and IL-2cx immunotherapy. a-d**, Flow cytometry analyses of indicated markers in spleen (**a** and **c**) and tumor-draining lymph nodes (TDLNs; **c**) from mice harbouring B16-F10 and treated as in Fig. 2b, and quantification of total cell counts and percentages of $CD3^+$ $CD8^+$ T cells, $CD3^+$ $CD4^+$ T cells, $CD4^+$ $CD25^+$ $FoxP3^+$

regulatory T cells, and CD3$^{-}$ CD11b$^{+}$ Gr-1$^{+}$ myeloid-derived suppressor cells (MDSCs) in spleen (**b**) and CD44$^{high}$ CD8$^{+}$ T cells in spleen and TDLNs (**d**). Data are represented as mean ± s.e.m. of $n$ = 17 (**b**, CD8$^{+}$, CD4$^{+}$ and CD4$^{+}$ CD25$^{+}$ FoxP3$^{+}$), $n$ = 9 (**b**, CD3$^{-}$ CD11b$^{+}$ Gr-1$^{+}$), and $n$ = 14 (**d**, CD44$^{high}$ CD8$^{+}$ T cells) of six independent experiments. $P$-values calculated with unpaired Student's $t$-test **(b**, **d)**. *$P$ < 0.05, **$P$ < 0.01, ***$P$ < 0.001, ****$P$ < 0.0001.

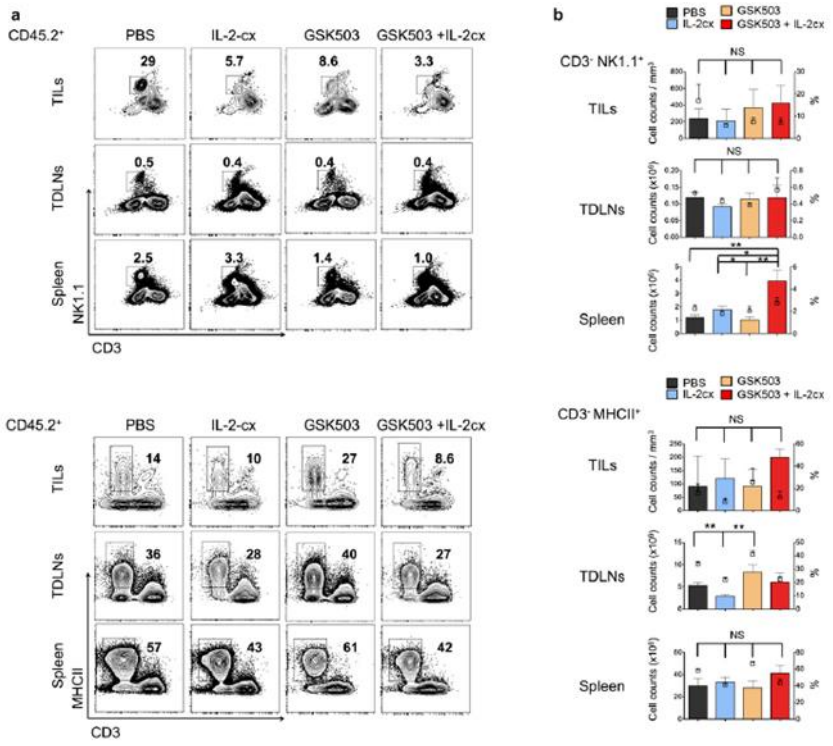


**Extended Data Figure 8. Effects of combination of Ezh2 inhibition and IL-2cx immunotherapy on NK cells, B cells, and antigen-presenting cells. a**,**b**, Flow cytometry analyses of indicated markers in tumor-infiltrating lymphocytes (TILs), TDLNs and spleen from mice harbouring B16-F10 and treated as in Fig. 2b, and quantification of total cell counts and percentages of CD3$^{-}$ NK1.1$^{+}$ NK cells (top three panels) and CD3$^{-}$ MHC-II$^{+}$ B and antigen-presenting cells (lower three panels). Data are represented as mean ± s.e.m. of $n$ = 3 (**b**, CD3$^{-}$ NK1.1$^{+}$ TILs), $n$ = 6 (**b**, CD3$^{-}$ NK1.1$^{+}$ TDLNs and spleen), $n$ = 3 (**b**, CD3$^{-}$ MHCII$^{+}$ TILs), $n$ = 10 (**b**, CD3$^{-}$ MHCII$^{+}$ TDLNs), and $n$ = 9 (**b**, CD3$^{-}$ MHCII$^{+}$ spleen) of six independent experiments. For TILs, samples of mice receiving the same treatment were pooled prior to analysis. $P$-values calculated using unpaired Student's $t$-test (**b**). *$P$ < 0.05, **$P$ < 0.01, ***$P$ < 0.001, ****$P$ < 0.0001.

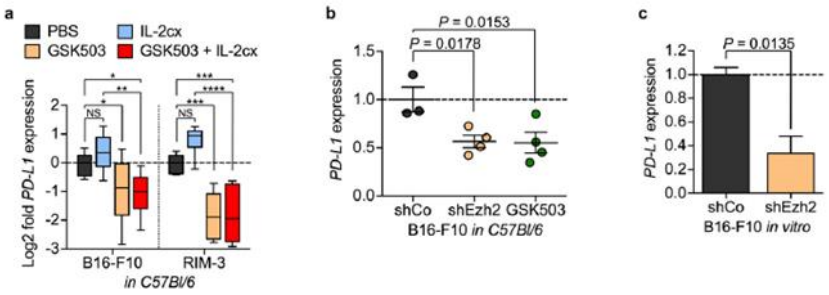


**Extended Data Figure 9. Ezh2 inactivation promotes PD-L1 downregulation. a**, RT-qPCR for *PD-L1* on B16-F10 and RIM-3 melanomas after IL-2cx administration and/or Ezh2 inhibition using GSK503. **b**, RT-qPCR for *PD-L1* on B16-F10 melanomas after Ezh2 inactivation using either shEzh2 or GSK503. **c**, RT-qPCR for *PD-L1* on B16-F10 cultures after *Ezh2* silencing using shEzh2. Data are represented as median ± 100% range of $n = 6$ (**a**), mean ± s.e.m. of $n = 3$ (**b**, shCo), $n = 4$ (**b**, shEzh2, shCo + GSK503), $n = 3$ (**c**) of two independent experiments (**a**, **c**) and one experiment (**b**). *P*-values calculated with ANOVA and Fisher's LSD test (**a**, **b**), or Student's *t*-test (**c**). $*P < 0.05$, $**P < 0.01$, $***P < 0.001$, $****P < 0.0001$.

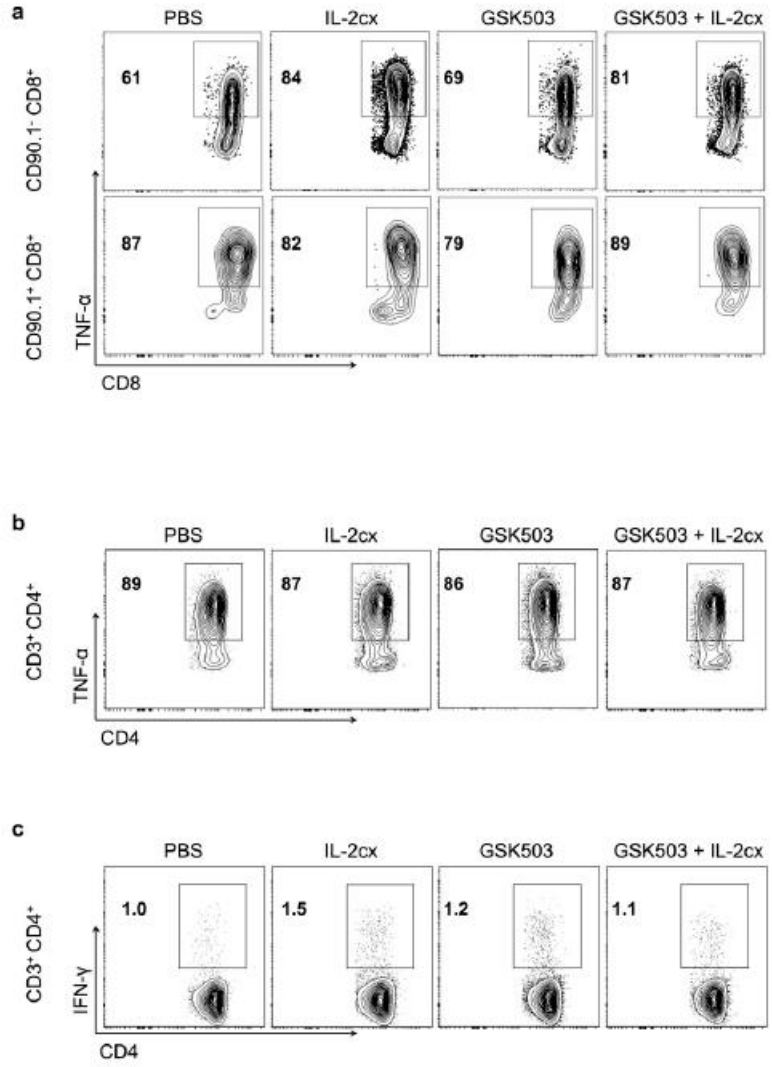


**Extended Data Figure 10. TNF-α and IFN-γ production in T cell subsets upon Ezh2 inhibition plus IL-2cx therapy. a–c**, TNF-α production by CD90.1$^{-}$ endogenous (upper) and CD90.1$^{+}$ Pmel-specific CD8$^{+}$ T cells (lower panels) (**a**), TNF-α production by endogenous CD4$^{+}$ T cells (**b**), and IFN-γ production by endogenous CD4$^{+}$ T cells (**c**) from TDLNs of B16-F10-grafted mice receiving PBS, IL-2cx, GSK503, or GSK503 + IL-2cx as in Fig. 2b. Data are representative of two independent experiments.

| Antigen | Fluorophore | Company | Serial number |
|---|---|---|---|
| CD107a | PE | eBioscience | 12-1071 |
| CD11b | BV650 | BD Biosciences | 563402 |
| CD122 | PE | eBioscience | 12-1221 |
| CD25 | APC | BD Biosciences | 557192 |
| CD3 | BV510 | BD Biosciences | 563024 |
| CD3 | FITC | eBioscience | 11-0031 |
| CD4 | BV605 | BioLegend | 100451 |
| CD44 | APC | eBioscience | 17-0441 |
| CD45.2 | Alexa-700 | BioLegend | 109822 |
| CD45.2 | BUV395 | BD Biosciences | 564616 |
| CD8a | Alexa 488 /efluor 450 | eBioscience | 53-0081/48-0081 |
| CD8b | APC-efluor 780 | eBioscience | 47-0083 |
| CD90.1 | eFluor 450 | eBioscience | 48-0900 |
| FoxP3 | PE | eBioscience | 12-5773 |
| Gr-1 | Alexa 488 | eBioscience | 53-5931 |
| I-A/E-A | BV711 | BD Biosciences | 563414 |
| IFN-γ | PE | eBioscience | 12-7311 |
| NK1.1 | FITC | eBioscience | 11-5941 |
| PD-1 | BV605 | BioLegend | 135219 |
| TNF-α | APC | eBiosciences | 17-7321 |

**Supplementary Table 1. FACS antibodies.**

| Antigen | Company | Serial number | Applications / Dilutions |
|---|---|---|---|
| β-Actin | Sigma-Aldrich | A5316 | WB, 1:10’000 |
| CD3 | Cell Signaling Technology | 4443 | IF, 1:100 |
| CD45 | BD Biosciences | 550539 | IF, 1:100 |
| Dct | Santa Cruz Biotechnology | sc-10451 | IF, 1:500 |
| Ezh2 | Cell Signaling Technology | 3147 | ChIP, 1:100; IF, 1:200; WB, 1:1’000 |
| H3K27me3 | Cell Signaling Technology | 9733 | ChIP, 1:100; WB, 1:1’000 |
| Histone 3 | Cell Signaling Technology | 3638 | WB, 1’000 |
| Mitf | H. Arnheiter Lab, NIH (ref. S1) | LH7 | IF, 1:100 |
| Pax3 | Life Technologies | 38-1801 | IF, 1:200 |
| PD-L1 | R&D Systems | AF1019 | IF, 1:100 |
| Pmel | Novus Biologicals | NBP1-69571 | IF, 1:100 |
| Tyrp1 | V. Hearing Lab, NIH (ref. S2) | αPEP1 | IF, 1:500 |
| Zeb1 | Bethyl Laboratories | IHC-00419 | IF, 1:100 |

**Supplementary Table 2. Primary antibodies.**

S1. Debbache, J. *et al.* In vivo role of alternative splicing and serine phosphorylation of the microphthalmia-associated transcription factor. *Genetics* **191,** 133–144 (2012).

S2. Kobayashi, T. & Hearing, V. J. Direct interaction of tyrosinase with Tyrp1 to form heterodimeric complexes in vivo. *J Cell Sci* **120,** 4261–4268 (2007).

| Fluorophore | Specificity | Company | Serial number | Applications / Dilutions |
|---|---|---|---|---|
| Alexa488 | goat | Jackson ImmunoResearch | 705-545-147 | IF, 1:500 |
| Alexa488 | rabbit | Jackson ImmunoResearch | 711-545-152 | IF, 1:500 |
| Alexa647 | rabbit | Jackson ImmunoResearch | 111-605-003 | IF, 1:500 |
| Cy3 | rat | Jackson ImmunoResearch | 712-165-153 | IF, 1:500 |
| IRDye-800CW | mouse | LI-COR Biosciences | 926-32212 | WB, 1:10'000 |
| IRDye-680LT | rabbit | LI-COR Biosciences | 926-68023 | WB, 1:10'000 |

**Supplementary Table 3. Secondary antibodies.**

| Gene | Forward sequence | Reverse sequence |
|---|---|---|
| *CD271* | ATGGATCACAAGGTCTACCCC | GGAGCAATAGACAGGAATGAGG |
| *Dct* | CCTGAATGGGACCAATGCCT | AGGCATCTGTGGAAGGGTTG |
| *Ezh2* | GTGACCACAGGATAGGCATCT | CAAGGGATTTCCATTTCTCG |
| *H2-D1* | GGAGCTATGGCCATCATTGGA | TCTCGGAGAGACATTTCAGAGC |
| *H2-K1* | CTGGAGCTGTGGTGGCTTT | GACAGATCAGAGGTCTGGGAG |
| *Mitf* | CCCCAAGTCAAATGATCCAG | GCAACTTCCGGATGTAGTCC |
| *Mlana* | CTTATCGGCTGCTGGTACTG | CTCTTGAGAAGACAGTCGGC |
| *Oca2* | TGTTGGAGAACAGACTGCCC | ATGATGCCAAGGCTGAGACC |
| *PD-L1* | GGACTACAAGCGAATCACGC | TTCTGGATAACCCTCGGCCT |
| *Pmel* | GGGGATGCATTTGAGCTGAC | CTGGCACCCTGGTGATGAAA |
| *Psmb8* | AGCATCCAAGCTGCTTTCCAA | CCGAGTCCCATTGTCATCTACG |
| *Psmb9* | GGTTCCGGAAGCTCCTACAT | AGAGCCATCTCGGTTCATGG |
| *Snai1* | GTGGAAAGGCCTTCTCTAGGC | GGTTGGAGCGGTCAGCAAAA |
| *Sox9* | ATGCTATCTTCAAGGCGCTG | TTGCACGTCGGTTTTGGGA |
| *Sox10* | GAAGAAGGCTCCCCCATGTC | GCTCTGTCTTTGGGGTGGTT |
| *Tap1* | TCCCTCAGGGCTATGACACA | ATAAGCAGGAGTGGCTTCCG |
| *Tap2* | ACTGTGAGGACGCTCAAGTG | TAACTGGCCCCCTTTTTCCC |
| *Tyr* | GTACTTGGGAGGTCGTCACC | GTCCCTCAGGTGTTCCATCG |
| *Tyrp1* | GCACACTTTCACTGATGCGG | TAGGTGCGTTTTCCAACGGG |
| *Usf1* | CAGGGCTCAGAGGCACTACT | GCTCCCTCCCTGCAATACTT |
| *Zeb1* | GATCCAGCCAAACGGAAACC | TGGCGTGGAGTCAGAGTCAT |

**Supplementary Table 4. Mouse RT-qPCR primers.**

| Promoter | Forward sequence | Reverse sequence |
|---|---|---|
| *Dct* | CTGGGACACATGAGCCCAATA | GACCCTAAGTGCACAATGAAGC |
| *H2-D1* | TTGTATTCCCGGAAGTGACCTT | TCACTGTTTCCTAACCTCCACC |
| *H2-K1* | ACTTTAAGGAAAAGCCTCTCTCTCC | AAAGCCTCTTCCGGGAATACAA |
| *Interg1* | GCTCCGGGTCCTATTCTTGT | TCTTGGTTTCCAGGAGATGC |
| *Mitf* | CGTGTCCTCGCAGATGTCTAAA | CGGTTTGCTTCAAGGATACAGAC |
| *Mlana* | CAGACACCCATTAGGAATCCAAAAC | ATGTGAAGACGGCTTCTCTGG |
| *Oca2* | CTGGCTTCTACAGCAAGGCT | CCAGCCCCCTCTTGAGAATG |
| *Pmel* | GCTGCCCATCAGTGAACTCT | GGGAAGAAGGAAAGGGCCAG |
| *Psmb8* | ACACATGAAAAGGCCCGACT | GCACAGGGGTCTTTAGGTCC |
| *Psmb9* | CCCCTTAACTTGCTTGCGTG | CCAGAGACAGGTGACGACAG |
| *Sox10* | AAACCCAAGCTGAGTCCAGG | CTTCATCCCCAACACCCAGG |
| *Tap1* | GAGAAGAACACGACAGGCCA | TCAGGCTGTTCTGGAAGCTG |
| *Tap2* | GGCTCAGGCAAGTTTTCTCAAC | GACCTCCGAGCATGTTTTAAGAAG |
| *Tyr* | CATGTGCTTTGCAGAAGATAAAAGC | GGAGTGACTATCACATGTTTTGGC |
| *Tyrp1* | GTGTGACATTGGCCTTAGTTCG | ACGCTGAAGAGATTTTGCTTTCG |

**Supplementary Table 5. Mouse ChIP primers.**

# VI. Conclusion and discussion

The concept of cancer immunotherapy has now opened the way for the development of therapeutics, which stimulate and potentiate the host's immune response against tumor cells. Different pharmaceuticals have been developed and approved for the treatment of metastatic melanoma such as recombinant IL-2 [188] and/or immuno-modulatory antibodies [189]. Although therapeutic benefits can be durable, only a subset of patients responds to current immunotherapies. Moreover, the use of most if not all immunotherapies is accompanied with severe side effects, many of which relate to the induction of autoimmunity and pro-inflammatory conditions [190]. Taken together, the low efficacy and the high incidence of therapy-related adverse effects represent a considerable clinical challenge that needs to be overcome by further pre-clinical research.

Taking these points into consideration, the first aim of the thesis was to develop a unique mAb to hIL-2, which could be further developed as high efficacy and low toxicity cancer immunotherapy for clinical use. We devised a rational approach for the generation of an anti-hIL-2 antibody to overcome the limitations of high-dose recombinant IL-2 currently used in the treatment of patients with metastatic melanoma and metastatic renal cell carcinoma patients. Following this approach we obtained an anti-hIL-2 mAb, named NARA1, which we could characterize in great detail combing structural, biophysical, and *in vitro* and *in vivo* functional analyses. Based on these results, we concluded that NARA1 binds with high affinity to the CD25 binding site of IL-2 acting as a high-affinity mimic of this IL-2-receptor subunit, allowing preferential stimulation of $CD122^{high}$ cells ($CD8^+$ T cells and NK cells) but disfavoring $CD25^+$ Treg cell proliferation and $CD25^+$ endothelial cell damage *in vivo*. The use of such antibody does not only preferentially direct IL-2 to the dimeric IL-2R but also allows

lowering the dose of IL-2 required for optimal *in vivo* bioactivity by increasing the half-life of IL-2. In line with these effects, using hIL-2/NARA1 complexes we were able to significantly better control tumor growth in murine models of melanoma which led to improved survival of mice engrafted with melanoma cells or in animals spontaneously developing metastatic melanoma.

For the clinical development of NARA1 and hIL-2/NARA1 complexes, some properties of hIL-2 and the interaction of hIL-2 with NARA1 merit consideration. Although hIL-2 and NARA1 are premixed prior to injection and associate with each other with high affinity, the two components could potentially detach *in vivo*, leading to unbound hIL-2 and NARA1. However, even if the hIL-2/NARA1 complex were to dissociate fully, the systemic levels of hIL-2 would be 20-fold lower compared to the high-dose IL-2 doses administered currently to cancer patients. At such low concentrations, IL-2-related side effects will be either absent or much milder. The free NARA1 antibody could in turn bind endogenous hIL-2 and thus generate hIL-2/NARA1 complexes favoring the stimulation of $CD122^{high}$ cells, similar to what has been observed with the anti-mIL-2 antibody S4B6 [134]. An additional therapeutic application of NARA1 could be the direct administration of the antibody to complex endogenous IL-2. However, for this approach to be successful systemic IL-2 levels need to be sufficiently high. In a clinical setting, the administration of NARA1 as a single agent could boost the efficacy of immune checkpoint blockade inhibitors in patients, especially when one considers recent data showing that CTLA-4 blockade increases IL-2-producing effector cells and reduces tumor growth [191].

Alternatively, the dissociation of NARA1 from IL-2 could also be overcome with the development of a fusion protein where the antibody and the cytokine will be linked with a

flexible linker as previously described for the anti-mIL-2 mAb S4B6 [192]. Nevertheless, to date, we cannot be sure that the *in vivo* effects observed using hIL-2/NARA1 complex would be reflected in the fusion protein. It is not known if the cytokine needs to dissociate from the antibody in order to get optimal *in vivo* selectivity for the dimeric receptor. To answer this question one would need to investigate IL-2 binding and signaling properties as well as internalization and recycling of hIL-2/NARA1 complexes and corresponding fusion proteins side by side with free recombinant IL-2.

Given the complexity of the immune system, combination of hIL-2/NARA1 complex with other immunotherapies, such as ACT, tumor peptide-specific vaccination, and immune checkpoint inhibitors, could induce stronger anti-tumor responses and lead to protective immunity in patients. We have indeed observed synergistic effects when combining hIL-2/NARA1 complex with particular checkpoint inhibitors or peptide-specific approaches (unpublished data).

The disadvantages of IL-2 can potentially also be circumvented with the development of IL-2 mutants (IL-2 muteins) [55, 142, 143], but further engineering may be needed in order to use them in a clinical setup. Recombinant human protein drugs are mostly recognized by the body as ‘self’ as shown by the administration of recombinant G-CSF (Neupogen) or hIL-2 (Proleukin) with less than 3% and 1% reported immunogenicity, respectively [193]. Moreover, the efforts done in predicting T cell epitopes and depleting them from the proteins therapeutics have been successful for humanized or human antibodies showing only low levels of anti-drug antibodies (ADAs) in patients to date [193]. However, immune tolerance of recombinant proteins can be lost with the introduction of mutations in the recombinant wild-type protein lowering the efficacy and safety of the therapeutic [194]. Indeed,

immunogenicity problems have been reported for the N88R IL-2 mutein (BAY 50-4798) leading to ADAs in 27% of treated patients [195]. Another way to reduce side effects and immunogenicity and increase efficacy of such IL-2 muteins would be to prolong their half-life by PEGylation, coupling to an Fc molecule, to a mAb or a mAb fragment binding to a tumor antigen [196]. The strategy of targeting IL-2 to the tumor site could also be tested for the IL-2/NARA1 complex by engineering a bispecific anti-IL-2 antibody. Such a molecule would raise the following questions: Is the IL-2/NARA1 complex specificity conserved? Can the protein be targeted to the site of disease, or should the tumor-draining lymphoid organs be targeted instead in order to get and sustain a potent immune response? Will it be necessary to engineer a smaller molecule (antibody fragments such as diabodies) in order to increase its accumulation at the tumor site? On one side one might think that small size molecules are able to better reach and stay in the site of disease while being eliminate fast from the body brining along less side effects. On the other hand, targeting IL-2 only to the tumor site could harm the anti-tumor response obtained with the stimulation of intratumoral Treg cells. The efficacy of the therapy could be compromised by the exhaustion levels of the stimulated $CD8^+$ T cells being in an immunosuppressive environment. It remains important to test different strategies in order to keep a favorable Tc vs Treg cells ratio in the tumor and to balance efficacy and toxicity.

The strategy used for the generation of an anti-IL-2 antibody with *in vivo* selectivity should be applicable to other cytokines including IL-3, IL-4, IL-6, IL-7, IL-15, and granulocyte colony-stimulating factor, for which *in vivo* agonist cytokine/antibody complexes have been described [197-200]. For example, we recently described polyclonal antibodies to IL-1β raised in mice that can either inhibit this pro-inflammatory cytokine or enhance its *in vivo*

effect by worsening IL-1β mediated diseases (submitted manuscript entitled 'Endogenous polyclonal anti-IL-1 antibodies potentiate IL-1 activity during pathogenic inflammation', data not shown).

The IL-2/NARA1-mediated immune stimulation allowing potent tumor control is lost over time, likely due to tumor immune escape mechanisms. For this reason, the 2$^{nd}$ part of this Ph.D. thesis was focused on investigating the mechanisms involved in tumor immune escape during IL-2cx immunotherapy. By analyzing the epigenetic signature in melanoma cells following treatment with IL-2-cx, we were able to show that the expression levels of the epigenetic regulator Ezh2 increases in melanoma cells during immunotherapy leading to dedifferentiation of melanoma cells and silencing of key molecules needed for tumor antigen presentation. We hypothesized that by inhibiting EZH2 with GSK503, melanoma cells are rendered 'immunogenic' again and therefore could be recognized by specific CD8$^{+}$ T cells expanded upon hIL-2/NARA1 complex treatment. This synergy could also be observed using an anti-CTLA-4 mAb. These results do not only show the benefit of combining cancer immunotherapy with epigenetics blockers but precisely describe the central role of Ezh2 during tumor immune escape. In addition, our results complement the data obtained by Weiping Zou and colleagues showing that in human ovarian cancer cells EZH2 and DNA methyltransferase 1-mediated DNA methylation repress tumor production of the chemokines CXCL-9 and CXCL-10, essential for the recruitment of effector T cells into the tumor. Blocking of such epigenetic pathways restores chemokines levels resulting in higher T cell infiltration and better tumor control [187].

Although many of the downstream targets of EZH2 are linked to tumor development and metastasis, it will be important to know which other genes could be further upregulated by

EZH2 inhibition to avoid long-term adverse effects. Furthermore, some loss-of-function mutations of EZH2 have been linked to hematological malignancies [201, 202], suggesting that this enzyme can also play a role in tumor suppression. It remains to be tested if EZH2 inhibitors are an appropriate treatment in all patients.

Moreover, it has been recently shown that cancer cells restrict T cell-mediated immunity via inhibition of EZH2 expression on T cells by limiting their glycolysis pathway [203]. The polyfunctional properties of $EZH2^{+}$ T cells convey survival advantages to those cells in the tumor microenvironment. Likewise, EZH2 expression on T cells correlates with better survival and prognosis in patients [203]. EZH2 seems therefore to play opposite roles on T cells and tumor cells, questioning systemic administration of epigenetic blockers that could potentially target T cell effector functions. Different strategies should be followed and studied in order to minimize such risks, such as administering lower doses, targeting epigenetic drugs to the tumor cells, or combining epigenetic drugs with other immunotherapy strategies that would enhance efficacy as observed using hIL-2/NARA1 complex and EZH2 blockers.

It would be interesting to assess whether EZH2 overexpression could be used as a biomarker defining different clinical forms of melanoma. Likewise, it will be important to understand the relationship between EZH2-mediated histone methylation and DNA methylation to know whether the inhibition of one pathway is enough to control tumor growth or the combination could be beneficial.

Our data shows that EZH2 plays a central role during tumor immune escape being responsible of impaired antigen presentation and expression of immunosuppressive molecules such as PD-L1. Nevertheless, it is important to keep in mind that tumor escape is most likely a highly complex process and cancer cells could use several strategies to evade the immune system.

Down-regulation of adhesion molecules within the tumor tissue might contribute to immunological ignorance [204]. When strategies such as vaccination or adoptive transfer of anti-tumor T cells are used to ensure proper immune activation, tumors might also escape through the expression of immunosuppressive cytokines such as IL-10 or TGF-β known to affect the proliferation, activation and differentiation state of immune cells [205, 206]. In parallel, tumor cells have been shown to promote the generation of immunosuppressive Treg cells, which actively inhibit the action of tumoricidal effector cells [207]. Moreover, the lack of a T cell response could be explained by tolerance induction. Although T cells might bind via their TCR to a peptide presented on MHC molecules on the surface of the tumor cells, the absence of co-stimulatory molecules might still induce T cell anergy [208]. Another tolerance mechanism under investigation is a process known as T cell deletion through activation-induced cell death [209]. It might be that cancer cells can also mutate their expression profile of molecules involved in apoptotic signaling making them resistant to cellular cytotoxicity. It is logical to think that tumor cells combine and adapt several immune escape mechanisms in response to different conditions. Of course, these mechanisms may also depend on the type of cancer and on the immune system of every patient. To date, it is clear that there is not a unique way to cure cancer. There is a need to get deeper knowledge on every single case (patient and cancer type) and to rationally combine the available therapeutics to improve current treatments, trying to keep a balance between efficacy and toxicity.

# VII. Material and methods

## Mice

3-month-old female *C57Bl/6J* mice and *Balb/c* were purchased (Charles River Laboratories). *Tcrb/d*$^{-/-}$, *Rag1*$^{-/-}$, *Ifng*$^{-/-}$, *Tnfa*$^{-/-}$, *IL-7tg.Ly5*$^{b}$ and *pmel*$^{Si}$ *Thy1*$^{a}$ transgenic mice were acquired and maintained according to suppliers recommendations (The Jackson Laboratory). *Tyr::N-Ras*$^{Q61K}$ *Ink4a*$^{-/-}$ transgenic mice were mated, genotyped and monitored for tumor development as previously described [170]. All mice were of a *C57Bl/6* background, born with the expected ratio of Mendelian inheritance and no changes in gender ratios were observed. No statistical methods were used to predetermine sample size. For all experiments presented in this study, the sample size was large enough to measure the effect size. The experiments were not randomized and the investigators were not blinded to allocation during experiments and outcome assessment. Mouse colonies were maintained in certified animal facilities in accordance with Swiss guidelines. All animal experiments were approved by the veterinary authorities of Canton of Zurich, Switzerland, and were performed in accordance with Swiss law and the GlaxoSmithKline policy on the Care, Welfare, and Treatment of Animals. Pre-established exclusion criteria were based on the Canton of Zurich veterinary authority's guidelines and included substantial weight loss of >15% of initial body weight. During the study period most of the animals appeared to be in good health.

## Generation of anti-human IL-2 mAbs

Balb/c mice were immunized with human (h) IL-2 (34-8029, eBioscience) in Freund’s adjuvant (F-5881, Sigma) on days 0, 14 (subcutaneously) and 28 (intravenously). Serum was collected before the first immunization and 9–11 days after every immunization in order to

check for anti-hIL-2 antibody titers. On day 35, mice were euthanized and spleen cells were collected following standard procedures. Splenocytes were mixed with myeloma cells at a 5:1 ratio with polyethylene glycol 1500 (10783641001, Roche). A feeder layer obtained from peritoneal lavage of Balb/c mice was used to grow clones in IMDM selective media (21980, Life Technologies) supplemented with 10% ultra-low IgG FBS (16250, Life Technologies), 50 μM mercaptoethanol (313050, Life technologies), 1:100 Insulin-Transferrin-Selenium (41400-045, Life Technologies), 2% IL-6-conditioned media, penicillin-streptomycin (15240, Life Technologies), gentamycin (15750, Life Technologies), and hypoxanthine-aminopterin-thymidine (HAT, H037, Sigma-Aldrich) for several days. Polyclonals were then screened for hIL-2 binding using a direct binding ELISA and for specificity using a competition ELISA, as shown in Fig. S1, and diluted to obtain monoclonal clones. For expansion of monoclonals, HAT media was replaced by hypoxanthine-thymidine media (HT, 41065, Life Technologies). Monoclonals were then concentrated using 100 kDa centrifugal filter units according to supplier's recommendations (UFC9100, Merck Millipore). Concentrate was further tested for specificity in a dose-dependent manner using a competition ELISA and *in vivo* using 4 daily intraperitoneally injections of 200 μl concentrate complexed with 1.5 μg hIL-2, followed by assessment by flow cytometry of T cell subsets and natural killer (NK) cells, as shown in Fig. S1. NARA1 was purified using Protein G agarose (20398. ThermoFisher Scientific) according to supplier's recommendations.

**Surface plasmon resonance (SPR) binding and titration experiments**

100 μg/ml NARA1 or 5344 (clone 5433.111, BD Biosciences) antibodies were immobilized into a GLM-Chip according to supplier's recommendations (176-5012, BioRad), followed by addition of hIL-2 (34-8029, eBioscience) at titrated concentrations in 3-fold dilutions starting

at 100 nM. For hCD25 and hCD122 titration experiments, hIL-2 was added at saturating concentration (1 μM) followed by coinjection of recombinant hCD25 or hCD122 (223-2A/CF, 224-2B/CF, R&D Systems) in 3-fold dilutions starting at 1 μM.

**Enzyme-Linked Immunosorbent Assay (ELISA)**

Flat Nunc-Immuno 96-well plates (M9410-1CS, Sigma-Aldrich) were coated overnight at 4°C with recombinant hIL-2 (direct binding ELISA; hIL-2, eBioscience, 34-8029) or with purified capture anti-hIL-2 mAb (competition ELISA, $mAb_{cap}$, clone 5344.111, BD) in PBS. The plates were then washed with PBS-Tween (0.1% Tween 20, P1379, Sigma-Aldrich) and blocked for at least 1 hour at room temperature (RT) in 1% BSA (A2058, Sigma-Aldrich), 0.1 % Tween solution at 450 rpm. After washing, hybridoma supernatants (direct ELISA) or hIL-2 (competition ELISA) were added to the plates in blocking solution and incubated for 1 hour at RT and 450 rpm, followed by washing. To check competition for a specific epitope, titrated amounts of hybridoma supernatants (concentrate) or purified NARA1 mAb, Fab or $(Fab')_2$ fragments were added. The plates were washed before addition of biotinylated anti-mouse IgG (direct ELISA, 405303, Biolegend) or biotinylated anti-hIL-2 detection mAb (competition ELISA, $mAb_{det}$, clone 5355, R&D systems) to the plates for 1 hour at RT and 450 rpm. Plates were then washed and streptavidin-conjugated horseradish peroxidase was added for 45 minutes at RT (554066, BD Biosciences) and, after a final vigorous wash, plates were developed using the single-component TMB Peroxidase EIA substrate (172-1068, BioRad). After 5–10 minutes the reaction was stopped by addition of 1.8 M $H_2SO_4$ (339741, Sigma-Aldrich) and readout was performed at 450 nM absorbance using an iMark microplate reader (BioRad). Biotinylation was performed using the EZ-link Sulfo-NHS.LC Biotinylation kit (21435, Thermo Scientific) according to supplier's recommendations.

**Complexing of hIL-2 with NARA1 mAb, Fab, and F(ab')$_2$**

The antigen, Proleukin, is commercially available as lyophilized powder and was purified by reverse-phase HPLC to remove the excipients before use for complex formation. The Fab fragment of NARA1 was generated by papain cleavage of the full-length monoclonal antibody (mAb) followed by Protein A chromatography. Briefly, 6.5 ml full-length NARA1 (9 mg/ml in 50 mM citrate buffer with 90 mM sodium chloride at pH 7.0) was mixed with 5 mM DTT and 590 µg Papain (Roche). The cleavage reaction was kept at room temperature for 16 hours and stopped by addition of 15 µl 56 mM E64 solution (Roche). The cleavage solution was then diluted 10 times with 25 mM Tris, 25 mM NaCl, pH 8.0 and purified using a 5 ml Protein A column (GE Healthcare) to remove Fc fragments. For generation of NARA1 F(ab')$_2$ fragments, about 5 mg of NARA1 mAb were digested overnight at 37°C with 5000 U IdeS protease (Genovis). Incompletely digested mAb and Fc fragments were removed using a 1 ml Protein A column. IdeS was then removed by size exclusion on Superdex 200 (GE Healthcare) run in PBS. To form hIL-2/NARA1 Fab complex for crystallization, Proleukin powder after HPLC was dissolved in $H_2O$ at a concentration of 5.5 mg/ml. 6.6 mg Proleukin, in excess, was added to 11.5 mg NARA1 Fab fragment solution drop by drop. Centrifugation was used to remove excess Proleukin that precipitated under these conditions. The complex was then purified by gel filtration with Superdex 200 10x300 using a running buffer of 25 mM Tris and 25 mM NaCl at pH 7.4.

**Crystallization and data collection and analysis**

Proleukin/NARA1 Fab complex after gel filtration was concentrated to 14 mg/ml and screened with vapour diffusion method as sitting drops. The protein solution was mixed 1:1 with reservoir buffer to a total size of 0.4 μl and crystallization plates were kept at 19°C. Crystals were harvested 4 days after screening under condition of 20% w/v polyethylene glycol 3350 and 0.2 M sodium nitrate. Crystals were cryoprotected using reservoir buffer plus 10% glycerol and flash frozen in liquid nitrogen prior to data collection. Diffraction data were collected at the Swiss Light Source (Villigen, Switzerland) at beam-line PX-II with a Pilatus pixel detector using X-ray radiation wavelength of 0.99998 Å. The dataset was processed with XDS and XSCALE (version Dec. 6, 2010) and the structure was resolved with molecular replacement method with the program PHASER by using Protein Data Bank (PDB) entry "3INK" as search model for hIL-2 and PDB entry "3TTI" as search model for Fab fragment. Iterative model building and refinement were performed with the programs Coot and AUTOBUSTER. All figures were generated with the program PyMOL. Proleukin residues were defined as residues that were within 4 Å distance from any atom of the NARA1 Fab and were further confirmed by CCP4 program CONTACT and AREAIMOL. Similarly, paratope residues were defined as those residues of NARA1 Fab that were within 4 Å distance from any atom in Proleukin.

**Linear peptide mapping**

Linear peptide mapping experiments were performed, as previously described [210]. Briefly, a library of 15-mer peptides was generated based on the sequence of hIL-2, followed by generation of a second library with 3 defined mutations on residues F42, Y65 and L92, based on available IL-2 muteins [55]. Peptides were designed thus each contained 12 overlapping

residues with the previous peptide and 12 with the following peptide. In total 41 peptides were generated, but only the 9 most prominent ones as shown. In order to avoid unspecific binding the cysteines of all peptides were replaced by a serine. The peptides were printed on microarray slides in triplicates and incubated with $mAb_{det}$, NARA1 or isotype control mAbs. Antibodies were then detected using fluorescently-labeled anti-mouse IgG antibodies (85454, Thermo Scientific, label DL650 or JIR 115-072, label Cy5). All steps were performed on a TECAN microarray processing station. After incubation of the mAbs and final washing the microarray were dried using nitrogen steam and scanned. The resulting images were analyzed using spot-recognition software GenePix (Molecular Devices), and the mean signal intensity was extracted for each spot.

**Cell cultures**

Sp2/0 myeloma cell line and IL-6 producing cell line were kindly provided by Antonius Rolink (University of Basel, Switzerland) and cultured in the media described above for the generation of mAbs. B16-F10 melanoma and CTLL-2 cell lines were purchased (ATCC). Cells were cultured in growth medium, which was RPMI 1640 (42401, Life Technologies) supplemented with 10% FCS (16140, Life Technologies), 4 mM L-Glutamine (25030, Life Technologies), Penicillin-Streptomycin (15070, Life Technologies), and Fungizone Antimycotic (15290, Life Technologies).

To stably silence *Ezh2*, cells were transfected with small hairpin RNA (shRNA)-expressing plasmids encoding either a scrambled shRNA (shCo, SHC002, Sigma-Aldrich) or an Ezh2 mRNA-targeting shRNA (shEzh2, TRCN0000039040, Sigma-Aldrich). 10 µg plasmid was applied in combination with jetPEI DNA Transfection Reagent (101-10N, Polyplus Transfection) according to manufacturer's guidelines. Transfected cells were selected using 1

μg/ml puromycin (A11138-02, Life Technologies) for 1 week before subjection to further assays. To pharmacologically inhibit Ezh2, cells were treated with 1 μM GSK503 for 8 days before subjection to further assays. Drug was only replenished when cells were passaged during the 8-day period. Efficiency of shEzh2 and GSK503 has been previously validated [170, 173, 211].

Human leukocytes were freshly isolated from peripheral blood mononuclear cells (PBMCs) using a standard Ficoll density gradient isolation protocol, maintained in growth media (as described above) supplemented with 10 % human serum, followed by purification of T cell subsets using kits (130-045-201, CD8 human Microbeads, Miltenyi Biotec).

### *In vitro* proliferation

CTLL-2 cells were seeded into 96-well plates (10 000 cells/well) and stimulated using mIL-2 (34-8021, eBiosciences), mIL-2/S4B6 complex (2:1 molar ratio; BioXcell), hIL-2, or hIL-2/NARA1 complex (2:1 molar ratio), and proliferation was assessed after 48 hours incubation at 37°C. After 72 hours at 37°C in complete medium, purified human $CD8^+$ T cells were seeded in 96-well plates (75 000 to 100 000 cells/well) and stimulated with hIL-2 or hIL-2/NARA1 complex (at a 2:1 molar ratio). Proliferation was assessed after 96 hours incubation at 37°C. Proliferation was measured using WST-1 (11644807001, Sigma-Aldrich), added to the cells. After 4 hours of incubation at 37°C readout was performed at 450 nM absorbance using an iMark microplate reader (BioRad).

### STAT5 phosphorylation

CTLL-2 cells (200 000 cells/well) or purified human $CD8^+$ T cells were seeded in a 96-well plate (400 000 cells/well) and stimulated using hIL-2 or hIL-2/NARA1 complex (at a 2:1

molar ratio). Phosphorylation of STAT5 was assessed after 15 minutes of stimulation, as previously described [142], and using manufacturer's buffer recommendation for human cells (612599, BD Phosflow Protocol for Human PBMCs, STAT5 antibody, BD Biosciences).

**Grafting of murine melanoma cells**

Skin melanoma cells derived from a *Tyr::N-Ras*$^{Q61K}$ *Ink4a*$^{-/-}$ mouse (RIM-3) were previously analysed [170]. Recipient mice were intradermally or subcutaneously engrafted with either 500 000 RIM-3 cells or 1 x $10^6$ B16-F10 cells. Mice engrafted with melanoma cells were sacrificed not later than at a time point defined by tumor volume (V > 1'000 $mm^3$). Tumor volume was calculated as follows: $V = 2/3 \times \pi \times ((a + b)/4)^3$, a (mm) was the length and b (mm) was the width of the tumor. For pulmonary tumor nodules, 3 x $10^5$ B16-F10 melanoma cells were injected intravenously in 100 µl DMEM.

***In vivo* treatments**

Recombinant hIL-2 (IL-2, Teceleukin, Roche), anti-CTLA-4 mAb (9D9, BioXcell), anti-PD-1 mAb (RMP1-14, BioXcell), anti-CD8 mAb (YTS169, BioXcell), anti CD4-mAbs (GK1.5, BioXcell) and GSK503 (GlaxoSmithKline) were purchased. hIL-2/NARA1 antibody complex (IL-2cx) was prepared in PBS by mixing 1.5 µg hIL-2 and 15 µg NARA1 antibody, as previously described [60, 133, 134]. GSK503 was diluted (15 mg/ml) in 20% Captisol solution (Cydex). Treatment of B16-F10 tumor-bearing mice was started, for intradermal tumors, when tumors became visible and palpable (usually day 4 ± 1 day) and, for pulmonary tumors, 3 days after B16-F10 injection and consisted of 4 daily injections of phosphate-buffered saline (PBS), hIL-2, or hIL-2/NARA1. For lung tumors, mice were killed on day 16 and lungs fixed for counting pulmonary melanoma nodules, as previously described [60].

Treatment of RIM-3-engrafted mice was induced when tumors reached a considerable size (V > 150 $mm^3$, ~20 days). Ezh2 inhibition has been previously defined [170, 173] and was achieved by daily intraperitoneal injections of 150 mg/kg GSK503 until termination of the experiment. Where indicated, mice received intraperitoneal injections of IL-2cx, 250 μg of anti-CTLA-4 mAb, or 250 μg of anti-PD-1 mAb for four consecutive days. To deplete T cells, 500 μg anti-CD8 mAb (YTS169, BioXcell) or 250 μg anti CD4-mAbs (GK1.5, BioXcell) were injected intraperitoneally to B16-F10-engrafted mice starting on the day of tumor engraftment. Treatment of *Tyr::N-Ras$^{Q61K}$ Ink4a$^{-/-}$* mice, consisting of 4 consecutive injections of hIL-2/NARA1 complex weekly, was started at the age of three months, before macroscopic skin melanomas were visible. Mice were monitored weekly for the appearance of macroscopic tumors (diameter>1.5mm). Quantifications of skin melanomas and metastases were done, as previously described [170].

Where indicated CD90.1$^+$ Pmel-specific CD8$^+$ T cells were obtained from pooled spleen and lymph nodes of *Pmel$^{Si}$ Thy1$^a$* transgenic mice and purified using negative T cell enrichment (19853, StemCell Technologies). At least 2 x $10^6$ purified cells were adoptively transferred to recipients. To assess IL-2-induced toxicity, mice received 4 consecutive injections of hIL-2 at 1.5 μg (low dose; LD) or 20 μg (high dose; HD), 15 μg NARA1, or hIL-2/NARA1 (1.5 μg and 15 μg, respectively). One day after the last injection, mice were sacrificed and pulmonary wet weight was determined as previously described [60]. To determine immune cell proliferation, two methods were used:

- CD8$^+$ T cells, obtained from pooled LNs of IL-7-transgenic mice (*IL-7tg.Ly5$^b$*) on a Ly5.1 background, were labelled with carboxyfluorescein succinimidyl ester (CFSE, C1157; ThermoFisher), as previously described [134]. At least 2 x $10^6$ purified cells were adoptively transferred to recipients, followed by 4 daily injections of PBS, hIL-2,

or hIL-2/NARA1 complex. IL-7-transgenic mice were used since they have an increase in T cell numbers especially at the level of memory phenotype $CD44^{high}CD122^{high}$ $CD8^{+}$ T cells.

- Bromodeoxyuridine (BrdU; B5002, Sigma-Aldrich) was given to mice in drinking water (0.8 mg/ml). BrdU-incorporated cells were labelled using the FITC BrdU Flow Kit (557891, BD Biosciences) according to manufacturer's instructions.

**Flow Cytometry**

Single cell suspensions of lymph nodes and spleen were prepared according to standard protocols. Tumors were cut into small pieces, pooled per groups in order to obtain enough cells for analysis, and incubated in 10 ml dissociation buffer (RPMI, 5% FCS, 10 μg/ml of DNAase I (D4527, Sigma-Aldrich) and 200 U/ml of collagenase type I (17100-017, Life Technologies) for 45 minutes at 37°C and 25 rpm. Cell suspension was then passed through a 70 μm cell strainer. After one wash a Percoll (17-5445-01, GE Healthcare) gradient centrifugation was performed. All cell suspensions were stained for flow cytometry analysis using PBS with 2% FCS, 2 mM EDTA and fluorochrome-conjugated Abs (Supplementary Table 1). Intracellular CD107a, FoxP3, IFN-γ, and TNF-α stainings were performed following manufacturers' instructions after *in vitro* restimulation using PMA and ionomycin (0.1 mg/ml and 1 mg/ml, P8139 and I0634, Sigma-Aldrich) or gp100 short peptide (10 nM; generated, purified, dissolved and stored as described previously [212] ) in the presence of brefeldin A and monensin (2 mg/ml, B7651 and M5273, Sigma-Aldrich). Samples were acquired with a BD LSR II flow cytometer (BD Biosciences) and analysed using FlowJo software.

**Histological analysis and immunofluorescence**

Mouse tumor samples were fixed in 4% buffered formaldehyde, embedded in paraffin, sliced into 5 μm sections, and subjected to immunofluorescent stainings as described before [213]. Briefly, sections were deparaffinised and subjected to an antigen-unmasking step in citrate buffer (S2369, Dako) using a vegetable steamer for 20 minutes. To minimize unspecific Ab binding, sections were subjected to two blocking steps using UltraVision Protein Block (TA-060-PBQ, Thermo Scientific) for 5 minutes and subsequently an immunofluorescence blocking buffer (0.2% BSA, 0.2% gelatin A, 0.2% casein, and 0.2% Triton X-100 in TBS) for 15 minutes at room temperature. Primary Abs (Supplementary Table 2) were applied in Antibody Diluent (S0809, Dako) overnight at 4°C and visualized using secondary Abs (Supplementary Table 3) in Antibody Diluent for 1 hour at room temperature. Subsequently, nuclei were stained with Hoechst 33342 (14533, Sigma-Aldrich) and slides were mounted with Fluorescent Mounting Medium (S3023, Dako). Immunofluorescent sections were recorded using a DMI 6000B microscope (Leica) and fluorescence intensity was quantified with CellProfiler software [214]. For tumor sections derived from PBS- or GSK503-treated mice, at least 10 fields containing $n \geq 1$ $CD45^+$ or $CD3^+$ cells were quantified. For tumor sections derived from IL-2cx or GSK503 + IL-2cx-treated mice, at least 10 fields containing either $n < 5$ or $n > 25$ $CD45^+$ or $CD3^+$ cells were quantified. $Ezh2^{high}$ cells were defined as previously described [170].

**Immunofluorescence on cells**

Cells were grown on cover slips, fixed with 50% ethanol, and subjected to immunofluorescent labelling using primary Abs (Supplementary Table 2) in blocking buffer (1% BSA in PBS) overnight at 4°C and secondary Abs (Supplementary Table 3) for 1 hour at room temperature.

Nuclei were stained with Hoechst 33342 and cells were recorded with a DMI 6000B microscope.

**RNA isolation and RT-qPCR**

Cells were lysed in Buffer RLT (79216, Qiagen) containing 1% 2-mercaptoethanol, while tumor biopsies were homogenised in such buffer using a Polytron PT 2100 tissue disperser (Kinematica). Subsequent RNA extraction and DNase treatment of samples was performed using the RNeasy Mini Kit (74104, Qiagen) and the RNase-Free DNase Set (79254, Qiagen) according to manufacturer's guidelines. Purified RNA was quantified using a NanoDrop ND-1000 Spectrophotometer (Thermo Scientific) and subjected to reverse transcriptase reaction using the Maxima First Strand cDNA Synthesis Kit (K1641, Thermo Scientific) followed by an RNase H (EN0202, Thermo Scientific) digestion step according to manufacturer's recommendations. Quantitative real-time PCR was performed on a LightCycler 480 System (Roche) using LightCycler 480 SYBR Green I Master (4707516001, Roche). Primers used are indicated in Supplementary Table 4. Each sample was analysed in technical triplicates, and relative quantified RNA was normalized using *Usf1* as housekeeping transcript.

**Chromatin isolation and ChIP**

Chromatin isolation and chromatin immunoprecipitation (ChIP) was performed using the SimpleChIP Plus Enzymatic Chromatin IP Kit (9005, Cell Signaling Technology) according to manufacturer's guidelines. Briefly, tumor biopsies of 150 mg were minced using razor blades and scissors and subjected to chromatin isolation. Crosslinked samples were disaggregated into single cells using a Polytron PT 2100 tissue disperser. Isolated nuclei were

digested with 5 µl micrococcal nuclease for 30 minutes at 37°C and nuclei were lysed using a SONOPULS HD 2070 Ultrasonic Homogenizer (Bandelin). Chromatin digestion efficiency was verified by agarose gel electrophoresis and chromatin concentration was determined with a NanoDrop ND-1000 Spectrophotometer. The ChIP was performed with 18 µg chromatin and primary Abs indicated in (Supplementary Table 2). Quantitative real-time PCR was performed on a LightCycler 480 System using the KAPA SYBR Fast qPCR Kit Master Mix (KR0389, KAPA Biosystems). Primers were designed to amplify genomic DNA from a region flanking the transcriptional starting site -500 bp to +100 bp devoid of local CpG islands defined by CpG island prediction [215]. Primers used are indicated in (Supplementary Table 5). Relative promoter enrichment was normalised to chromatin inputs and to the intergenic region 1 (*Interg1*), which was previously defined as a negative control [216].

**Protein isolation and Western blotting**

For protein isolation, tumor biopsies were homogenised in RIPA buffer (89900, Thermo Scientific) containing Halt Phosphatase and Protease Inhibitor Cocktails (78420 and 87786, Thermo Scientific) using a Polytron PT 2100 tissue disperser. Cell lysis was completed using a SONOPULS HD 2070 Ultrasonic Homogenizer. Total protein concentration was determined with the BCA Protein Assay Kit (23227, Thermo Scientific) using a DTX 880 Multimode Detector (Beckman Coulter). Western blotting was performed as previously described [170]. Briefly, SDS–PAGE was carried out on 4–20% Mini-PROTEAN TGX Gels (456–1094, Bio Rad). Primary Abs (Supplementary Table 2) were applied in Odyssey blocking buffer (927–40000, LI-COR Biosciences) overnight at 4°C and visualized using secondary Abs (Supplementary Table 3) in Odyssey blocking buffer for 45 minutes at room temperature. Blots were scanned and quantified with an Odyssey imaging system (LI-COR

Biosciences). Quantified band intensities were normalized using either β-Actin or Histone 3 as housekeeping protein.

**Statistical analyses**

*P*-values were calculated as indicated using either analysis of variance (ANOVA), Fisher's least significant difference (LSD) test, or a two-sided unpaired Student's *t*-test. The expected variance was similar between the groups that were compared.

# VIII. Acknowledgements

I would like to thank Prof. Onur Boyman for his constant support as supervisor for during my thesis. I am really proud to be his first PhD student, together with Janine Woytschak. Many interesting discussions and input during these years helped me to advance further, personally as well as scientifically. I felt very fortunate that I had the chance to work in a great environment, cover different aspects of science and develop several methods.

I would also like to thank my family which was always there to support me and give me strength when I need it, in spite of the fact that they live thousands of kilometers away. My special thanks go to my husband Dario, for his never-ending love, encouragement and great assistance throughout the years and to his family whose affection really means a lot to me.

I greatly acknowledge the interdisciplinary and multinational members of the lab, immunologists, pharmacists and medical doctors with whom I had the luck to work together during these years. Special thanks goes to Emerita Ammann for her help with animal experiments and constant care of lab issues, to Dr. Rodney Rosalia, Dr. Janine Woytschak and Daniela Impellizzieri for stimulating discussions and troubleshooting and for being regular coffee break companions. It is a great pleasure to work in such helpful and friendly environment making my time, inside and outside of the lab very pleasant.

I would also like to express my gratitude to former members of the lab, Dr. Usriansyah Hadis, Dr. Grégory Bouchaud, and Dr. Carsten Krieg who introduced us into the lab and for our constructive discussions and to my student Monika Huembelin for her experimental contributions.

I would like to thanks the Novartis team, especially Dr. Catherine Regnier and Dr. Andreas Katopodis for the collaboration in the NARA1 antibody project. Their confidence and valuable scientific activity with us led to the development of the humanized antibody which will potentially be tested in clinical studies.

I also highly appreciated the collaboration with Prof. Lukas Sommer and Dr. Daniel Zingg in the project on EZH2 and tumor immune escape. Our valuable meetings, troubleshooting and experiments brought the project to a good end, showing how two different branches of cancer research can complement each other.

# IX. References


1. Delves, P.J. and I.M. Roitt, *The immune system. First of two parts.* N Engl J Med, 2000. **343**(1): p. 37-49.

2. Delves, P.J. and I.M. Roitt, *The immune system. Second of two parts.* N Engl J Med, 2000. **343**(2): p. 108-17.

3. Aderem, A. and D.M. Underhill, *Mechanisms of phagocytosis in macrophages.* Annu Rev Immunol, 1999. **17**: p. 593-623.

4. Karre, K., et al., *Selective rejection of H-2-deficient lymphoma variants suggests alternative immune defence strategy.* Nature, 1986. **319**(6055): p. 675-8.

5. Wardlaw, A.J., R. Moqbel, and A.B. Kay, *Eosinophils: biology and role in disease.* Adv Immunol, 1995. **60**: p. 151-266.

6. Abraham, S.N. and M. Arock, *Mast cells and basophils in innate immunity.* Semin Immunol, 1998. **10**(5): p. 373-81.

7. Moretta, A., et al., *Major histocompatibility complex class I-specific receptors on human natural killer and T lymphocytes.* Immunol Rev, 1997. **155**: p. 105-17.

8. Lanier, L.L., *Activating and inhibitory NK cell receptors.* Adv Exp Med Biol, 1998. **452**: p. 13-8.

9. Walker, J.A., J.L. Barlow, and A.N. McKenzie, *Innate lymphoid cells--how did we miss them?* Nat Rev Immunol, 2013. **13**(2): p. 75-87.

10. Steinman, R.M. and H. Hemmi, *Dendritic cells: translating innate to adaptive immunity.* Curr Top Microbiol Immunol, 2006. **311**: p. 17-58.

11. Tonegawa, S., *Somatic generation of antibody diversity.* Nature, 1983. **302**(5909): p. 575-81.

12. Kapsenberg, M.L., *Dendritic-cell control of pathogen-driven T-cell polarization.* Nat Rev Immunol, 2003. **3**(12): p. 984-93.

13. Garcia, K.C., L. Teyton, and I.A. Wilson, *Structural basis of T cell recognition.* Annu Rev Immunol, 1999. **17**: p. 369-97.

14. Davis, M.M., et al., *Ligand recognition by alpha beta T cell receptors.* Annu Rev Immunol, 1998. **16**: p. 523-44.

15. Fink, P.J. and M.J. Bevan, *Positive selection of thymocytes.* Adv Immunol, 1995. **59**: p. 99-133.

16. Sebzda, E., et al., *Selection of the T cell repertoire.* Annu Rev Immunol, 1999. **17**: p. 829-74.

17. Rajewsky, K., *Clonal selection and learning in the antibody system.* Nature, 1996. **381**(6585): p. 751-8.

18. Lenschow, D.J., T.L. Walunas, and J.A. Bluestone, *CD28/B7 system of T cell costimulation.* Annu Rev Immunol, 1996. **14**: p. 233-58.

19. Ott, P.A., F.S. Hodi, and C. Robert, *CTLA-4 and PD-1/PD-L1 blockade: new immunotherapeutic modalities with durable clinical benefit in melanoma patients.* Clin Cancer Res, 2013. **19**(19): p. 5300-9.

20. Smith, K.A., *Interleukin-2: inception, impact, and implications.* Science, 1988. **240**(4856): p. 1169-76.

21. Mosmann, T.R. and R.L. Coffman, *TH1 and TH2 cells: different patterns of lymphokine secretion lead to different functional properties.* Annu Rev Immunol, 1989. **7**: p. 145-73.

22. Dong, C., *TH17 cells in development: an updated view of their molecular identity and genetic programming.* Nat Rev Immunol, 2008. **8**(5): p. 337-48.

23. Dardalhon, V., et al., *IL-4 inhibits TGF-beta-induced Foxp3+ T cells and, together with TGF-beta, generates IL-9+ IL-10+ Foxp3(-) effector T cells.* Nat Immunol, 2008. **9**(12): p. 1347-55.

24. Kaplan, M.H., M.M. Hufford, and M.R. Olson, *The development and in vivo function of T helper 9 cells.* Nat Rev Immunol, 2015. **15**(5): p. 295-307.

25. Craft, J.E., *Follicular helper T cells in immunity and systemic autoimmunity.* Nat Rev Rheumatol, 2012. **8**(6): p. 337-47.

26. Medana, I.M., et al., *MHC class I-restricted killing of neurons by virus-specific CD8+ T lymphocytes is effected through the Fas/FasL, but not the perforin pathway.* Eur J Immunol, 2000. **30**(12): p. 3623-33.

27. Metkar, S.S., et al., *Cytotoxic cell granule-mediated apoptosis: perforin delivers granzyme B-serglycin complexes into target cells without plasma membrane pore formation.* Immunity, 2002. **16**(3): p. 417-28.

28. Munoz-Fernandez, M.A., M.A. Fernandez, and M. Fresno, *Synergism between tumor necrosis factor-alpha and interferon-gamma on macrophage activation for the killing of intracellular Trypanosoma cruzi through a nitric oxide-dependent mechanism.* Eur J Immunol, 1992. **22**(2): p. 301-7.

29. Cerutti, A., M. Cols, and I. Puga, *Marginal zone B cells: virtues of innate-like antibody-producing lymphocytes.* Nat Rev Immunol, 2013. **13**(2): p. 118-32.

30. Parker, D.C., *T cell-dependent B cell activation.* Annu Rev Immunol, 1993. **11**: p. 331-60.

31. Kurosaki, T., K. Kometani, and W. Ise, *Memory B cells.* Nat Rev Immunol, 2015. **15**(3): p. 149-59.

32. Brekke, O.H. and I. Sandlie, *Therapeutic antibodies for human diseases at the dawn of the twenty-first century.* Nat Rev Drug Discov, 2003. **2**(1): p. 52-62.

33. Weiner, L.M., R. Surana, and S. Wang, *Monoclonal antibodies: versatile platforms for cancer immunotherapy.* Nat Rev Immunol, 2010. **10**(5): p. 317-27.

34. Raghavan, M. and P.J. Bjorkman, *Fc receptors and their interactions with immunoglobulins.* Annu Rev Cell Dev Biol, 1996. **12**: p. 181-220.

35. Kohler, G. and C. Milstein, *Continuous cultures of fused cells secreting antibody of predefined specificity. 1975.* Biotechnology, 1992. **24**: p. 524-6.

36. Kohler, G. and C. Milstein, *Derivation of specific antibody-producing tissue culture and tumor lines by cell fusion.* Eur J Immunol, 1976. **6**(7): p. 511-9.

37. Hwang, W.Y. and J. Foote, *Immunogenicity of engineered antibodies.* Methods, 2005. **36**(1): p. 3-10.

38. Morrison, S.L., et al., *Chimeric human antibody molecules: mouse antigen-binding domains with human constant region domains.* Proc Natl Acad Sci U S A, 1984. **81**(21): p. 6851-5.

39. Jones, P.T., et al., *Replacing the complementarity-determining regions in a human antibody with those from a mouse.* Nature, 1986. **321**(6069): p. 522-5.

40. McCafferty, J., et al., *Phage antibodies: filamentous phage displaying antibody variable domains.* Nature, 1990. **348**(6301): p. 552-4.

41. Winter, G., et al., *Making antibodies by phage display technology.* Annu Rev Immunol, 1994. **12**: p. 433-55.

42. Boder, E.T. and K.D. Wittrup, *Yeast surface display for screening combinatorial polypeptide libraries.* Nat Biotechnol, 1997. **15**(6): p. 553-7.

43. Lonberg, N., et al., *Antigen-specific human antibodies from mice comprising four distinct genetic modifications.* Nature, 1994. **368**(6474): p. 856-9.

44. Sievers, E.L. and P.D. Senter, *Antibody-drug conjugates in cancer therapy.* Annu Rev Med, 2013. **64**: p. 15-29.

45. Lee, Y.J. and K.J. Jeong, *Challenges to production of antibodies in bacteria and yeast.* J Biosci Bioeng, 2015. **120**(5): p. 483-90.

46. Rochman, Y., R. Spolski, and W.J. Leonard, *New insights into the regulation of T cells by gamma(c) family cytokines.* Nat Rev Immunol, 2009. **9**(7): p. 480-90.

47. Okuda, Y., *Review of tocilizumab in the treatment of rheumatoid arthritis.* Biologics, 2008. **2**(1): p. 75-82.

48. Bissonnette, R., et al., *Efficacy and safety of adalimumab in patients with plaque psoriasis who have shown an unsatisfactory response to etanercept.* J Am Acad Dermatol, 2010. **63**(2): p. 228-34.

49. Gisondi, P., C. Dalle Vedove, and G. Girolomoni, *Efficacy and safety of secukinumab in chronic plaque psoriasis and psoriatic arthritis therapy.* Dermatol Ther (Heidelb), 2014. **4**(1): p. 1-9.

50. Atkins, M.B., et al., *High-dose recombinant interleukin 2 therapy for patients with metastatic melanoma: analysis of 270 patients treated between 1985 and 1993.* J Clin Oncol, 1999. **17**(7): p. 2105-16.

51. Paty, D.W. and D.K. Li, *Interferon beta-1b is effective in relapsing-remitting multiple sclerosis. II. MRI analysis results of a multicenter, randomized, double-blind, placebo-controlled trial. UBC MS/MRI Study Group and the IFNB Multiple Sclerosis Study Group.* Neurology, 1993. **43**(4): p. 662-7.

52. Gallin, J.I., *Interferon-gamma in the management of chronic granulomatous disease.* Rev Infect Dis, 1991. **13**(5): p. 973-8.

53. Eggermont, A.M., et al., *Isolated limb perfusion with tumor necrosis factor and melphalan for limb salvage in 186 patients with locally advanced soft tissue extremity sarcomas. The cumulative multicenter European experience.* Ann Surg, 1996. **224**(6): p. 756-64; discussion 764-5.

54. Rosalia, R.A., et al., *Use of enhanced interleukin-2 formulations for improved immunotherapy against cancer.* Curr Opin Chem Biol, 2014. **23**: p. 39-46.

55. Arenas-Ramirez, N., J. Woytschak, and O. Boyman, *Interleukin-2: Biology, Design and Application.* Trends Immunol, 2015.

56. Boyman, O. and J. Sprent, *The role of interleukin-2 during homeostasis and activation of the immune system.* Nat Rev Immunol, 2012. **12**(3): p. 180-90.

57. Malek, T.R. and I. Castro, *Interleukin-2 receptor signaling: at the interface between tolerance and immunity.* Immunity, 2010. **33**(2): p. 153-65.

58. Taniguchi, T. and Y. Minami, *The IL-2/IL-2 receptor system: a current overview.* Cell, 1993. **73**(1): p. 5-8.

59. Zubler, R.H., et al., *Activated B cells express receptors for, and proliferate in response to, pure interleukin 2.* J Exp Med, 1984. **160**(4): p. 1170-83.

60. Krieg, C., et al., *Improved IL-2 immunotherapy by selective stimulation of IL-2 receptors on lymphocytes and endothelial cells.* Proc Natl Acad Sci U S A, 2010. **107**(26): p. 11906-11.

61. Roediger, B., et al., *Cutaneous immunosurveillance and regulation of inflammation by group 2 innate lymphoid cells.* Nat Immunol, 2013. **14**(6): p. 564-73.

62. Zelante, T., et al., *Interleukin-2 production by dendritic cells and its immuno-regulatory functions.* Front Immunol, 2012. **3**: p. 161.

63. Malek, T.R., *The biology of interleukin-2.* Annu Rev Immunol, 2008. **26**: p. 453-79.

64. Liao, W., J.X. Lin, and W.J. Leonard, *Interleukin-2 at the crossroads of effector responses, tolerance, and immunotherapy.* Immunity, 2013. **38**(1): p. 13-25.

65. Yu, A., et al., *A low interleukin-2 receptor signaling threshold supports the development and homeostasis of T regulatory cells.* Immunity, 2009. **30**(2): p. 204-17.

66. Amado, I.F., et al., *IL-2 coordinates IL-2-producing and regulatory T cell interplay.* J Exp Med, 2013. **210**(12): p. 2707-20.

67. O'Shea, J.J. and W.E. Paul, *Mechanisms underlying lineage commitment and plasticity of helper CD4+ T cells.* Science, 2010. **327**(5969): p. 1098-102.

68. Aoki, C.A., et al., *IL-2 receptor alpha deficiency and features of primary biliary cirrhosis.* J Autoimmun, 2006. **27**(1): p. 50-3.

69. Caudy, A.A., et al., *CD25 deficiency causes an immune dysregulation, polyendocrinopathy, enteropathy, X-linked-like syndrome, and defective IL-10 expression from CD4 lymphocytes.* J Allergy Clin Immunol, 2007. **119**(2): p. 482-7.

70. Gregersen, P.K. and L.M. Olsson, *Recent advances in the genetics of autoimmune disease.* Annu Rev Immunol, 2009. **27**: p. 363-91.

71. Yu, A., et al., *Selective IL-2 responsiveness of regulatory T cells through multiple intrinsic mechanisms supports the use of low-dose IL-2 therapy in type 1 diabetes.* Diabetes, 2015. **64**(6): p. 2172-83.

72. Long, S.A., et al., *Rapamycin/IL-2 combination therapy in patients with type 1 diabetes augments Tregs yet transiently impairs beta-cell function.* Diabetes, 2012. **61**(9): p. 2340-8.

73. Hartemann, A., et al., *Low-dose interleukin 2 in patients with type 1 diabetes: a phase 1/2 randomised, double-blind, placebo-controlled trial.* Lancet Diabetes Endocrinol, 2013. **1**(4): p. 295-305.

74. Saadoun, D., et al., *Regulatory T-cell responses to low-dose interleukin-2 in HCV-induced vasculitis.* N Engl J Med, 2011. **365**(22): p. 2067-77.

75. Koreth, J., et al., *Interleukin-2 and regulatory T cells in graft-versus-host disease.* N Engl J Med, 2011. **365**(22): p. 2055-66.

76. Klatzmann, D. and A.K. Abbas, *The promise of low-dose interleukin-2 therapy for autoimmune and inflammatory diseases.* Nat Rev Immunol, 2015. **15**(5): p. 283-94.

77. Rosenberg, S.A., *Raising the bar: the curative potential of human cancer immunotherapy.* Sci Transl Med, 2012. **4**(127): p. 127ps8.

78. Rosenberg, S.A., *IL-2: the first effective immunotherapy for human cancer.* J Immunol, 2014. **192**(12): p. 5451-8.

79. Hanahan, D. and R.A. Weinberg, *The hallmarks of cancer*. Cell, 2000. **100**(1): p. 57-70.

80. Hanahan, D. and R.A. Weinberg, *Hallmarks of cancer: the next generation.* Cell, 2011. **144**(5): p. 646-74.

81. McCarthy, E.F., *The toxins of William B. Coley and the treatment of bone and soft-tissue sarcomas.* Iowa Orthop J, 2006. **26**: p. 154-8.

82. Old, L.J. and E.A. Boyse, *IMMUNOLOGY OF EXPERIMENTAL TUMORS.* Annu Rev Med, 1964. **15**: p. 167-86.

83. Schreiber, R.D., L.J. Old, and M.J. Smyth, *Cancer immunoediting: integrating immunity's roles in cancer suppression and promotion.* Science, 2011. **331**(6024): p. 1565-70.

84. Mellman, I., G. Coukos, and G. Dranoff, *Cancer immunotherapy comes of age.* Nature, 2011. **480**(7378): p. 480-9.

85. Van den Eynde, B., et al., *Presence on a human melanoma of multiple antigens recognized by autologous CTL.* Int J Cancer, 1989. **44**(4): p. 634-40.

86. De Plaen, E., et al., *Structure, chromosomal localization, and expression of 12 genes of the MAGE family.* Immunogenetics, 1994. **40**(5): p. 360-9.

87. Lurquin, C., et al., *Two members of the human MAGEB gene family located in Xp21.3 are expressed in tumors of various histological origins.* Genomics, 1997. **46**(3): p. 397-408.

88. Lucas, S., et al., *Identification of a new MAGE gene with tumor-specific expression by representational difference analysis.* Cancer Res, 1998. **58**(4): p. 743-52.

89. Lucas, S., E. De Plaen, and T. Boon, *MAGE-B5, MAGE-B6, MAGE-C2, and MAGE-C3: four new members of the MAGE family with tumor-specific expression.* Int J Cancer, 2000. **87**(1): p. 55-60.

90. Brichard, V., et al., *The tyrosinase gene codes for an antigen recognized by autologous cytolytic T lymphocytes on HLA-A2 melanomas.* J Exp Med, 1993. **178**(2): p. 489-95.

91. Kawakami, Y., et al., *Identification of the immunodominant peptides of the MART-1 human melanoma antigen recognized by the majority of HLA-A2-restricted tumor infiltrating lymphocytes.* J Exp Med, 1994. **180**(1): p. 347-52.

92. Wolfel, T., et al., *Two tyrosinase nonapeptides recognized on HLA-A2 melanomas by autologous cytolytic T lymphocytes.* Eur J Immunol, 1994. **24**(3): p. 759-64.

93. Boon, T., et al., *Human T cell responses against melanoma.* Annu Rev Immunol, 2006. **24**: p. 175-208.

94. Vonderheide, R.H. and M.J. Glennie, *Agonistic CD40 antibodies and cancer therapy.* Clin Cancer Res, 2013. **19**(5): p. 1035-43.

95. Kenter, G.G., et al., *Vaccination against HPV-16 oncoproteins for vulvar intraepithelial neoplasia.* N Engl J Med, 2009. **361**(19): p. 1838-47.

96. Kantoff, P.W., et al., *Overall survival analysis of a phase II randomized controlled trial of a Poxviral-based PSA-targeted immunotherapy in metastatic castration-resistant prostate cancer.* J Clin Oncol, 2010. **28**(7): p. 1099-105.

97. Schuler, G., *Dendritic cells in cancer immunotherapy.* Eur J Immunol, 2010. **40**(8): p. 2123-30.

98. Leffers, N., et al., *Immunization with a P53 synthetic long peptide vaccine induces P53-specific immune responses in ovarian cancer patients, a phase II trial.* Int J Cancer, 2009. **125**(9): p. 2104-13.

99. Brichard, V.G. and D. Lejeune, *GSK's antigen-specific cancer immunotherapy programme: pilot results leading to Phase III clinical development.* Vaccine, 2007. **25 Suppl 2**: p. B61-71.

100. Rosenberg, S.A., et al., *Adoptive cell transfer: a clinical path to effective cancer immunotherapy.* Nat Rev Cancer, 2008. **8**(4): p. 299-308.

101. Kalos, M., et al., *T cells with chimeric antigen receptors have potent antitumor effects and can establish memory in patients with advanced leukemia.* Sci Transl Med, 2011. **3**(95): p. 95ra73.

102. Hudis, C.A., *Trastuzumab--mechanism of action and use in clinical practice.* N Engl J Med, 2007. **357**(1): p. 39-51.

103. Weiner, G.J., *Rituximab: mechanism of action.* Semin Hematol, 2010. **47**(2): p. 115-23.

104. Suntharalingam, G., et al., *Cytokine storm in a phase 1 trial of the anti-CD28 monoclonal antibody TGN1412.* N Engl J Med, 2006. **355**(10): p. 1018-28.

105. Topalian, S.L., C.G. Drake, and D.M. Pardoll, *Immune checkpoint blockade: a common denominator approach to cancer therapy.* Cancer Cell, 2015. **27**(4): p. 450-61.

106. Hodi, F.S., et al., *Improved survival with ipilimumab in patients with metastatic melanoma.* N Engl J Med, 2010. **363**(8): p. 711-23.

107. Brahmer, J.R., et al., *Phase I study of single-agent anti-programmed death-1 (MDX-1106) in refractory solid tumors: safety, clinical activity, pharmacodynamics, and immunologic correlates.* J Clin Oncol, 2010. **28**(19): p. 3167-75.

108. Tumeh, P.C., et al., *PD-1 blockade induces responses by inhibiting adaptive immune resistance.* Nature, 2014. **515**(7528): p. 568-71.

109. Ratner, M., *Genentech's glyco-engineered antibody to succeed Rituxan.* Nat Biotechnol, 2014. **32**(1): p. 6-7.

110. Ascierto, P.A. and F.M. Marincola, *2015: The Year of Anti-PD-1/PD-L1s Against Melanoma and Beyond.* EBioMedicine, 2015. **2**(2): p. 92-3.

111. Topp, M.S., et al., *Targeted therapy with the T-cell-engaging antibody blinatumomab of chemotherapy-refractory minimal residual disease in B-lineage acute lymphoblastic leukemia patients results in high response rate and prolonged leukemia-free survival.* J Clin Oncol, 2011. **29**(18): p. 2493-8.

112. Marvel, D. and D.I. Gabrilovich, *Myeloid-derived suppressor cells in the tumor microenvironment: expect the unexpected.* J Clin Invest, 2015. **125**(9): p. 3356-64.

113. Pillay, V., H.K. Gan, and A.M. Scott, *Antibodies in oncology.* N Biotechnol, 2011. **28**(5): p. 518-29.

114. Ferris, R.L., E.M. Jaffee, and S. Ferrone, *Tumor antigen-targeted, monoclonal antibody-based immunotherapy: clinical response, cellular immunity, and immunoescape.* J Clin Oncol, 2010. **28**(28): p. 4390-9.

115. Kaplan, D.H., et al., *Demonstration of an interferon gamma-dependent tumor surveillance system in immunocompetent mice.* Proc Natl Acad Sci U S A, 1998. **95**(13): p. 7556-61.

116. Shankaran, V., et al., *IFNgamma and lymphocytes prevent primary tumour development and shape tumour immunogenicity.* Nature, 2001. **410**(6832): p. 1107-11.

117. Enzler, T., et al., *Deficiencies of GM-CSF and interferon gamma link inflammation and cancer.* J Exp Med, 2003. **197**(9): p. 1213-9.

118. Voronov, E., et al., *IL-1 is required for tumor invasiveness and angiogenesis.* Proc Natl Acad Sci U S A, 2003. **100**(5): p. 2645-50.

119. Atkins, M.B., et al., *Phase I evaluation of intravenous recombinant human interleukin 12 in patients with advanced malignancies.* Clin Cancer Res, 1997. **3**(3): p. 409-17.

120. Kirkwood, J.M., et al., *High-dose interferon alfa-2b significantly prolongs relapse-free and overall survival compared with the GM2-KLH/QS-21 vaccine in patients with resected stage IIB-III melanoma: results of intergroup trial E1694/S9512/C509801.* J Clin Oncol, 2001. **19**(9): p. 2370-80.

121. Spitler, L.E., et al., *Adjuvant therapy of stage III and IV malignant melanoma using granulocyte-macrophage colony-stimulating factor.* J Clin Oncol, 2000. **18**(8): p. 1614-21.

122. Rini, B.I., et al., *Prostate-specific antigen kinetics as a measure of the biologic effect of granulocyte-macrophage colony-stimulating factor in patients with serologic progression of prostate cancer.* J Clin Oncol, 2003. **21**(1): p. 99-105.

123. Barnetson, R.S. and G.M. Halliday, *Regression in skin tumours: a common phenomenon.* Australas J Dermatol, 1997. **38 Suppl 1**: p. S63-5.

124. Donohue, J.H. and S.A. Rosenberg, *The fate of interleukin-2 after in vivo administration.* J Immunol, 1983. **130**(5): p. 2203-8.

125. Konrad, M.W., et al., *Pharmacokinetics of recombinant interleukin 2 in humans.* Cancer Res, 1990. **50**(7): p. 2009-17.

126. Albertini, M.R., et al., *Phase II trial of hu14.18-IL2 for patients with metastatic melanoma.* Cancer Immunol Immunother, 2012. **61**(12): p. 2261-71.

127. Johannsen, M., et al., *The tumour-targeting human L19-IL2 immunocytokine: preclinical safety studies, phase I clinical trial in patients with solid tumours and expansion into patients with advanced renal cell carcinoma.* Eur J Cancer, 2010. **46**(16): p. 2926-35.

128. Gutbrodt, K.L., et al., *Antibody-based delivery of interleukin-2 to neovasculature has potent activity against acute myeloid leukemia.* Sci Transl Med, 2013. **5**(201): p. 201ra118.

129. Antony, P.A., et al., *CD8+ T cell immunity against a tumor/self-antigen is augmented by CD4+ T helper cells and hindered by naturally occurring T regulatory cells.* J Immunol, 2005. **174**(5): p. 2591-601.

130. Klages, K., et al., *Selective depletion of Foxp3+ regulatory T cells improves effective therapeutic vaccination against established melanoma.* Cancer Res, 2010. **70**(20): p. 7788-99.

131. Dubois, S., et al., *Preassociation of IL-15 with IL-15R alpha-IgG1-Fc enhances its activity on proliferation of NK and CD8+/CD44high T cells and its antitumor action.* J Immunol, 2008. **180**(4): p. 2099-106.

132. Bessard, A., et al., *High antitumor activity of RLI, an interleukin-15 (IL-15)-IL-15 receptor alpha fusion protein, in metastatic melanoma and colorectal cancer.* Mol Cancer Ther, 2009. **8**(9): p. 2736-45.

133. Letourneau, S., et al., *IL-2/anti-IL-2 antibody complexes show strong biological activity by avoiding interaction with IL-2 receptor alpha subunit CD25.* Proc Natl Acad Sci U S A, 2010. **107**(5): p. 2171-6.

134. Boyman, O., et al., *Selective stimulation of T cell subsets with antibody-cytokine immune complexes.* Science, 2006. **311**(5769): p. 1924-7.

135. Spangler, J.B., et al., *Antibodies to Interleukin-2 Elicit Selective T Cell Subset Potentiation through Distinct Conformational Mechanisms.* Immunity, 2015. **42**(5): p. 815-25.

136. Webster, K.E., et al., *In vivo expansion of T reg cells with IL-2-mAb complexes: induction of resistance to EAE and long-term acceptance of islet allografts without immunosuppression.* J Exp Med, 2009. **206**(4): p. 751-60.

137. Phelan, J.D., T. Orekov, and F.D. Finkelman, *Cutting edge: mechanism of enhancement of in vivo cytokine effects by anti-cytokine monoclonal antibodies.* J Immunol, 2008. **180**(1): p. 44-8.

138. Molloy, M.J., W. Zhang, and E.J. Usherwood, *Cutting edge: IL-2 immune complexes as a therapy for persistent virus infection.* J Immunol, 2009. **182**(8): p. 4512-5.

139. Hamilton, S.E., et al., *IL-2 complex treatment can protect naive mice from bacterial and viral infection.* J Immunol, 2010. **185**(11): p. 6584-90.

140. Shanafelt, A.B., et al., *A T-cell-selective interleukin 2 mutein exhibits potent antitumor activity and is well tolerated in vivo.* Nat Biotechnol, 2000. **18**(11): p. 1197-202.

141. Laurent, J., et al., *T-cell activation by treatment of cancer patients with EMD 521873 (Selectikine), an IL-2/anti-DNA fusion protein.* J Transl Med, 2013. **11**: p. 5.

142. Levin, A.M., et al., *Exploiting a natural conformational switch to engineer an interleukin-2 'superkine'.* Nature, 2012. **484**(7395): p. 529-33.

143. Carmenate, T., et al., *Human IL-2 mutein with higher antitumor efficacy than wild type IL-2.* J Immunol, 2013. **190**(12): p. 6230-8.

144. Landsberg, J., et al., *Melanomas resist T-cell therapy through inflammation-induced reversible dedifferentiation.* Nature, 2012. **490**(7420): p. 412-6.

145. Wherry, E.J. and M. Kurachi, *Molecular and cellular insights into T cell exhaustion.* Nat Rev Immunol, 2015. **15**(8): p. 486-99.

146. Sharma, P. and J.P. Allison, *The future of immune checkpoint therapy.* Science, 2015. **348**(6230): p. 56-61.

147. Hurwitz, A.A., et al., *CTLA-4 blockade synergizes with tumor-derived granulocyte-macrophage colony-stimulating factor for treatment of an experimental mammary carcinoma.* Proc Natl Acad Sci U S A, 1998. **95**(17): p. 10067-71.

148. Li, B., et al., *Anti-programmed death-1 synergizes with granulocyte macrophage colony-stimulating factor--secreting tumor cell immunotherapy providing therapeutic benefit to mice with established tumors.* Clin Cancer Res, 2009. **15**(5): p. 1623-34.

149. Curran, M.A., et al., *PD-1 and CTLA-4 combination blockade expands infiltrating T cells and reduces regulatory T and myeloid cells within B16 melanoma tumors.* Proc Natl Acad Sci U S A, 2010. **107**(9): p. 4275-80.

150. Humphrey, R.W., et al., *Opportunities and challenges in the development of experimental drug combinations for cancer.* J Natl Cancer Inst, 2011. **103**(16): p. 1222-6.

151. Waddington, C.H., *The epigenotype. 1942.* Int J Epidemiol, 2012. **41**(1): p. 10-3.

152. Bernstein, B.E., A. Meissner, and E.S. Lander, *The mammalian epigenome.* Cell, 2007. **128**(4): p. 669-81.

153. Karpf, A.R. and S. Matsui, *Genetic disruption of cytosine DNA methyltransferase enzymes induces chromosomal instability in human cancer cells.* Cancer Res, 2005. **65**(19): p. 8635-9.

154. Feinberg, A.P. and B. Vogelstein, *Hypomethylation distinguishes genes of some human cancers from their normal counterparts.* Nature, 1983. **301**(5895): p. 89-92.

155. Costello, J.F., et al., *Aberrant CpG-island methylation has non-random and tumour-type-specific patterns.* Nat Genet, 2000. **24**(2): p. 132-8.

156. Esteller, M., et al., *Promoter hypermethylation and BRCA1 inactivation in sporadic breast and ovarian tumors.* J Natl Cancer Inst, 2000. **92**(7): p. 564-9.

157. Merlo, A., et al., *5' CpG island methylation is associated with transcriptional silencing of the tumour suppressor p16/CDKN2/MTS1 in human cancers.* Nat Med, 1995. **1**(7): p. 686-92.

158. McHugh, J.B., et al., *Expression of polycomb group protein EZH2 in nevi and melanoma.* J Cutan Pathol, 2007. **34**(8): p. 597-600.

159. Sauvageau, M. and G. Sauvageau, *Polycomb group proteins: multi-faceted regulators of somatic stem cells and cancer.* Cell Stem Cell, 2010. **7**(3): p. 299-313.

160. Cao, R., et al., *Role of histone H3 lysine 27 methylation in Polycomb-group silencing.* Science, 2002. **298**(5595): p. 1039-43.

161. Martinez-Garcia, E. and J.D. Licht, *Deregulation of H3K27 methylation in cancer.* Nat Genet, 2010. **42**(2): p. 100-1.

162. Margueron, R. and D. Reinberg, *The Polycomb complex PRC2 and its mark in life.* Nature, 2011. **469**(7330): p. 343-9.

163. O'Carroll, D., et al., *The polycomb-group gene Ezh2 is required for early mouse development.* Mol Cell Biol, 2001. **21**(13): p. 4330-6.

164. Ben-Porath, I., et al., *An embryonic stem cell-like gene expression signature in poorly differentiated aggressive human tumors.* Nat Genet, 2008. **40**(5): p. 499-507.

165. McCabe, M.T., et al., *Mutation of A677 in histone methyltransferase EZH2 in human B-cell lymphoma promotes hypertrimethylation of histone H3 on lysine 27 (H3K27).* Proc Natl Acad Sci U S A, 2012. **109**(8): p. 2989-94.

166. McCabe, M.T., et al., *EZH2 inhibition as a therapeutic strategy for lymphoma with EZH2-activating mutations.* Nature, 2012. **492**(7427): p. 108-12.

167. Morin, R.D., et al., *Somatic mutations altering EZH2 (Tyr641) in follicular and diffuse large B-cell lymphomas of germinal-center origin.* Nat Genet, 2010. **42**(2): p. 181-5.

168. Bachmann, I.M., et al., *EZH2 expression is associated with high proliferation rate and aggressive tumor subgroups in cutaneous melanoma and cancers of the endometrium, prostate, and breast.* J Clin Oncol, 2006. **24**(2): p. 268-73.

169. Fan, T., et al., *EZH2-dependent suppression of a cellular senescence phenotype in melanoma cells by inhibition of p21/CDKN1A expression.* Mol Cancer Res, 2011. **9**(4): p. 418-29.

170. Zingg, D., et al., *The epigenetic modifier EZH2 controls melanoma growth and metastasis through silencing of distinct tumour suppressors.* Nat Commun, 2015. **6**: p. 6051.

171. Holling, T.M., et al., *A role for EZH2 in silencing of IFN-gamma inducible MHC2TA transcription in uveal melanoma.* J Immunol, 2007. **179**(8): p. 5317-25.

172. Tan, J., et al., *Pharmacologic disruption of Polycomb-repressive complex 2-mediated gene repression selectively induces apoptosis in cancer cells.* Genes Dev, 2007. **21**(9): p. 1050-63.

173. Beguelin, W., et al., *EZH2 is required for germinal center formation and somatic EZH2 mutations promote lymphoid transformation.* Cancer Cell, 2013. **23**(5): p. 677-92.

174. Wang, X., M. Rickert, and K.C. Garcia, *Structure of the quaternary complex of interleukin-2 with its alpha, beta, and gammac receptors.* Science, 2005. **310**(5751): p. 1159-63.

175. Stauber, D.J., et al., *Crystal structure of the IL-2 signaling complex: paradigm for a heterotrimeric cytokine receptor.* Proc Natl Acad Sci U S A, 2006. **103**(8): p. 2788-93.

176. Rickert, M., et al., *The structure of interleukin-2 complexed with its alpha receptor.* Science, 2005. **308**(5727): p. 1477-80.

177. Rojas, G., et al., *Deciphering the molecular bases of the biological effects of antibodies against Interleukin-2: a versatile platform for fine epitope mapping.* Immunobiology, 2013. **218**(1): p. 105-13.

178. Ackermann, J., et al., *Metastasizing melanoma formation caused by expression of activated N-RasQ61K on an INK4a-deficient background.* Cancer Res, 2005. **65**(10): p. 4005-11.

179. Shakhova, O., et al., *Sox10 promotes the formation and maintenance of giant congenital naevi and melanoma.* Nat Cell Biol, 2012. **14**(8): p. 882-90.

180. Steingrimsson, E., N.G. Copeland, and N.A. Jenkins, *Melanocytes and the microphthalmia transcription factor network.* Annu Rev Genet, 2004. **38**: p. 365-411.

181. Bloom, M.B., et al., *Identification of tyrosinase-related protein 2 as a tumor rejection antigen for the B16 melanoma.* J Exp Med, 1997. **185**(3): p. 453-9.

182. Overwijk, W.W., et al., *gp100/pmel 17 is a murine tumor rejection antigen: induction of "self"-reactive, tumoricidal T cells using high-affinity, altered peptide ligand.* J Exp Med, 1998. **188**(2): p. 277-86.

183. Civenni, G., et al., *Human CD271-positive melanoma stem cells associated with metastasis establish tumor heterogeneity and long-term growth.* Cancer Res, 2011. **71**(8): p. 3098-109.

184. Caramel, J., et al., *A switch in the expression of embryonic EMT-inducers drives the development of malignant melanoma.* Cancer Cell, 2013. **24**(4): p. 466-80.

185. Cheng, P.F., et al., *Methylation-dependent SOX9 expression mediates invasion in human melanoma cells and is a negative prognostic factor in advanced melanoma.* Genome Biol, 2015. **16**: p. 42.

186. Chen, L., et al., *Metastasis is regulated via microRNA-200/ZEB1 axis control of tumour cell PD-L1 expression and intratumoral immunosuppression.* Nat Commun, 2014. **5**: p. 5241.

187. Peng, D., et al., *Epigenetic silencing of TH1-type chemokines shapes tumour immunity and immunotherapy.* Nature, 2015. **527**(7577): p. 249-53.

188. Atkins, M.B., et al., *High-dose recombinant interleukin-2 therapy in patients with metastatic melanoma: long-term survival update.* Cancer J Sci Am, 2000. **6 Suppl 1**: p. S11-4.

189. Prieto, P.A., et al., *CTLA-4 blockade with ipilimumab: long-term follow-up of 177 patients with metastatic melanoma.* Clin Cancer Res, 2012. **18**(7): p. 2039-47.

190. Ma, C. and A.W. Armstrong, *Severe adverse events from the treatment of advanced melanoma: a systematic review of severe side effects associated with ipilimumab, vemurafenib, interferon alfa-2b, dacarbazine and interleukin-2.* J Dermatolog Treat, 2014. **25**(5): p. 401-8.

191. Hannani, D., et al., *Anticancer immunotherapy by CTLA-4 blockade: obligatory contribution of IL-2 receptors and negative prognostic impact of soluble CD25.* Cell Res, 2015. **25**(2): p. 208-24.

192. Tomala, J., et al., *Chimera of IL-2 linked to light chain of anti-IL-2 mAb mimics IL-2/anti-IL-2 mAb complexes both structurally and functionally.* ACS Chem Biol, 2013. **8**(5): p. 871-6.

193. Baker, M.P., et al., *Immunogenicity of protein therapeutics: The key causes, consequences and challenges.* Self Nonself, 2010. **1**(4): p. 314-322.

194. Boyman, O., D. Comte, and F. Spertini, *Adverse reactions to biologic agents and their medical management.* Nat Rev Rheumatol, 2014. **10**(10): p. 612-27.

195. Margolin, K., et al., *Phase I trial of BAY 50-4798, an interleukin-2-specific agonist in advanced melanoma and renal cancer.* Clin Cancer Res, 2007. **13**(11): p. 3312-9.

196. Hess, C., D. Venetz, and D. Neri, *Emerging classes of armed antibody therapeutics against cancer.* MedChemComm, 2014. **5**(4): p. 408-431.

197. Finkelman, F.D., et al., *Anti-cytokine antibodies as carrier proteins. Prolongation of in vivo effects of exogenous cytokines by injection of cytokine-anti-cytokine antibody complexes.* J Immunol, 1993. **151**(3): p. 1235-44.

198. May, L.T., et al., *Antibodies chaperone circulating IL-6. Paradoxical effects of anti-IL-6 "neutralizing" antibodies in vivo.* J Immunol, 1993. **151**(6): p. 3225-36.

199. Boyman, O., et al., *IL-7/anti-IL-7 mAb complexes restore T cell development and induce homeostatic T Cell expansion without lymphopenia.* J Immunol, 2008. **180**(11): p. 7265-75.

200. Rubinstein, M.P., et al., *G-CSF/anti-G-CSF antibody complexes drive the potent recovery and expansion of CD11b+Gr-1+ myeloid cells without compromising CD8+ T cell immune responses.* J Hematol Oncol, 2013. **6**: p. 75.

201. Muto, T., et al., *Concurrent loss of Ezh2 and Tet2 cooperates in the pathogenesis of myelodysplastic disorders.* J Exp Med, 2013. **210**(12): p. 2627-39.

202. Ntziachristos, P., et al., *Genetic inactivation of the polycomb repressive complex 2 in T cell acute lymphoblastic leukemia.* Nat Med, 2012. **18**(2): p. 298-301.

203. Zhao, E., et al., *Cancer mediates effector T cell dysfunction by targeting microRNAs and EZH2 via glycolysis restriction.* Nat Immunol, 2016. **17**(1): p. 95-103.

204. Piali, L., et al., *Endothelial vascular cell adhesion molecule 1 expression is suppressed by melanoma and carcinoma.* J Exp Med, 1995. **181**(2): p. 811-6.

205. Gorelik, L. and R.A. Flavell, *Immune-mediated eradication of tumors through the blockade of transforming growth factor-beta signaling in T cells.* Nat Med, 2001. **7**(10): p. 1118-22.

206. Ochsenbein, A.F., et al., *Roles of tumour localization, second signals and cross priming in cytotoxic T-cell induction.* Nature, 2001. **411**(6841): p. 1058-64.

207. Sakaguchi, S., *Regulatory T cells: key controllers of immunologic self-tolerance.* Cell, 2000. **101**(5): p. 455-8.

208. Staveley-O'Carroll, K., et al., *Induction of antigen-specific T cell anergy: An early event in the course of tumor progression.* Proc Natl Acad Sci U S A, 1998. **95**(3): p. 1178-83.

209. Russell, J.H., et al., *Receptor-stimulated death pathway is opened by antigen in mature T cells.* Proc Natl Acad Sci U S A, 1991. **88**(6): p. 2151-5.

210. Maksimov, P., et al., *Analysis of clonal type-specific antibody reactions in Toxoplasma gondii seropositive humans from Germany by peptide-microarray.* PLoS One, 2012. **7**(3): p. e34212.

211. Tiwari, N., et al., *Sox4 is a master regulator of epithelial-mesenchymal transition by controlling Ezh2 expression and epigenetic reprogramming.* Cancer Cell, 2013. **23**(6): p. 768-83.

212. Feltkamp, M.C., et al., *Vaccination with cytotoxic T lymphocyte epitope-containing peptide protects against a tumor induced by human papillomavirus type 16-transformed cells.* Eur J Immunol, 1993. **23**(9): p. 2242-9.

213. O'Connell, M.P., et al., *Hypoxia induces phenotypic plasticity and therapy resistance in melanoma via the tyrosine kinase receptors ROR1 and ROR2.* Cancer Discov, 2013. **3**(12): p. 1378-93.

214. Carpenter, A.E., et al., *CellProfiler: image analysis software for identifying and quantifying cell phenotypes.* Genome Biol, 2006. **7**(10): p. R100.

215. Li, L.C. and R. Dahiya, *MethPrimer: designing primers for methylation PCRs.* Bioinformatics, 2002. **18**(11): p. 1427-31.

216. Schwarz, D., et al., *Ezh2 is required for neural crest-derived cartilage and bone formation.* Development, 2014. **141**(4): p. 867-77.

# X. Curriculum vitae

**Natalia Arenas-Ramirez**

Hopfenstrasse 19
8045, Zürich, Switzerland

natalia.arenasramirez@uzh.ch

## Professional experience

---

**Department of Immunology**
**University Hospital Zürich,**
**University of Zürich**
Prof: Onur Boyman
January 2012 to Present

**PhD Student**
Project**:** Cancer immunotherapy**.**
Goals:

- Develop antibodies able to modulate IL-2 activity *in vivo* and reduce IL-2 related side effects.
- Prolong anti-tumor effects studying tumor immune escape mechanisms.

**Molecular Partners AG**
Cell biology
**R&D department**
Schlieren, Switzerland
Manager: Dr. Stefan Deuber
November 2008- December 2011

**Senior Research Associate in Cell Biology**
Subject: Develop DARPin-based (scaffold proteins) medicines. Currently involved in the research and development of DARPins against important targets for the treatment of inflammatory diseases and oncology.

- **Cellular Biology** (culture cell, establishment of *in vitro* assays for screening and characterization of proteins).
- Study of protein **pharmacodynamics** (Half-life determination in animal models).
- **Development and transfer of assays to CMO, CRO** (potency assays, TK and ADA assays) for preclinical development.
- Introduction to animal experiments.
- Small scale Protein Purification.
- Responsible of the Tissue Culture laboratory.

**Genentech, Inc**
Protein engineering
**Research department**
San Francisco, CA, USA
Manager:
Dr. Rami Hannoush
March2008-Sept 2008

**Intern as a research associate**
Subject: study of Wnt proteins (signaling molecules with key roles during embryonic development, adult life and **oncogenesis**).

- Protein –**cellular biochemistry (culture cell,** conditioned media).
- Protein purification.
- Protein post-translational modification (glycan/lipid composition).
- Treatment of cells (*in vivo*) with palmitate analogs.

**Roche/ESIL**
Switzerland, France
Advisor: Elodie de Roo
Oct-Jan 2007/08

**Engineering project in collaboration with Roche.**
Subject: Increase the yield of the production of Avastin™

- Cell culture process design (perfusion and batch bioreactors) for AvastinTM production.

**CNRS**: National Center of Scientific Research
"Fe-S" proteins department
Marseille, France
Managers:
Dr Py, Dr.Angelini
March 2007-April 2007

**Intern as a research assistant**
Subject: identification of interaction between *Escherichia coli* proteins and YhgI (proposed to be a potential iron-donor protein for Fe-S proteins).

- Protein purification (affinity purification *in vitro*).
- Bacterial two hybrid system (*in vivo*).

| | |
|---|---|
| **Practical works** | **Cellular biology** (**mammalian cell culture, Vi-Cell assay**, **development of cell based assay**, **SDS-Page** protein gels).<br>**LTK-1 Introductory Course in Laboratory Animal Science , animal experiments**<br>**Immunology; Pharmacodynamics (development of ELISAS**, **TK and ADA** determination, **western Blot: ECL, LICOR,**), gel staining (Sypro Ruby, Typhoon). **FACS analysis**<br>Protein biochemistry (labeling reactions, western Blot, ProteOn, purification)<br>Bioinformatics (GraphPrism) |

## Academic background

| | |
|---|---|
| **ESIL**: Ecole Supérieure d'Ingénieurs de Luminy. University of Provence<br>Marseilles, France<br>2008-2005 | University for advanced studies in engineering technology.<br>**Equivalent of Master of Sciences Degree and Pre-doctorate Preparation**.<br>Specialization in **Biotechnology for Healthcare industries**.<br>1st year: 2nd /36; 2nd year: 8th/35; 3rd year: 5th/35<br>Graduated in October 2008<br>Course work: **cellular and molecular biology (**conjugation, transfection, sequencing), **therapeutical biomolecules, cell therapies**, expression systems, **immunology**, virology, general and applied microbiology, protein production and purification, enzymology, biochemistry engineering, genetic engineering, protein engineering, genomics, communication, economics. |
| **Lycée Pierre de Fermat**<br>Toulouse, FRANCE<br>2003-2005 | "Classe préparatoire" BCPST (Biology, Chemistry, Physics, Earth Sciences, Geology). A two year intensive course for entering French high rated engineering school. |
| **Lycée Français Louis Pasteur**<br>Bogota, COLOMBIA<br>1989-2003 | "Baccalauréat" majoring in Biology. I obtained the excellence prize and therefore the scholarship of the French government to make the university studies in France |

## Main Skills

High capacity to learn complex matters.
Oriented to work by goals with the proactive participations on teams
Dynamics, methodical and with a positive attitude
Team leader with strong motivational, leadership and organization skills

| | |
|---|---|
| | Excellent communication skills manifested in written reports and oral presentations<br>Able to set up priorities and ensuring high quality output<br>Reliability, loyalty and full involvement in the projects |

## Languages

| | |
|---|---|
| Spanish | Mother tongue. |
| French | Bilingual. |
| English | **Very good working knowledge.**<br>TOEIC. Current level 850/1000 |
| German | B2 level |

## Activities and interests

| | |
|---|---|
| Other activities | ESIL: students associations.<br>Responsible for the organization of the integration weekend for new students. Treasurer of the ESIL student association (2006-2007) |
| Leisure | Music, reading, sports, travelling, hiking. |

## Publications

**Interleukin-2: Biology, Design and Application.**
Arenas-Ramirez N, Woytschak J, Boyman O.
Trends Immunol. 2015. Review.

**IL-17 receptor A and adenosine deaminase 2 deficiency in siblings with recurrent infections and chronic inflammation.**
Fellmann F, Angelini F, Wassenberg J, Perreau M, Arenas Ramirez N, Simon G, Boyman O, Demaria O, Christen-Zaech S, Hohl D, Belfiore M, von Scheven-Gete A, Gilliet M, Bochud PY, Perrin Y, Beck Popovic M, Bart PA, Beckmann JS, Martinet D, Hofer M.
J Allergy Clin Immunol. 2015 Nov 19

**The epigenetic modifier EZH2 controls melanoma growth and metastasis through silencing of distinct tumour suppressors.**
Zingg D, Debbache J, Schaefer SM, Tuncer E, Frommel SC, Cheng P, Arenas-Ramirez N, Haeusel J, Zhang Y, Bonalli M, McCabe MT, Creasy CL, Levesque MP, Boyman O, Santoro R, Shakhova O, Dummer R, Sommer L.
Nat Commun. 2015 Jan 22

**Use of enhanced interleukin-2 formulations for improved immunotherapy against cancer.**
Rosalia RA, Arenas-Ramirez N, Bouchaud G, Raeber ME, Boyman O.
Curr Opin Chem Biol. 2014 Dec. Review.

**Membrane targeting of palmitoylated Wnt and Hedgehog revealed by chemical probes.**
Gao X, Arenas-Ramirez N, Scales SJ, Hannoush RN.
FEBS Lett. 2011 Aug 4

**Imaging the lipidome: omega-alkynyl fatty acids for detection and cellular visualization of lipid-modified proteins.**
Hannoush RN, Arenas-Ramirez N.
ACS Chem Biol. 2009 Jul 17.